ADAPTING RIVER BRIDGE INFRASTRUCTURES TO CLIMATE CHANGE

By
Akinola Ifelola, R. Eng, PMP
B.Eng. (Civil), University of Ado Ekiti, Nigeria, 2006

A thesis
presented to Ryerson University
in partial fulfillment of the
requirements for the degree of
Master of Applied Science
in the program of
Civil Engineering

Toronto, Ontario, Canada, 2017

Author's Declaration for Electronic Submission of a Thesis

I hereby declare that I am the sole author of this thesis. This is a true copy of the thesis, including any required final revisions, as accepted by my examiners.

I authorize Ryerson University to lend this thesis to other institutions or individuals for the purpose of scholarly research.

I further authorize Ryerson University to reproduce this thesis by photocopying or by other means, in total or in part, at the request of other institutions or individuals for the purpose of scholarly research.

I understand that my thesis may be made available electronically to the public.

Adapting River Bridge Infrastructures to Climate Change

Master of Applied Science, 2017

Akinola Ifelola, Civil Engineering, Ryerson University.

Abstract

Climate change forecasts project up to 20% increase in precipitation for southern Ontario based on several climate change scenarios and models and an unpredictable change an average wind speed that may range from 5% reduction to 15% increase by the year 2100 compared to 1971 to 2000 reference period. Average annual air temperatures are predicted to increase between 2.5 and 3.7°C by 2050 from baseline average between 1961 and 1990.

This research studied the impact of climate change on bridge infrastructure using the Portage bridge on the Ottawa river in southern Ontario as a case study. Result shows that increase in precipitation due to climate change will cause 0.3m/s increase in stream velocity and about 0.85m increase in water level for a 100-year storm. This increase will result in scour depths at bridge piers to increase by 0.86 m while bending moments on piers increased by 21 kNm. Shear forces also increased by 43 kN.

Acknowledgements

First and foremost, I am extremely grateful to my supervisor, Dr. Lamya Amleh, for her incredible guidance, expert advice, kindness, patience and great support throughout my graduate study. I especially thank her for her endless concern and encouragement.

I wish to thank Dr. Luaay Hassein, Assistant program director, First - Year Engineering office for his encouragement, kind help and useful comments on my research. I would also like to thank my mum and siblings for their constant encouragement and support. I am most thankful to my wife, Rachael Ifelola, for her support and contributions. Finally, I also thank my lovely kids. Without their encouragement and support, I would not have been able to complete my studies.

I am extremely grateful to all these people and I pray that God in his infinite mercies and wisdom will bring perfection into their lives.

Dedication

To my Dad,

Late Samuel Olubunmi Ifelola

Table of Contents

Author's Declaration for Electronic Submission of a Thesis ii

Abstract iii

Acknowledgements iv

Dedication v

Table of Contents vi

List of Figures x

List of Tables xiii

List of Appendices xiv

1 Introduction 1

1.1 Objective and Scope 3

1.2 Organization of the Thesis 3

2 Literature Review 5

2.1 Climate Change 5

2.2 Causes of Climate change 5

2.2.1 Natural Causes 6

2.2.2 Human Causes 6

2.3 Climate Models 8

2.3.1 Regional Climate Models and Dynamic Downscaling 8

2.3.2 Canadian Climate Models 9

2.4 Climate Change Scenarios 10

2.4.1 A1 Family 11

2.4.2 A2 Family 11

2.4.3 B1 Family 11
2.4.4 B2 Family 12
2.5 Climate Change in Canada 12
2.5.1 Surface air temperature 12
2.5.2 Precipitation 17
2.6 Historical Climate and Projected Changes for Ontario 20
2.7 Climate Change and Infrastructure 22
2.8 Climate Change Impact and Risk Assessment For Civil Infrastructure 22
2.8.1 Extreme Events Risk Assessment 22
2.8.2 Physical Vulnerability Risk Assessment 23
2.8.3 Functional Vulnerability Risk Assessment 23
2.8.4 Total risk assessment 24
2.9 Mechanism of Climate Change Impact on Bridge Infrastructure 24
2.9.1 Carbonation-Induced Corrosion 25
2.9.2 Chloride-induced Corrosion 26
2.9.3 Scouring 28
2.9.4 Extreme weather events 31
3 Current Research 32
3.1 Portage Bridge 32
3.2 Methodology for the present study 33
3.3 Hydraulic analysis 33
3.4 Scour Depth Prediction 37
3.5 Finite Element Analysis 38
3.6 Loading 40

3.6.1 Dead Loads 40
3.6.2 Hydrostatic Pressure 40
3.6.3 Hydrodynamic Pressure 40
3.6.4 Wind Loads 42
3.6.5 Horizontal drag load 42
3.6.6 Vertical Wind Load 43
3.6.7 Traffic Loadings 44
3.6.8 Design Lane 45
3.6.9 Load combinations 46
3.7 Analysis 48
4 Results and Discussions 48
4.1 Hydrological Results and Water Levels For Analyzed 100-Year Storm 48
4.2 Hydrological Results for 100-Year Storm in Projected Changed Climate 50
4.3 Design scour for 100-year storm 52
4.4 Scour for 100-year storm in projected climate 53
4.5 Results of bridge elements under normal design loading 54
4.5.1 Axial and Shear forces 54
4.5.2 Bending Moments and Design Requirements 56
4.6 Response of Bridge to Loading and Effects of Scouring In Projected Climate 61
4.6.1 Axial and shear forces 61
4.6.2 Bending moments and design requirements 62
4.7 Effects of Age and Exposure Conditions and Climate Change Interactions on Concrete Infrastructures 67
5 Conclusion and recommendations 68
5.1 Adapting To Climate Change 68

5.1.1 Jacketing 68

5.1.2 Scour Protection 69

5.2 Future Study 71

Appendices 72

References 90

List of Figures

Figure 2.1 Increasing gas concentration in the atmosphere for 2000 years. (Forster et al., 2007) 7
Figure 2.2 Increment in CO2 concentrations in the atmosphere form 1960. (Forster, et al., 2007) 7
Figure 2.3 Change in mean annual temperature in Canada, from 1950 to2007 (Zhang et al., 2010) 13
Figure 2.4 Change in mean Spring temperature in Canada from1950 to 2007 (Zhang et al., 2010) 14
Figure 2.5 Change in mean Summer temperature in Canada from 1950 to 2007 (Zhang et al., 2010) 15
Figure 2.6 Change in mean Fall temperature in Canada from 1950-2007 (Zhang et al., 2010) 15
Figure 2.7 Change in mean Winter temperature in Canada from 1950 to 2007 (Zhang et al., 2010) 16
Figure 2.8 Projected change in mean surface air temperature (°C) in Canada in 2041-2060 relative to 1941-1960 as simulated by CGCM3/T47 in the IPCC SRES A1B experiment (Environment and Climate Change Canada, 2017) 16
Figure 2.9 Projected change in mean surface air temperature (°C) in Canada in 2041-2060 relative to 1941-1960 as simulated by CGCM3/T47 in the IPCC SRES B1 experiment (Environment and Climate Change Canada, 2017) 17
Figure 2.10 Precipitation trends over Canada from 1950 to 2007 (Zhang et al., 2010) 18
Figure 2.11 Projected change in 5-year mean precipitation rate (mm/day) in 2055 relative to 1981-2000 as simulated by CGCM3/T47 in the IPCC SRES A1B experiment (Environment and Climate Change Canada, 2017) 19
Figure 2.12 Projected change in 5-year mean precipitation rate (mm/day) in 2055 relative to 1981-2000 as simulated by CGCM3/T47 in the IPCC SRES B1 experiment. (Environment and Climate Change Canada, 2017) 20

Figure 2.13 Projected change in 5-year mean precipitation rate (mm/day) in 2055 relative to 1981-2000 as simulated by CGCM3/T47 in the IPCC SRES A2 experiment. (Environment and Climate Change Canada, 2017) 20
Figure 2.14 Projected change in average annual temperature in Ontario in 2071 to 2100 compared to 1971 – 2000 using the A2 scenario in the Canadian Coupled Global Climate model. (Colombo et al, 2007) 21
Figure 2.15 Typical risk matrix for an extreme event scenario 24
Figure 2.16 Corrosion and spalling induced by carbonation (Xiaoming et al. 2010) 26
Figure 2.17 Electrochemical cell at rebar surface induced by chloride penetration (Xiaoming, et al., 2010) 27
Figure 2.18 Corrosion of steel reinforcement in concrete Structures (Xiaoming et al., 2010) 28
Figure 3.1 Stretch of Ottawa River Showing Portage Bridge and MacDonald-Cartier Bridge along the Ottawa River 33
Figure 3.2 Digital Elevation map (DEM) of study area showing heights above sea level. (source: USGS) 34
Figure 3.3 Hydraulic analysis result table for 100-year return period of portage bridge site 35
Figure 3.4 Hydraulic analysis result table for 100-year return period downstream at portage bridge site 35
Figure 3.5 Hydraulic analysis result table for 100-year return period plus 20% increase in discharge upstream at portage bridge site 36
Figure 3.6 Hydraulic analysis result table for 100-year return period plus 20% increase in discharge downstream at portage bridge site 36
Figure 3.7 3D Model of Bridge Analysis section 39
Figure 3.8 Transverse section of Bridge model 39
Figure 3.9 Longitudinal view of bridge model. 39
Figure 3.10 Hydrodynamic pressure on bridge piers 42
Figure 3.11 Idealized horizontal wind pressure on piers 43
Figure 3.12 CL-W loading (CSA,2014) 45
Figure 3.13 Cl-W Load Envelope (CSA, 2014) 45

Figure 4.1 Variations in water level for a 100-year storm event along a stretch of Ottawa River 49
Figure 4.2 Water surface levels at the portage bridge site for 100-year storm event 49
Figure 4.3 Variations in velocities along the river reaches 50
Figure 4.4 Variations in water level for a 100-year storm event along a stretch of Ottawa River for projected climate 51
Figure 4.5 Water surface levels at the portage bridge site for 100-year storm event in projected climate 51
Figure 4.6 Variations in velocities along the river reaches in projected climate 52
Figure 4.7 Bridge scour in a 100-year storm 53
Figure 4.8 Bridge scour for a 100-year storm in projected Climate 54
Figure 4.9 Plan of bridge piers arrangement 54
Figure 4.10 Axial load envelope for pier 7 55
Figure 4.11 Shear force envelope for pier 7 55
Figure 4.12 Axial load envelope for pier 8 55
Figure 4.13 Shear force envelope for pier 8 56
Figure 4.14 Bending moment envelope for pier 7. 56
Figure 4.15 Bending moment envelope for pier 8. 57
Figure 4.16 Shear force envelope for pier 7 in projected climate 62
Figure 4.17 Shear force envelope for pier 8 in projected climate 62
Figure 4.18 Bending moment envelope for pier 7 in projected climate 63
Figure 4.19 Bending moment envelope for pier 8 in projected climate 63
Figure 5.1 Typical cross section of a Pier before and after Jacketing 69

List of Tables

Table 3.1 Unit weights of construction materials (CSA, 2014) 40
Table 3.2 Longitudinal drag coefficient (CSA, 2014) 41
Table 3.3 Wind exposure coefficient (CSA S6-14) 44
Table 3.4 Ultimate Load combinations (CSA, 2014) 46
Table 3.5 Live load factors ultimate limit state (CSA,2014) 47
Table 3.6 Permanent loads – Maximum and minimum values of load factors for ULS (CSA,2014) 47
Table 4.1- Summary of Bending Moment, Shear Force and reinforcement requirements 67

List of Appendices

Appendix 1 Output table of hydraulic analysis 72
Appendix 2 Historical discharge data for Ottawa river measured at Carillon (Ottawa river regulation planning board) 74
Appendix 3 Scour calculations input and output for 100- year storm 76
Appendix 4 Scour calculations input and output for 100- year storm in projected climate 77
Appendix 5 STAAD Pro input for 100-year design 80
Appendix 6 STAAD Pro input for projected climate 85

1 Introduction

River bridges are a critical component of transport networks; therefore, the functionality and sustainability of river bridges will have a significant effect on the social, economic and physical development of the society. Infrastructural systems such as bridges often form the core foundation of many aspects of modern society such as economy and quality of life. In the last century, there has been a significant change in weather patterns across different zones of the world. This shift is termed climate change.

The Intergovernmental Panel on Climate Change (IPCC), established by the United Nations (the world's most authoritative and recognized body of climate change research) has released several assessment reports on climate change impact to all zones of the world and made predictions on how climate change will affect different zones of the world (Intergovernmental Panel on Climate Change (IPCC, 2007)

According to predictions, climate change will have both detrimental and advantageous effects. Harmful consequences of climate change which are already being noticed include; sea level rise, global temperature rise, warming ocean, shrinking ice sheet, declining Arctic ice ocean acidification and an increase in the frequency of extreme events. Of noteworthy is the increase in the severity of extreme events apart from their increased frequency. (Intergovernmental Panel on Climate Change (IPCC, 2007).

One of the strategies to reduce the vulnerability of infrastructures to these changes is to anticipate and adapt. Before any meaningful adaptation studies and strategies can be implemented for infrastructures, a clear understanding of the process and impact of climate change is required. Although a lot of studies have been conducted by researchers generally on climate change, most of the available studies concentrated on causes, impact and mitigation methods with few studies done on the adaptation of infrastructures to climate change. Climate change requires a focus on both slowing climate change, that is, mitigation and adapting to the anticipated impacts of it. Adaptation, however, has not received as much attention from researchers as much as mitigations. (Blanco and Alberti, 2009).

The anticipated impact of climate change which would directly or indirectly affect bridge infrastructure by an increase in environmental loading and degradation mechanism and rate of which the materials with which infrastructures are built are, carbonation, chloride penetration, sulfate attacks, alkali aggregate reactions, precipitation depending on region and increase in storm surges. (flooding).

There have been studies investigating all these phenomena as discrete occurrences but they have mostly not been investigated in the context of climate change. These studies did not investigate the mechanisms of these phenomena and climate change interactions. Yin-hui, et al. (2015) investigated the effect of water flow pressure on bridge piers. They also studied the scour associated with water pressure on bridge piers. Cheng, (2012) evaluated the Lateral behavior of Pile-supported Bridges under scouring conditions. Stewart, Wang, and Nguyen, (2011) however, investigated Climate change impact and risks of concrete infrastructure deterioration.

In the area of adapting infrastructures to climate change impacts, very few studies have been carried out and these studies mostly explored strategic management adaptations regarding policy changes that can be implemented by government agencies and policy makers. Structural adaptations to the physical infrastructure itself were seldom discussed. Buurman and Babovic, (2016) discussed the uncertainty in policy making for adaptation to climate change and proposed several approaches for quantifying and dealing with these uncertainties. Demuzere, et al., (2014) advocated adaptation on a holistic societal scale through green urban infrastructure development and averred that green urban infrastructure directly mitigates climate change and adapt the environment since it directly removes CO2 from the atmosphere via photosynthetic uptake during the day and releases CO2 at night via respiration.

The big question however is; how do we adapt individual existing infrastructure to climate change in terms of structural capacity and user's safety since these structures will be exposed to new loading in scales and patterns that were non-existence as at the time of design and construction? How do we also adapt future (yet to be built) infrastructure to climate change as our existing codes and standards were formulated mostly for past climate? These questions require answers especially since resources are limited, and all existing infrastructures can't be rebuilt.

1.1 Objective and Scope

The overall goal is to investigate the structural impact of climate change on river bridge infrastructure using a bridge on the Ottawa River as a case study and to demonstrate the utilization of the finite element modelling and analysis to investigate the response of the bridge and how the bridge can be adapted to the structural impacts of climate change. These objectives were achieved by:

- Apply the HecRas tool to simulate precipitation and water level changes in the future climate based on selected climate scenarios (HecRas is a computer program that models the hydraulics of water flow through natural rivers and other channels);
- Simulate historical and future data for the Ottawa river by calibrating the HecRas model for the river and basin;
- Compare simulation of past scenarios to historical data as a verification for simulations of future scenarios;
- Apply the HecRas tool to estimate the scour at the base of the bridge pier;
- Apply the tool to estimate the river flow velocity at the location of the bridge;
- Use the finite element software STAAD.PRO to analyze the bridge and investigate the bridge response to different climate change impact based on the results of scour depth, water level, and flow velocities;
- Study the effect of climate change on existing structures whose strength has been affected due to age, use and exposure conditions; and
- Discuss adaptive retrofits to the bridge.

1.2 Organization of the Thesis

Following the introduction, chapter 2 reviews the literature on adapting infrastructure to climate change. The present body of knowledge and research was explored. Climate change scenarios and models were looked into and mechanism of climate change impact on bridge infrastructures was discussed. Material deterioration was discussed in terms of carbonation, chloride penetration, sulfate attacks and freeze thaw effects. Structural impact of climate change was also discussed. Factors that will impact the structural integrity of bridges such as flooding and it attendant hydrostatic and hydrodynamic loading as well as scour effect of flooding on the bridge piers is discussed.

Chapter 3 describes the methodology employed in the current research. In chapter 4, results were discussed. Axial forces, bending moments and reinforcement requirements for the present climate and the projected future climate were compared. Chapter discussed conclusions to present study and looked at recommendations to adapt to climate change and suggested future studies.

2 Literature Review

2.1 Climate Change

Climate refers to the average weather conditions prevailing in an area over a long period of time. In statistical terms, it may be described as the mean and variability of atmospheric variables such as temperature, precipitation, wind and humidity over a period of time, which can range from months to centuries. The averaging period for estimating these variables is usually 30 years. (IPCC, 2014).

However, Rood (2007) averred that climate is much more than weather and atmosphere, He stated that climate involves contributions of other components of the earth system such as the cryosphere, ocean, land and their chemical state including the sun and the geological state of the earth which are significant contributors to climate. He also hinted that the averaging period of 30 years used in defining climate is dependent on the quality and completeness of observed records which might be inadequate since extended data record shows an important mode of variabilities longer than 30 years, especially the non-atmospheric components.

"Climate change in IPCC usage refers to a change in the state of the climate that can be identified (e.g. using statistical tests) by changes in the mean and/or the variability of its properties, and that persists for an extended period, typically decades or longer." (IPCC, 2014). Environment and natural resources Canada defines "climate change as a long-term shift in weather conditions identified by changes in temperature, precipitation, winds, and other indicators. Climate change can involve both changes in average conditions and changes in variability, including, for example, extreme events" (Environment and natural resources Canada, 2015).

2.2 Causes of Climate change

The causes of climate change can best be explained concerning earth energy balance or energy factors. The earth's temperature is regulated by outgoing and incoming energy and any factor that that causes a sustained disruption to the amount of outgoing or incoming energy causes climate change. Because these factors are external to the earth system, they are referred to as 'climate forcers' to create the impression that they push the climate towards a new state. The new state can

be cooler or warmer depending on the climate forces. Causes of climate change can be broadly categorized into natural and human causes.

2.2.1 Natural Causes

Climate can be affected by natural occurrences that are external to the earth's climatic system. These may include changes in the sun's solar output and volcanic activities

2.2.2 Human Causes

Human causes refer to climate forces that are caused by human activities. The primary cause is burning of fossil fuels and deforestation as a direct result of logging for timber and clearing for agriculture and development and results in the release of greenhouse gasses, mainly carbon dioxide, methane, nitrous oxide and water vapor. Chlorofluorocarbons (CFC) are another major greenhouse gas contributing to climate change by reacting with and destroying the ozone layer. The United Nations has acknowledged that present climate change is happening due to human caused factors (Fung et al., 2011). Figure 2.1 shows the rate of increase in greenhouse gases for 2000 years. It can be deduced that the industrial revolution heralded the sharp increase in a number of greenhouse gases in the atmosphere. Figure 2.2 also shows the increment in CO2 concentrations in the atmosphere from 1960.

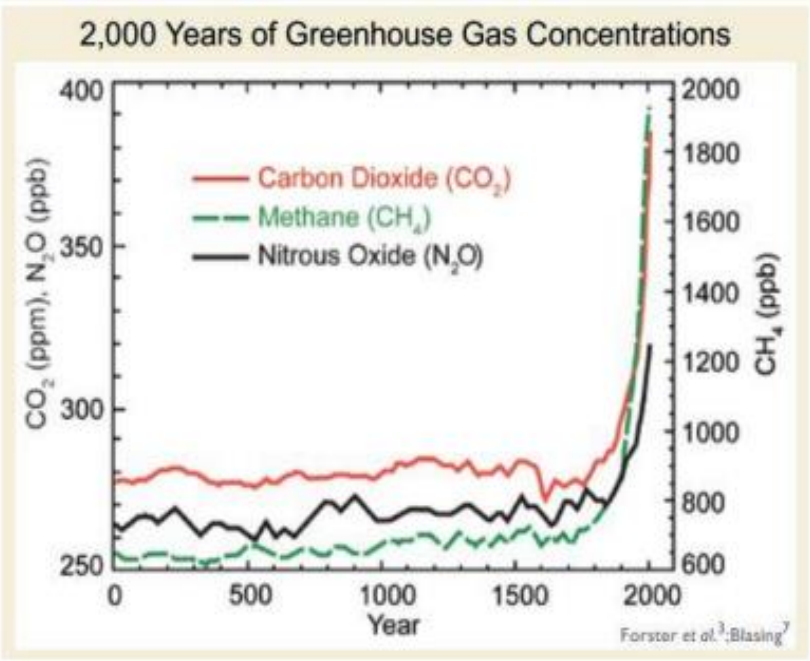

Figure 2.1 Increasing gas concentration in the atmosphere for 2000 years. (Forster et al., 2007)

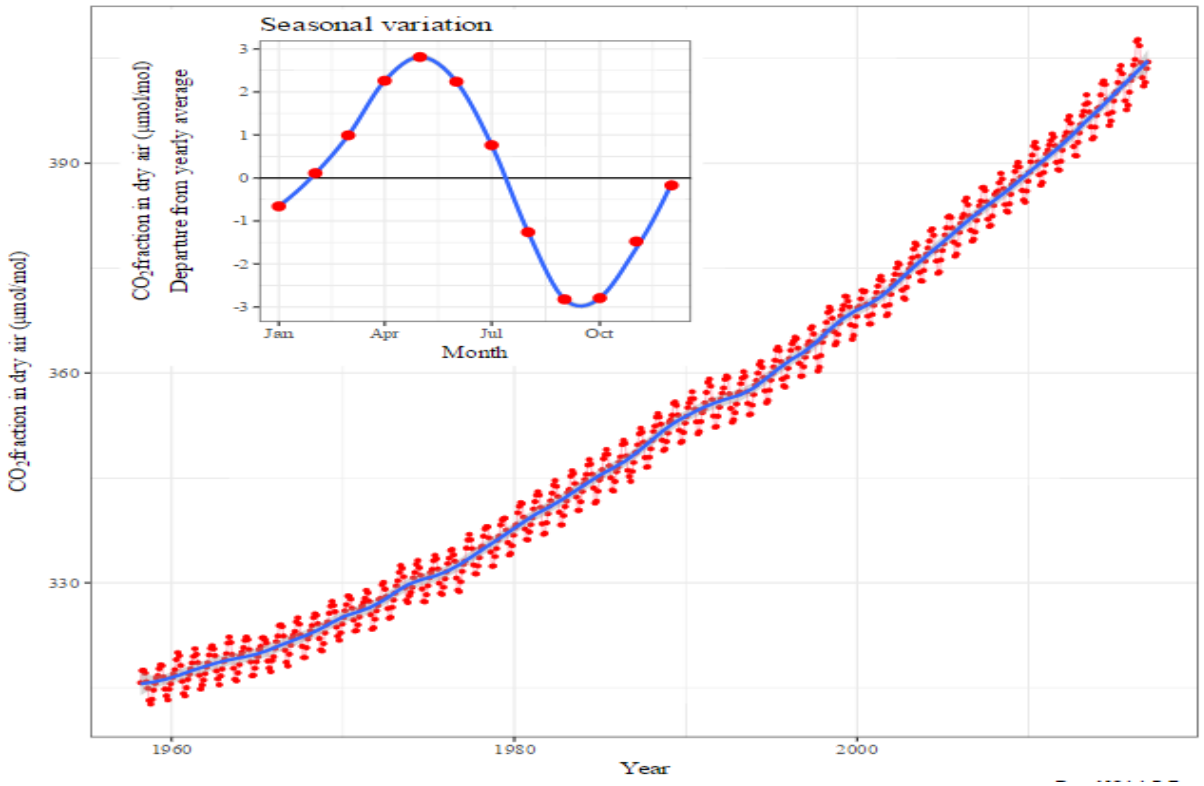

Figure 2.2 Increment in CO2 concentrations in the atmosphere form 1960. (Forster, et al., 2007)

2.3 Climate Models

Climate models are used to study the effect of higher greenhouse gases in the atmosphere based on increasing amounts of heat that is trapped in the atmosphere. Increased heat affects all aspects of weather and climate, which includes precipitation, winds, and humidity. Lots of global climate models have been developed with each one being unique, based on different assumptions and each one produces different projections of future climate when the same data (scenarios) are provided as inputs.

The intergovernmental panel on climate change has developed several climate models to analyze and project what the future climate would likely be. These models development has witnessed several fine-tuning as technology improves and can be said to be generational. These models are called Global climate models or General circulation models (GCMs).

A global climate model also called a general circulation model intends to predict climate behavior by integrating a variety of fluid-dynamical, chemical, or biological equations that are either derived from physical laws or constructed by empirical means. GCMs have been developed for both the atmosphere, that is atmospheric GCMs (AGCMs) and the ocean, that is ocean GCMs (OGCMs). An AGCM and an OGCM can be combined (coupled) together to form an atmosphere-ocean coupled general circulation model (AOGCM). Other components such as a sea ice model or a land model are added, and this AOGCM becomes the basis for a full climate model. This allows for different variations and their varying degrees of response to climate change can be studied.

2.3.1 Regional Climate Models and Dynamic Downscaling

GCMs depict the world climate using a three-dimensional grid over the global space, and the grids typically have a horizontal resolution of between 250 and 600 km, 10 to 20 vertical layers in the atmosphere and may have as many as 30 layers in the oceans. This resolution is quite coarse relative to the scale of exposure units in most impact assessments, therefore only partially fulfilling criteria of GCM developments. (IPCC, 2017). Many physical processes, such as those related to clouds occur at smaller scales than the GCMs resolutions and cannot be adequately modeled using the GCMs. Instead, their known properties are averaged over the larger scale using a technique

known as parameterization. This creates a source of uncertainty in GCM based simulations of future climate.

Also, in the simulation of feedback mechanisms in models relating to water vapor and warming, clouds and radiation, ocean circulation, ice and snow albedo which occur at scales smaller than the resolutions of GCMs, results of future climate simulations obtained are marred with a high level of uncertainties. Because of these, GCMs may simulate quite different responses to the same forcing because of the way certain processes and feedbacks are modelled. (IPCC, 2017)

In other to solve the problems of uncertainty created by too large resolutions of GCMs, Improved information on regional climate change can be achieved with the use of different regionalization techniques, including high-resolution and variable resolution (Jacob, et al., 2007). This results in Regional Climate Models (RCMs). RCMs are therefore GCMs that has been dynamically downscaled to produce models of higher resolutions.

Dynamical downscaling is basically the method used to obtain high-resolution climate or climate change information from coarse-resolution global climate models (GCMs) which does not adequately capture the effects of local and regional forcing in areas with complex surface physiography. GCMs are run at a spatial resolution of 150-300 km by 150-300 km and are unable to resolve important sub-grid scale features such as clouds and topography. Many impacts models require information at scales of 50 km or less for proper analysis. Hence several downscaling methods are developed to estimate the smaller-scale information. Dynamical downscaling uses limited-area, high-resolution model (a regional climate model, or RCM) driven by boundary conditions from a GCM to derive smaller-scale information which cannot be adequately derived from global climate models, GCMs, (IPCC, 2017)

2.3.2 Canadian Climate Models

Canada and Canadian climate scientists have not been left out in the development of global climate models and regional climate models. The Canadian Centre for Climate Modelling and Analysis (CCCma) has developed a number of climate models. These climate models are used to study climate change and its variability and to understand the various processes which govern the climate system. They are also used to make quantitative projections of future long-term climate change

given various greenhouse gas and aerosol forcing scenarios and increasingly to make initialized climate predictions on time scales ranging from seasons to decades. (Environment and Climate Change Canada, 2017)

Climate models developed by the Canadian Centre for Climate Modelling and Analysis (CCCma) includes the current and previous models.

2.3.2.1 Current models

Climate models developed and currently in use by Canadian climate reseachers include the following (Environment and Climate Change Canada, 2017)

CanESM2	The second generation Canadian Earth System Model
CGCM4/CanCM4	The fourth generation and current coupled global climate model
AGCM4/CanAM4	The fourth generation and current atmospheric general circulation model
CGCM3	The third generation coupled global climate model
AGCM3	The third generation atmospheric general circulation model

2.3.2.2 Previous model versions

AGCM1	The first generation atmospheric general circulation model
AGCM2	The second generation atmospheric general circulation model
CGCM1	The first generation coupled global climate model
CGCM2	The second generation coupled global climate model
CRCM	The Canadian Regional Climate Model

2.4 Climate Change Scenarios

Future levels of greenhouse gas in itself are not certain and are therefore modeled based on scenarios, which describe different ways in which the world may develop in the next 100 years. The Intergovernmental Panel on Climate Change has approved 40 scenarios which may be used in assessments of climate change and its impacts. The scenario has a different set of assumptions about future environmental, social and economic conditions. The real amount of greenhouse gas in the future will depend on variable factors such as global population, human behavior,

technological development, carbon source, the behavior of land and water ecosystems. No scenario is more likely to occur than others, therefore none of the scenarios represent a "best guess" of future emission. The intergovernmental panel on climate change further grouped these 40 emission scenarios into four (4) distinct families as described below:

2.4.1 A1 Family

The A1 scenarios are of a more integrated world. The A1 family of scenarios is characterized by Rapid economic growth. A global population that reaches 9 billions in 2050 and then gradually declines. The quick spread of new and efficient technologies. A convergent world - income and way of life converge between regions. Extensive social and cultural interactions worldwide.
There are subsets to the A1 family based on their technological emphasis:
A1FI - An emphasis on fossil-fuels (Fossil Intensive).
A1B - A balanced emphasis on all energy sources.
A1T - Emphasis on non-fossil energy sources (IPCC, 2014).

2.4.2 A2 Family

The A2 scenarios are of a more divided world. The A2 family of scenarios is characterized by:
(a) A world of independently operating, self-reliant nations. (b) Continuously increasing population and regionally oriented economic development. (IPCC, 2014).

2.4.3 B1 Family

The B1 scenarios are of a world more integrated, and more ecologically friendly. The B1 scenarios are characterized by:
(a) Rapid economic growth as in A1, but with rapid changes towards a service and information economy. (b) Rising population to 9 billion in 2050 and then declining as in A1. (c) Reductions in material intensity and the introduction of clean and resource efficient technologies. (d) Emphasis on global solutions to economic, social and environmental stability (IPCC, 2014).

2.4.4 B2 Family

The B2 scenarios are of a world more divided, but more ecologically friendly. The B2 scenarios are characterized by:
(a) Continuously increasing population, but at a slower rate than in A2 (b) Emphasis on local rather than global solutions to economic, social and environmental stability (c) Intermediate levels of economic development and (d) Less rapid and more fragmented technological change than in A1 and B1. (IPCC, 2014).

2.5 Climate Change in Canada

Canadian scientists have studied climate change over the last two decades. Various federal government agencies, the provincial government, city councils and industry have sponsored a series of researches related to climate change, its impacts, mitigation, and adaptations. However, these studies are scattered around these different agencies and make them somewhat difficult to access. Examples of these studies include "The impact of climate change on Canadian municipalities infrastructure," "Changing weather patterns, uncertainty, and infrastructure risks: Emerging adaptation requirements", "Climate change for Ontario: an updated synthesis for policy makers and planners", "Adapting infrastructure to climate change in Canadian cities and communities", "Cities and communities: The changing climate and increasing vulnerability", "Canadian climate trends, 1950 to 2007" and "Temperature and precipitation trends in Canada during the 20th century".

These studies were performed to try to understand the observed climate changes, it causes and to project future trends. Major results of climate trends in Canada and future projections may be summarized as follows:

2.5.1 Surface air temperature

Zhang et al. (2010) studied temperature trends using data from 210 stations scattered across the country over a period from 1950 to 2007. These data were rigorously checked and corrected for known sources of systematic error such as station shifts, changes in procedures used for observation and excluded stations where there were high urban warming effects. (Zhang, et al.,

2010). The daily mean temperature was then computed from the average daily maximum and minimum temperatures.

From the studies, they concluded that the mean daily temperatures across Canada showed a significant increase in most regions. Within the time studied, annual mean temperature has increased by about 1.4ºC. (Zhang et al., 2010). This increase differs from zone to zone as shown in Figure 2.3, the largest increase was observed in northwestern and western region with lowest in eastern Canada.

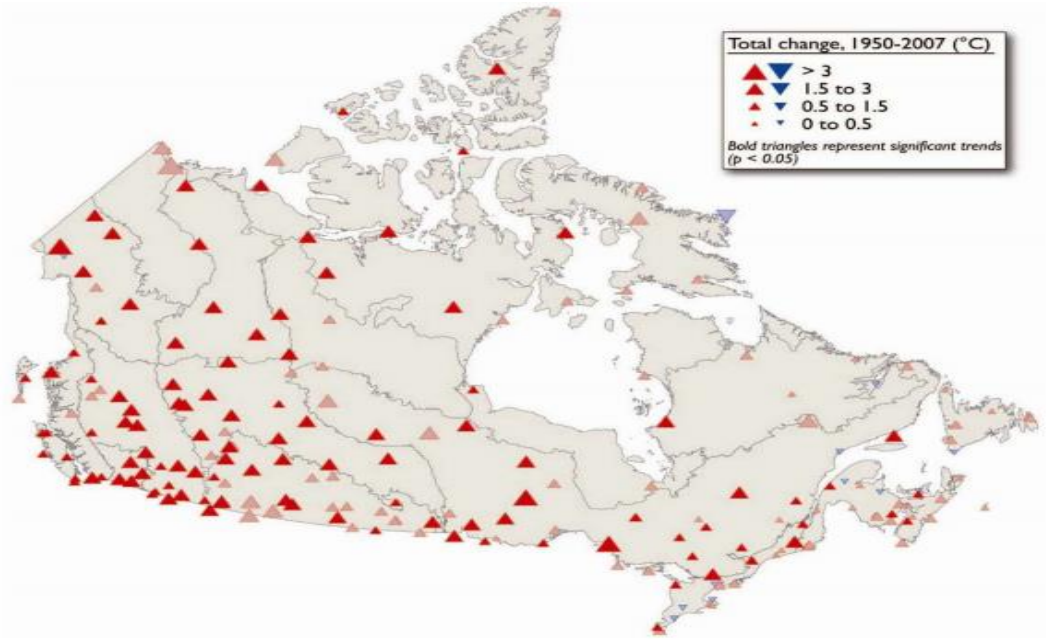

Figure 2.3 Change in mean annual temperature in Canada, from 1950 to2007 (Zhang et al., 2010)

These results agree with results obtained by several other researchers like Bonsal et al. (2000), Chiotti and Lavender (2008). Historical trends show that the average annual global temperature warmed by about 0.76°C over the last century (IPCC 2007a:5), but warming in Canada was double the world average. The average temperature in Canada has increased about 1.2°C in the last 58 years (Environment Canada, 2006). The warming was not uniform across the country. For example, average annual temperatures increased about 2°C in northwestern British Columbia and the Kluane region of the Yukon Territory, and by 1.2°C in south-central Canada, but did not change

in Atlantic Canada (Environment Canada, 2006). During this period, temperatures across Ontario increased 0 to 1.4°C (Chiotti and Lavender, 2008).

Seasonal trends have also been studied, change in temperature differs from one season to another as shown in Figures 2.4 - 2.7. Warming trends are more frequently observed in winter and spring, with more warming concentrated over western Canada. Some evidence of cooling was observed in the fall, but these were not significant (Zhang et al. 2010). The only stations showing significant fall trends are warming over northern Canada. Similarly, in summer the only significant trends are warming, and these stations tend to be located in southern Canada. Analyses of daily temperature extremes indicate trends consistent with warming including fewer cold nights, cold days, and frost days, but more frequent warm nights and warm days. (Vincent and Mekis, 2006). Zhang et al. (2010) found evidence that increases in atmospheric concentrations of greenhouse gases from human activities were contributing to temperature increases in Canada.

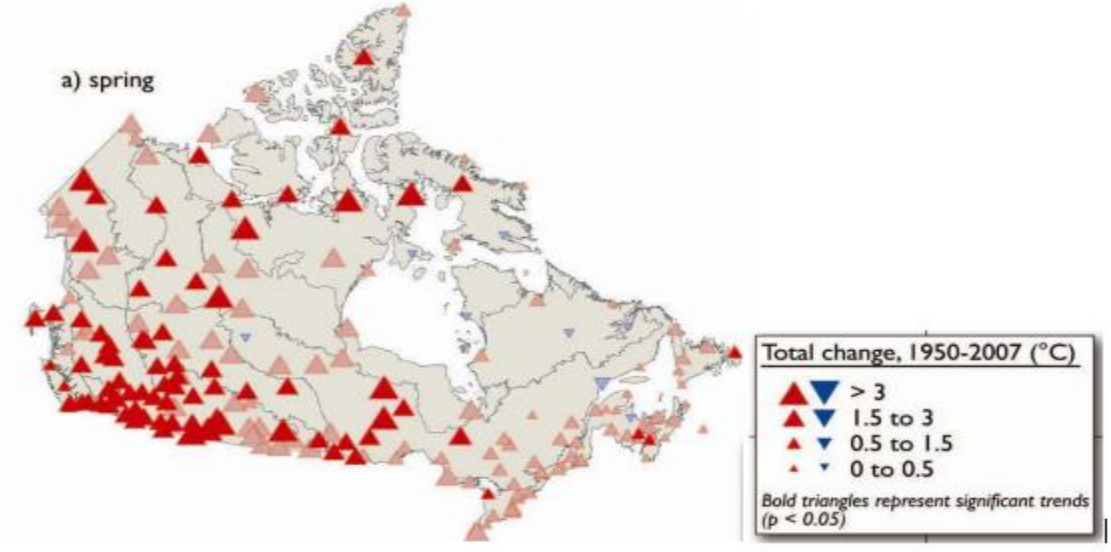

Figure 2.4 Change in mean Spring temperature in Canada from1950 to 2007 (Zhang et al., 2010)

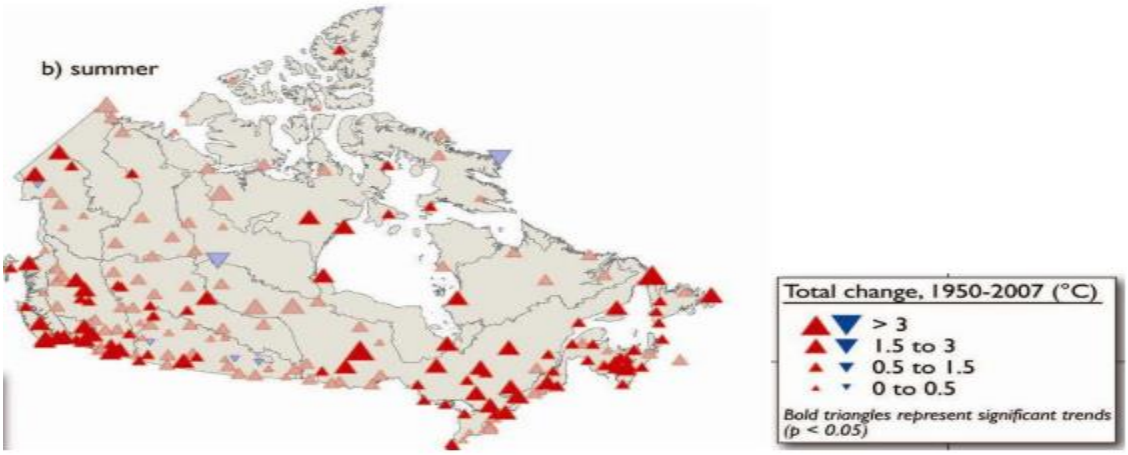

Figure 2.5 Change in mean Summer temperature in Canada from 1950 to 2007 (Zhang et al., 2010)

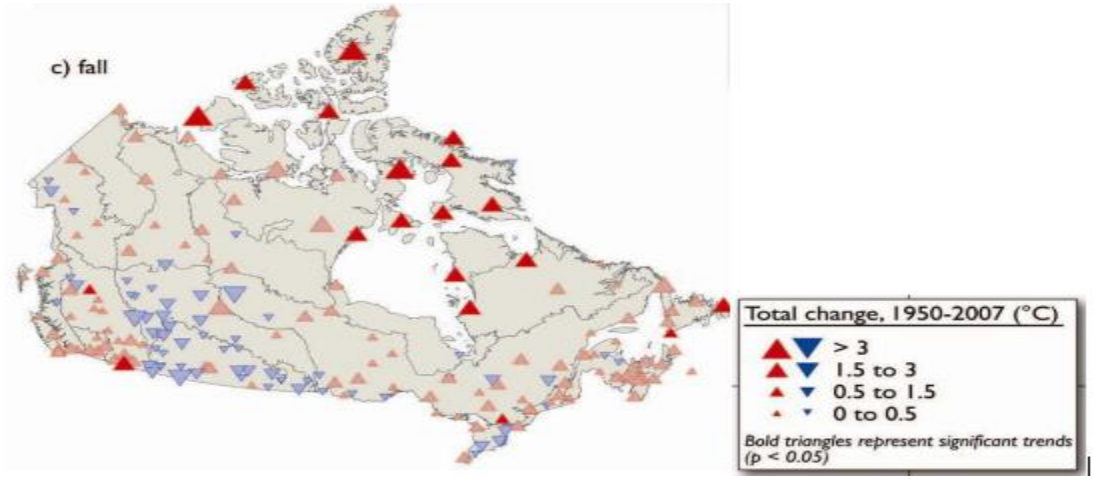

Figure 2.6 Change in mean Fall temperature in Canada from 1950-2007 (Zhang et al., 2010)

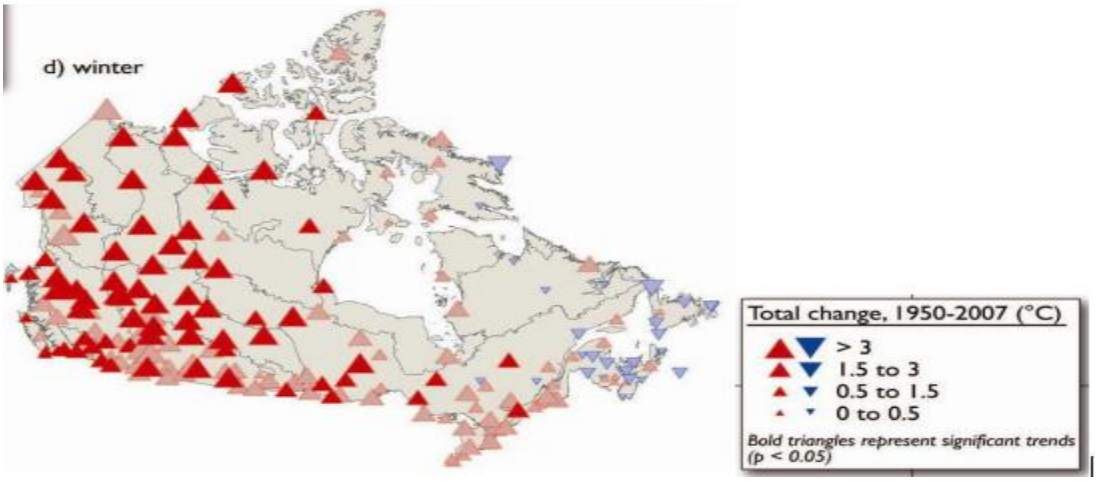

Figure 2.7 Change in mean Winter temperature in Canada from 1950 to 2007 (Zhang et al., 2010)

Future projections for temperature in Canada have been studied. Figure 2.8 shows the result of simulations by The Canadian Centre for Climate Modelling and Analysis (CCCma) when they simulated and projected the likely change in mean surface air temperature (°C) in Canada in 2041-2060 relative to 1941-1960 as simulated by CGCM3/T47 in the IPCC SRES A1B experiment. Figure 2.9 shows the projections for the same period while using the IPCC SRES B1 scenario.

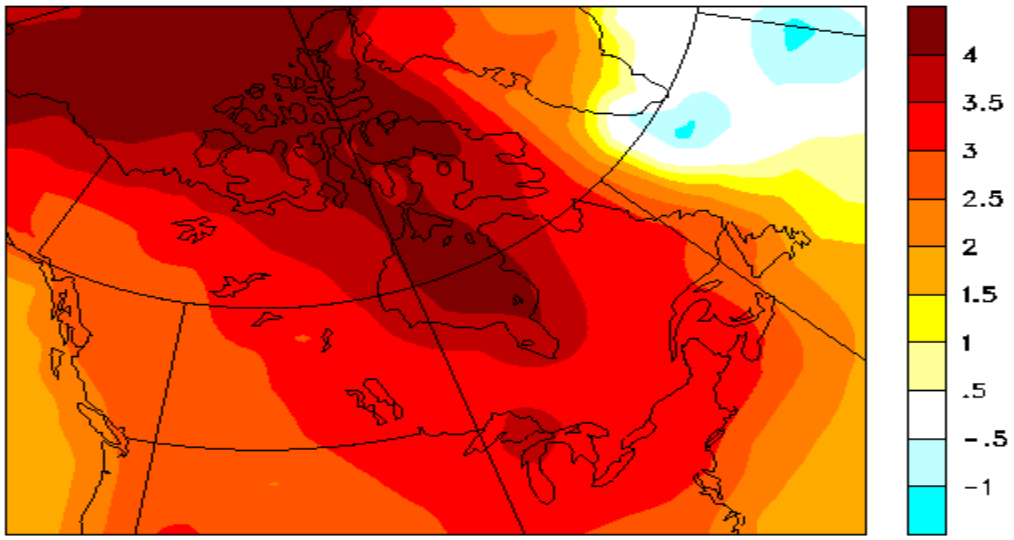

Figure 2.8 Projected change in mean surface air temperature (°C) in Canada in 2041-2060 relative to 1941-1960 as simulated by CGCM3/T47 in the IPCC SRES A1B experiment (Environment and Climate Change Canada, 2017)

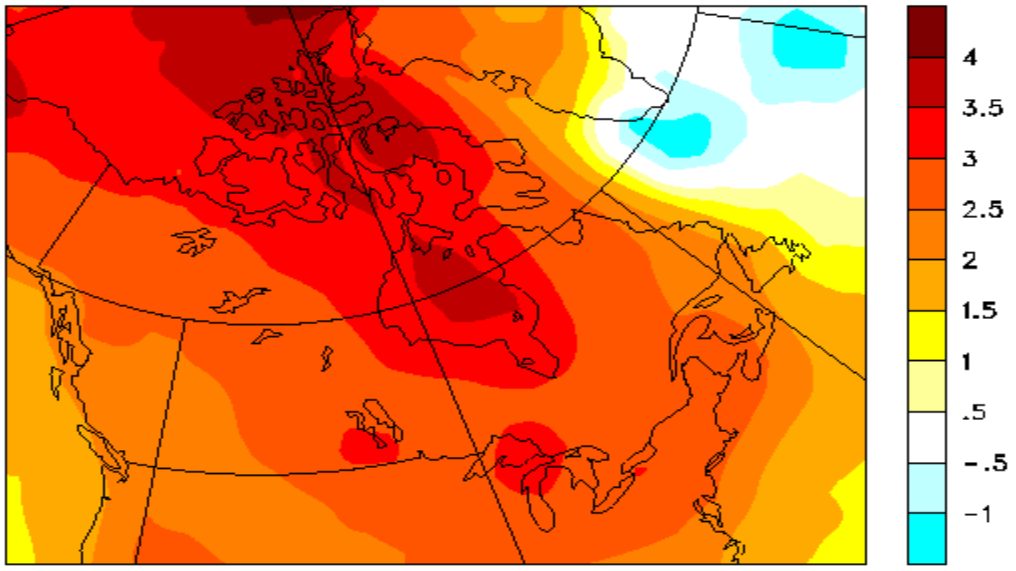

Figure 2.9 Projected change in mean surface air temperature (°C) in Canada in 2041-2060 relative to 1941-1960 as simulated by CGCM3/T47 in the IPCC SRES B1 experiment (Environment and Climate Change Canada, 2017)

Both projections show that temperature by the 2050s will increase by an amount of a range 2.5ºC to 4ºC relative to the 1950s with northern Canada experiencing the maximum increase.

2.5.2 Precipitation

Zhang et al. (2010) showed that precipitation had increased over Canada since 1950 when he studied data from 210 different weather stations. The majority of stations with significant trends showing increases as shown in Figure 2.10. The increasing trend is most obvious over northern Canada where many stations show significant increases. There is not much evidence of clear regional patterns in stations showing significant changes in seasonal precipitation except for significant decreases which tend to be concentrated in the winter season over southwestern and southeastern Canada. Also, increasing precipitation over the Arctic appears to be occurring in all seasons except summer. The trend toward increasing precipitation has been accompanied by increases in extreme daily precipitation amounts during the growing season (Qian et al., 2010).

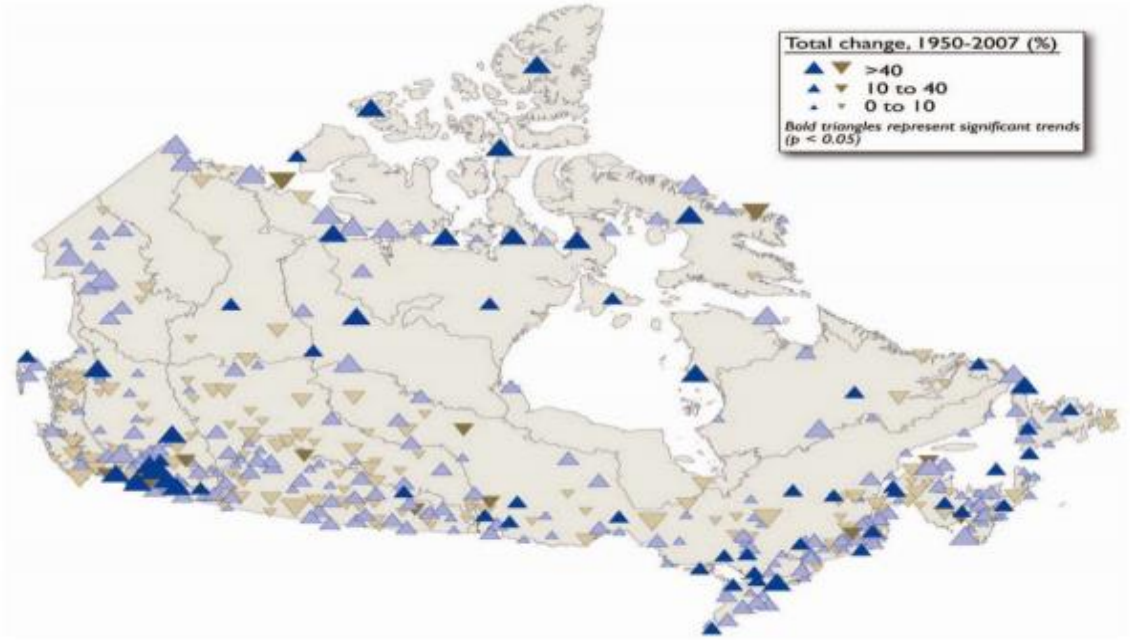

Figure 2.10 Precipitation trends over Canada from 1950 to 2007 (Zhang et al., 2010)

Trends in the annual number of days with measurable precipitation have a similar pattern to trends in total annual precipitation but with larger numbers of stations showing significant increases and decreases. This is particularly evident in summer where significant increases in the number of days with precipitation were observed over most regions of Canada (Zhang et al., 2010). Zhang et al. (2010) reported that it is difficult to generalize a spatial pattern in precipitation trends apart from a tendency for stations with significant increases in precipitation amount and the number of days with precipitation to be located over southern coastal and northern regions of Canada. While it is not yet clear what is responsible for the precipitation changes in Canada, a recent study found evidence of anthropogenic influences in observed precipitation increases over Northern Hemispheric land areas north of 55°N including Canada (Min et al., 2008).

Projections for future precipitation in Canada as simulated by the CCCma shows that annual and seasonal precipitations are likely to increase across Canada for all the simulated SRES scenarios, with the greatest increase in northwest Canada.

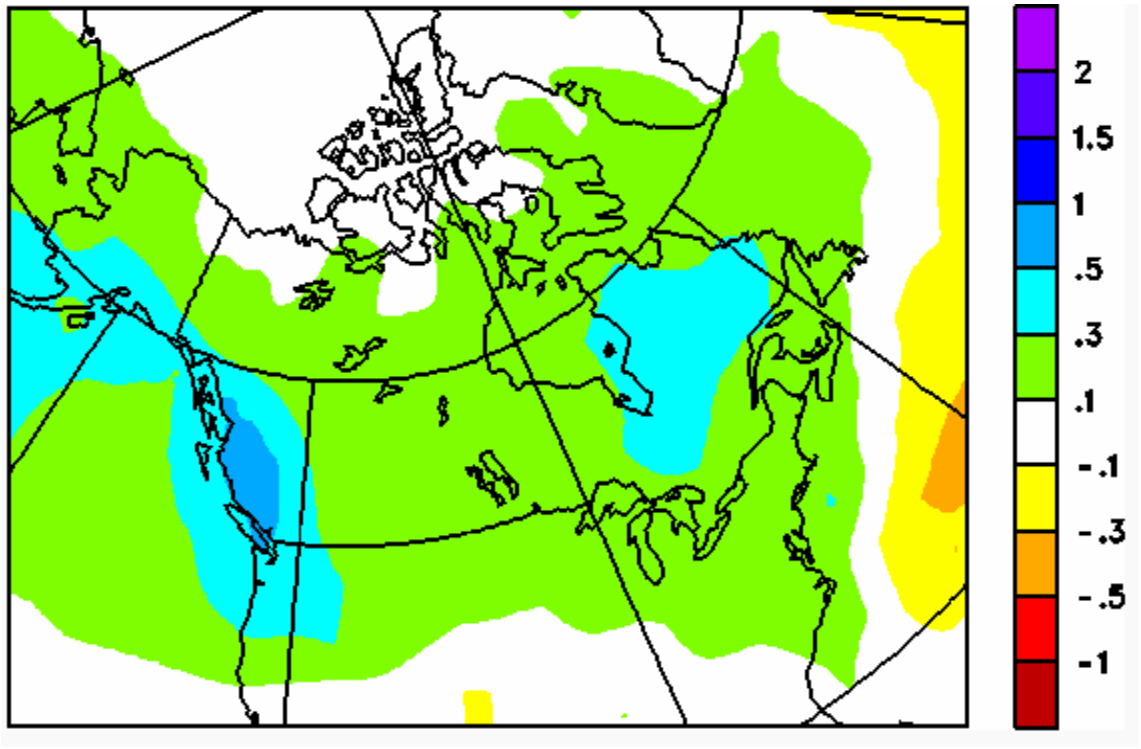

Figure 2.11 Projected change in 5-year mean precipitation rate (mm/day) in 2055 relative to 1981-2000 as simulated by CGCM3/T47 in the IPCC SRES A1B experiment (Environment and Climate Change Canada, 2017)

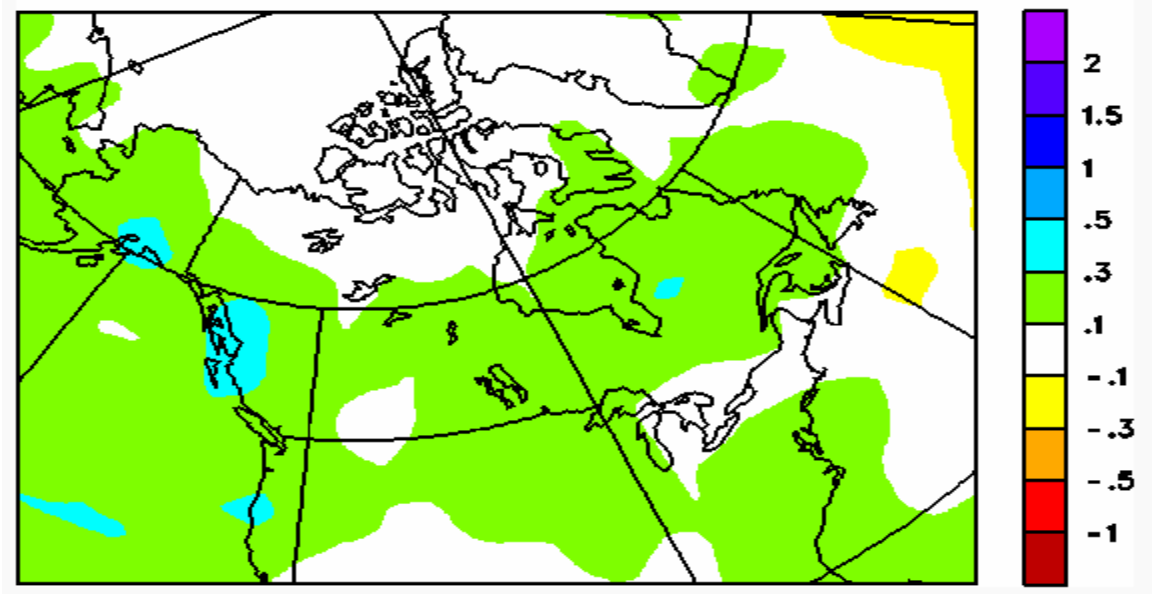

Figure 2.12 Projected change in 5-year mean precipitation rate (mm/day) in 2055 relative to 1981-2000 as simulated by CGCM3/T47 in the IPCC SRES B1 experiment. (Environment and Climate Change Canada, 2017)

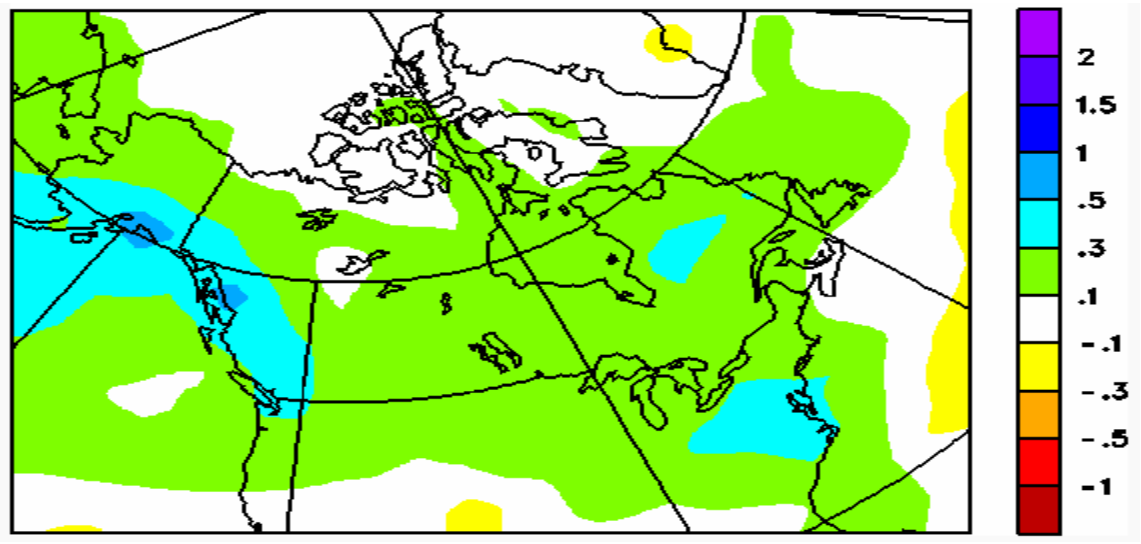

Figure 2.13 Projected change in 5-year mean precipitation rate (mm/day) in 2055 relative to 1981-2000 as simulated by CGCM3/T47 in the IPCC SRES A2 experiment. (Environment and Climate Change Canada, 2017)

2.6 Historical Climate and Projected Changes for Ontario

Scientists have studied Ontario's historical climate and have projected future climate using Canadian regional climate models as well as global climate models. Chiotti and Lavander (2008) projected the seasonal changes in mean temperature in the 2050's compared with 1961 to 1990 based on a median of seven global climate models (GCMs) and SRES A1F1 to B2. Ontario climate is changing and will witness an increase in mean temperature and precipitation in the coming decades. (Chiotti & Lavender, 2008)

Temperature increases in Ontario were significant in several locations during the 20th century. For example, the average annual temperature near Belleville in Ontario on the north shore of Lake Ontario has increased by 1.14°C since 1921 (Lemieux et al. 2007). In northwestern Ontario, east of Sioux Lookout, the average annual temperature has increased by 1.19°C since 1930. Significant warming in northeastern Ontario has also occurred. Since 1938, the average annual temperature

north of Sudbury has increased by 1.14°C, and along the James Bay coastline, the average annual temperature has increased 1.24°C since 1895 (Lemieux et al. 2007). Warming has been more significant in winter and spring and is believed to have contributed to changes in evaporation rates, less snowfall, more rainfall, and shorter periods with ice cover (Lemieux et al. 2005, Vincent and Mekis 2005). Figure 2.14 shows projected annual temperature difference between 1971 and 2000 and 2071-2100 following the A2 scenario for Ontario.

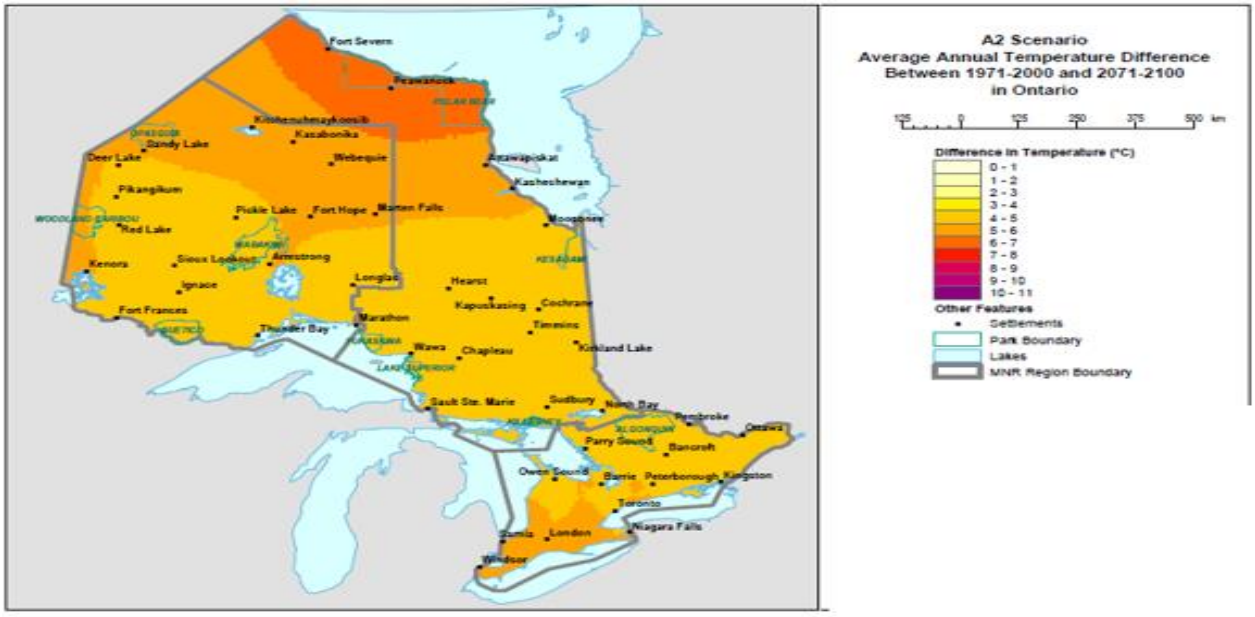

Figure 2.14 Projected change in average annual temperature in Ontario in 2071 to 2100 compared to 1971 – 2000 using the A2 scenario in the Canadian Coupled Global Climate model. (Colombo et al, 2007)

Precipitation has also been on the increase in Ontario in the past decades, Colombo et al. (2007) reported that even though winter season precipitation is on a reducing trend, warm season precipitation and average annual precipitation will increase by up to 20% by 2071 to 2100 compared to 1971 to 2000 for the investigated scenarios.

2.7 Climate Change and Infrastructure

Researchers over the years have recognized the impacts of climate change on infrastructures and emphasized the need to evaluate the severity of the infrastructure vulnerability and impacts. Research has also shown that threats are posed to both existing and future infrastructures. The current and potential impacts of climate change on infrastructure include both beneficial and detrimental effects (Research & Analysis Division Infrastructure Canada, 2006). Flooding is an example of detrimental effects, which causes scouring and in some cases, total bridge washouts. (Wright et al, 2012) evaluated the impact of climate change on bridge performance associated with climate change and submitted that although many bridges are already vulnerable to scour, incremental vulnerability is caused because of climate change.

With building infrastructures, material deterioration and flooding are of major concern, concrete, steel and wood that are the main materials for building infrastructure are sensitive to climate change. More carbon dioxide in the atmosphere is a problem to reinforced concrete whose deterioration may occur as a direct result of carbonation. Atmospheric humidity will impact steel buildings in terms of corrosion rate while the wood structures and products will rot in moist environments. Overall, climate change will cause the rate of material deterioration to be exacerbated.

2.8 Climate Change Impact and Risk Assessment For Civil Infrastructure

Before any meaningful discussion can be carried out on climate change adaptation, a risk assessment framework must be developed. This helps in assessing vulnerabilities and impending hazards that adaptation measures are implemented as a mitigation strategy. It is imperative to assess the risk of climate change impact on each particular type of infrastructure. These risks assessment may be defined or carried out based on:

2.8.1 Extreme Events Risk Assessment

This requires an assessment of extreme events that may occur due to climate change and its impacts. According to intergovernmental panel on climate change reports, the following extreme climate changes are expected: drought periods increase, the extreme hot temperature increase in

intensity and temporal occurrence, the number of days of heat wave increase, extreme precipitation increase in intensity, the number of days with snowfall decrease. Moreover, extreme events: forest fires, flooding, ground movements, temporary sea flooding, biodiversity (avifauna corridors evolutions, algal blooms in waterways), etc., are likely to evolve. (Marie et al, 2016).

A list of these extreme events should be made and scores assigned to them based on intensity and frequency of occurrence.

2.8.2 Physical Vulnerability Risk Assessment

This is a physical assessment based on factors such as the age of the infrastructure, materials, expected lifetime, design rules or localization. It is also of importance to consider extreme events the infrastructure has faced in the past for existing infrastructures. A scoring regime should be developed for this assessment. Physical vulnerability should consider both ultimate and serviceability limits of failure of the specific infrastructure.

2.8.3 Functional Vulnerability Risk Assessment

Civil infrastructure supports different types of functionalities, for example, transportation infrastructure supports crucial functionalities such as rescue services, firemen or police access, evacuation of persons; accessibility functionalities, such as food and health centers and common functionalities such as goods and passengers common transport services (Marie et al, 2016)

Functional vulnerability refers to the loss of functionality that may occur in the event of an extreme weather event. Functional vulnerability risk assessment is the analysis of the expected impacts on services that would be affected, for example, destruction of a hospital access road may not directly cause death but the delay in reaching a health facility due to detours may cause death, or permanent disabilities.

Extreme climate event’s impact on functionalities of transport network will include degradation of the quality of service, capacity, increase in cost and time and even vehicle deterioration.

2.8.4 Total risk assessment

The total risk assessment is determined by the combination of risk scores of the extreme events, functional vulnerabilities, and physical vulnerabilities. This risk level or score forms the baseline or metrics on which adaptation strategies are developed. Each type of risk assessment should be carried out using a risk matrix as shown in Figure 2.15. Each extreme event should be analyzed. The risk for a particular event is the product of the probability of occurrence and the severity. Immediate adaptation strategies must be developed for events with high-risk values.

Impact / Probability		A	B	C	D	E
		Negligible	Minor	Moderate	Significant	Severe
E	Very Likely	Low Med	Medium	Med Hi	High	High
D	Likely	Low	Low Med	Medium	Med Hi	High
C	Possible	Low	Low Med	Medium	Med Hi	Med Hi
B	Unlikely	Low	Low Med	Low Med	Medium	Med Hi
A	Very Unlikely	Low	Low	Low Med	Medium	Medium

Figure 2.15 Typical risk matrix for an extreme event scenario

2.9 Mechanism of Climate Change Impact on Bridge Infrastructure

Climate change will affect transport infrastructure and bridge infrastructure in particular by exacerbating the standard bridge deterioration mechanisms, and these include material deterioration and structural failures due to increased loadings. These mechanisms will include carbonation, chloride penetration which ultimately leads to corrosion of steel and scouring which undermines the integrity of the bridge foundation.

Most river bridges are constructed with materials such as steel, concrete and wood either in combinations as composite as in reinforced and pre-stressed concrete bridges or as stand-alone as

in steel and wooden bridges. All these materials react to elements of climate and will be impacted by change in climate since their designs and construction are based on inputs which includes climate characteristics such as temperature, relative humidity and atmospheric pollution. Corrosion, a widespread cause of deterioration in bridges containing steel causes material loss and if not treated, increasing corrosion damage may lead to reduced safety, premature in-service failures as well as altered structural behavior and failure modes (Kallias and Imam, 2013). Exposure design conditions of these structures are directly dependent on climate parameters and a change in these exposure conditions will cause changes in deterioration process.

2.9.1 Carbonation-Induced Corrosion

Carbonation is a phenomenon, which occurs in concrete as a result of the dissolution of carbon di-oxide (CO_2) in the concrete pore fluid to form carbonic acid (H_2CO_3). This reacts with calcium from calcium hydroxide and calcium silicate hydrate present in the concrete to form calcium carbonate ($CaCO_3$).

$$CO_2 + H_2O \leftrightarrow H_2CO_3 \quad (2.1)$$

$$H_2CO_3 + Ca(OH)_2 \rightarrow CaCO_3 + 2H_2O \quad (2.2)$$

The presence of $Ca(OH)_2$ in concrete gives it a PH value of about 12.5. The highly alkaline environment of concrete creates a protective, passivating oxide layer around steel when present in the concrete protecting the reinforcement from corrosion. Carbonation of concrete reduces a concrete's pH to a value less than 9, which weakens, or could even eliminate the steel's protective layer and herald the process of corrosion. It should be noted that carbonation gradually propagates from the concrete surface towards the reinforcement and when carbonation depth equals the concrete cover, corrosion of the reinforcement starts.

Carbonation depth depends on many parameters such as concrete quality, concrete cover, relative humidity, ambient carbon dioxide concentration and others. Many researchers have studied the impact of carbonation and various mathematical models have been developed with the purpose of predicting carbonation depths. Stewart, et al. (2011) showed that climate change, which is associated with increased level of carbon di-oxide in the atmosphere and increased atmospheric temperatures effectively accelerates the deterioration of concretes containing steel reinforcements.

Figure 2.16 shows a section of a reinforced concrete structure that is undergoing degradation by corrosion and spalling induced by carbonation

Figure 2.16 Corrosion and spalling induced by carbonation (Xiaoming et al. 2010)

2.9.2 Chloride-induced Corrosion

Steel bars used as reinforcement in concrete are covered by a thin passive layer of oxide that protects them from oxygen and water, which causes corrosion and the production of rust when they get to the steel, as shown in Figure 2.17. This passive layer can only be maintained at an alkaline pH values i.e. pH>12 or at a chloride ion content less than a corrosion threshold. When chloride ions penetrate the concrete and then accumulate to a critical level on the surface of steel reinforcement, the protective layer is destroyed in a process known as de-passivation. (Xiaoming, et al, 2010). This causes an electrochemical cell to be formed. Figure 2.17 shows the Electrochemical cell at rebar surface induced by chloride penetration.

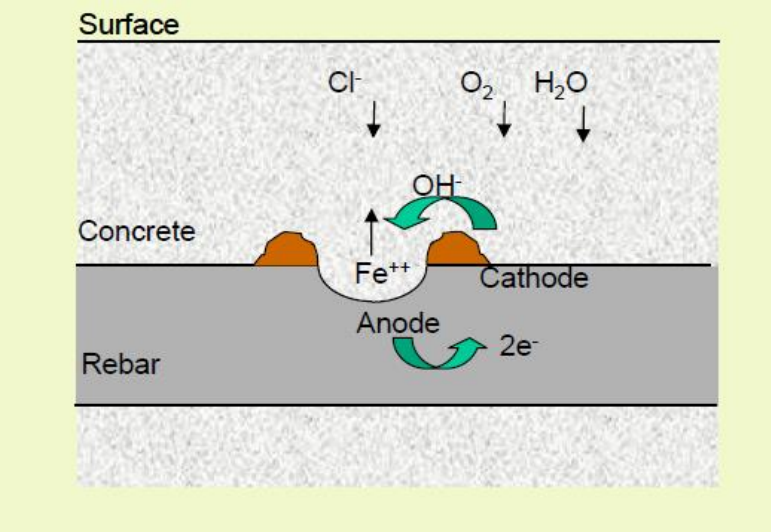

Figure 2.17 Electrochemical cell at rebar surface induced by chloride penetration (Xiaoming et al., 2010)

The chemical reactions for chloride-induced corrosion at the steel surface involves the following reaction as shown by Xiaoming, et al. (2010).

$$Fe^{++} + 2Cl^{-} \rightarrow FeCl2 \quad (2.3)$$

$$FeCl2 + 2H2O \rightarrow Fe(OH)2 + 2HCl \quad (2.4)$$

The de-passivated area becomes an anode, while the passivated surface becomes a cathode. At the anode of the cell, the reaction is described by:

$$Fe \rightarrow Fe^{++} + 2e^{-} \quad (2.5)$$

$$Fe^{++} + 2(OH)^{-} \rightarrow Fe(OH)_2 \quad (2.6)$$

$$4Fe(OH)_2 + 2H_2O + O_2 \rightarrow 4Fe(OH)_3 \quad (2.7)$$

and the reaction at the cathode is given by:

$$4e^{-} + O_2 + 2H_2O \rightarrow 4(OH)^{-} \quad (2.8)$$

During the corrosion process, two major rust and corrosion products are $Fe(OH)_2$ (ferrous hydroxide) and $Fe(OH)_3$ (ferric hydroxide).

Figure 2.18 Corrosion of steel reinforcement in concrete Structures (Xiaoming et al., 2010)

Chlorides induced corrosion depends on three main factors which are diffusion coefficient of concrete, surface chloride concentration and critical chloride level beyond which corrosion of reinforcement will be initiated. (Xiaoming, et al. 2010). The coefficient of diffusion depends on the microstructure of the concrete.

Climate change will hence speed up chloride-induced corrosion as it is associated with increased carbon dioxide and carbonation which affects the concrete micro structure. Saeki (2002) studied the effect of carbonation on chloride penetration of concrete and submitted that chloride penetrated is accelerated in carbonated concrete.

2.9.3 Scouring

Scouring refers to the erosion of bed material around structures such as abutments and piers caused by water flowing around the structure. It occurs when more sediment material is transported out of an area than into it. Bridge piers or other obstacles that obstruct the flow and cause a change to the flow field initiate the scouring process. The material on the bed and banks of a river erodes when the drag and uplift forces from the flow exceed those of gravity on the bed materials, friction

and cohesion. The depth and extent of scour depends on many factors such as the water flow, size and shape of the obstruction and type of sediment material. Different materials erode at varying speeds. it will take longer for a cohesive soil to erode than for a loose granular soil due to cohesive and Van der Waal forces, but the final scour depth can be the same in both types of soils (Chase and Holnbeck, 2004).

The total scour at a bridge consists of three components; long-term aggradation and degradation, general scour and local scour. With climate change, increased precipitation intensity and extremes, which is usually associated with flooding is bound to increase scouring at bridge foundations and jeopardizing the stability of bridges.

2.9.3.1 Clear-Water and Live Bed Scour

The two different types of sediment transport mechanisms are clear-water and live-bed scour. Clearwater scour occurs when there is no transportation of sediment from upstream of the bridge or the sediment being transported remains in suspension and is not deposited into the scour-hole.

Live-bed scour, also known as continuous sediment transport scour, occurs when sediment material is being transported into the area from upstream during the scour process. The equilibrium state is dynamic, and the scour depth oscillates non-periodically as bed material is being transported in and out of the scour hole. The equilibrium state for this type of sediment transportation is reached faster than for clear-water scour. The scour depth at a certain pier is about ten percent greater in a clear-water situation compared to a live-bed situation (Chase and Holnbeck, 2004). Clear water scour tends to occur at a slower rate than that of the live-bed scour.

2.9.3.2 Long-Term Aggradation and Degradation

Aggradation and degradation are long-term changes to the elevation of a streambed. Aggradation means that sediment is brought into the area from upstream and is being deposited at the downstream. This causes a rise in the bed elevation of the downstream. Degradation refers to situations when the bed materials are being transported away resulting in a decrease in elevation of the stream or riverbed. These changes can be either a natural trend of the river or a result of some man-made modifications of the stream.

2.9.3.3 General Scour

General scour is when the streambed lowers due to changes in the water flow caused by flow through a contraction or around a bend. This type of scour can lead to various scour depths at different parts along the cross-section or it can result in to a uniform lowering of the streambed. The difference between general scour and long-term degradation is that the general scour can be a cyclic process. Contraction scour occurs when the available flow area decreases. This happens at a bridge if the piers are placed in the river or the abutments are placed at the bank lines or in the river resulting in a decrease in flow area and causes an increase in flow velocity. The increased velocity causes an increase of erosive forces and the streambed starts to erode. As the bed elevation is lowered the available flow area increases and the flow velocity and scour decrease until equilibrium state is reached.

2.9.3.4 Local Scour

Local scour around bridge piers is the result of the acceleration of the flow and formation of vortices around the piers. As the flow is interrupted a strong pressure field decreasing with the depth is formed in front of the obstruction. If the pressure field is strong enough, it causes a three-dimensional separation of the boundary layer. It drives the approaching flow downwards, and a recirculating primary vortex is formed on the upstream side of the pier. As the flow passes through the bridge, the vortices wrap around the sides of the piers in the shape of a horseshoe and continue downstream. This is called a horseshoe vortex

The primary vortex system in front of the pier is the main scour force, and it removes bed material from the base of the pier. Since the rate at which material is carried away from the area is greater than the transport rate into it, a scour hole is formed around the pier. As the scour hole gets deeper the strength of the vortices at the base of the pier decrease and eventually a state of equilibrium is reached. For a clear-water situation that happens when the shear stress from the vortices equals the critical stress for the sediment particles, and no more bed material is scoured. For a live-bed situation, equilibrium is reached when the amount of sediment inflow equals the amount of outflow from the scour hole. In that situation, the scour depth fluctuates, while the average depth remains constant.

The horseshoe vortices act mainly on the upstream face and the sides of a pier, whereas on the downstream side of the pier another type of vortices dominate, called wake vortices. They are formed along the surface of the pier, then detached from both sides and continue downstream The wake vortices together with the accelerated side flow and the upward flow behind the pier causes the downstream scouring. The pier itself generates the wake vortices, and their size and strength depend mainly on the velocity of the flow and the pier size and shape. The strength of a wake vortex declines rapidly downstream of a pier and therefore there is often a deposit of material downstream of piers (Chase and Holnbeck, 2004).

2.9.4 Extreme weather events

The focus of earlier climate model studies of global warming was mainly on changes in mean climate. It has been only since the early 1990s that climate models have started to be analyzed to study possible changes of future weather and climate extremes (Meehl et al., 2000).

There is also clear evidence of changes in extremes of precipitation. For the contiguous United States and Canada. Kunkel et al. (2003) and Groisman et al. (2008) find statistically significant increases in heavy (upper 5%) and very heavy (upper 1%) precipitation by 14% and 20%, respectively. Much of this increase occurred during the last three decades of the century especially over the eastern parts of United States. Groisman et al. (2008) showed that even as the top 0.3% of heavy rains has increased by 27% from 1967 to 2006, so have dry spells increased in most places. Also, there is evidence for Europe and the United States that the relative increase in precipitation extremes is larger than the increase in mean precipitation, and this is manifested as an increasing contribution of heavy events to total precipitation (Alexander et al., 2006). Globally-averaged over the land area with sufficient data, the percentage contribution to total annual precipitation from very wet days (upper 5%) has increased in the past 50 years even in places where mean precipitation amounts are not increasing (Kunkel et al. (1999).

Flooding records are often confounded by changes in land use and increasing human settlement in flood plains. Nevertheless, great floods have been found to be increasing in the twentieth century (Paasche and Storen, 2014).

3 Current Research

To investigate the structural impact of climate change on river bridge infrastructure, a bridge on the Ottawa river was used as a case study to demonstrate the utilization of the finite element modelling and analysis to investigate the response of the bridge and how the bridge can be adapted to the structural impacts of climate change.

3.1 Portage Bridge

The Portage bridge is a bridge on the Ottawa River. It crosses the river downstream of the Chaudiere bridge. It is the link between Laurier street and Alexander-Tache boulevard. The bridge was completed and opened in 1973 by the National Capital Commission. The Portage bridge is 160 meters long.

The Ottawa river is a river in the Canadian provinces of Ontario and Quebec. For most of its length, it defines the border between the two provinces. It is a major tributary of the St. Lawrence River. The river rises at Lake Capimitchigama, in the Laurentian Mountains of central Quebec, and flows west to Lake Timiskaming. From there its route has been used to define the interprovincial border with Ontario. From Lake Timiskaming, the river flows southeast to Ottawa and Gatineau, where it tumbles over the Chaudière Falls and further takes in the Rideau and Gatineau rivers.

The Ottawa River drains into the Lake of Two Mountains and the St. Lawrence River at Montreal. The river is 1,271 kilometers long. it drains an area of 146,300 square kilometers, 65 percent in Quebec and the rest in Ontario, with a mean discharge of 1,950 cubic meters per second. The average annual mean water-flow measured at Carillon dam, near the Lake of Two Mountains, is 1,939 cubic meters per second with average annual extremes of 749 to 5,351 cubic meters per second. Record historic levels since 1964 are a low of 529 cubic meters per second in 2005 and a high of 8,190 cubic meters per second. Figure 3.1 shows a stretch of Ottawa river showing portage bridge.

Figure 3.1 Stretch of Ottawa River Showing Portage Bridge and MacDonald-Cartier Bridge

3.2 Methodology for the present study

Precipitation and flood level historical data for the study area was obtained from the Ottawa River Regulation Planning Board, data included the historical water levels and discharges along the Ottawa river at Lake Timiskaming, Mattawa, Pembroke, Lake Coulonge, Arnprior, Britannia, Hull, Grenville and Carillon. These flood data were used to determine the 1:100- year flood discharge of the basin. A 20% increase in discharge was determined to simulate the likely increase in flood levels due to climate change as projected for the basin. These data were used for hydraulic analysis to derive the channel velocity, inundation depths and scour depths around bridge piers in a flood event. The flood data is included in Appendix 2.

Results of the hydraulic analysis, which were Stream Velocity (m/s), Scour depth (m) and flood levels (inundation depths) (m) were then used in a structural model alongside other structural loads to determine the response of bridges along the basin.

3.3 Hydraulic analysis

Digital elevation models (DEM) for the study area which were derived from LIDAR data was obtained from the United States Geological Survey (USGS) for the purposes of this study. The

DEMs were processed into Triangulated irregular network maps (TIN) and cross sections, stream center line, river bank and over banks were digitized using ArcGIS software version 10.4.1. The purpose of these is to create a dataset compatible with HEC-RAS which was used for the hydraulic analysis and scour prediction.

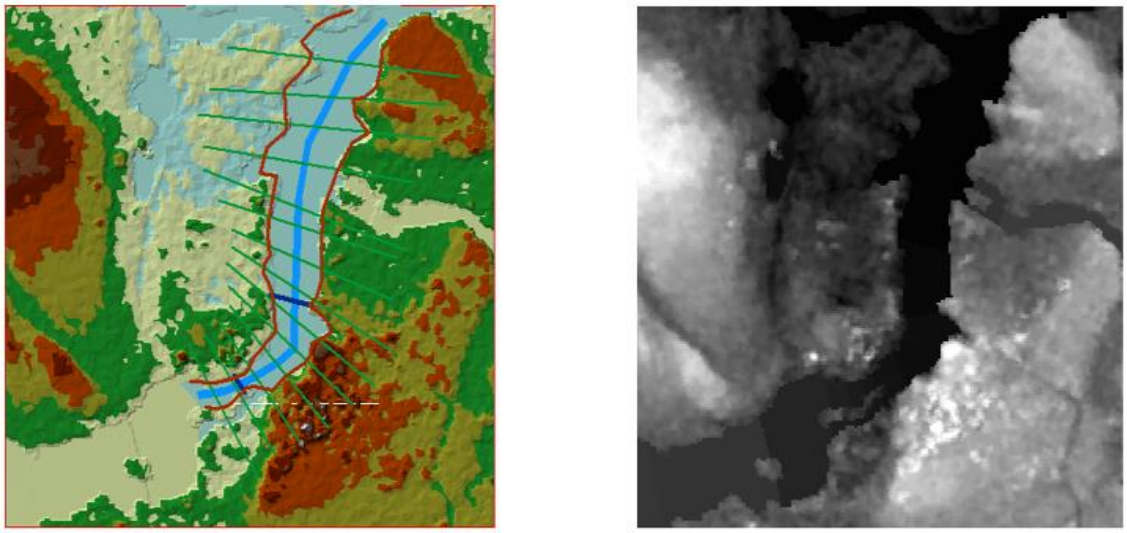

Figure 3.2 Digital Elevation map (DEM) of study area showing heights above sea level. (source: USGS)

The HEC-RAS (version 5.0.3) is a software developed by the US Army Corps of Engineers (USACE, 2016). It uses the backwater calculation procedure as HEC-2 (USACE, 1990) which has been the industry standard in flood water hydraulic modelling but with improved data processing and graphical capabilities. (Ferdous, et al. 2014). A steady-state hydraulic model was then developed in HEC-RAS using the data set and cross sections generated in ArcGIS as imported inputs. In total, twenty-one cross sections and the bridge site was included in the analysis. The final model was run with the estimated flood discharges for a 100-year storm, which is the standard used in bridge designs. Additional runs were conducted for 100-year plus 20% to simulate the projected increase in precipitation due to climate change at the portage bridge site on the Ottawa River. Figure 3.3 and

Figure 3.4 show hydraulic analysis output for the basin for a 100-year storm at upstream and downstream cross-section of the bridge respectively while Figure 3.5 and Figure 3.6 show the

hydraulic analysis results for 100-year 100 plus 20% increase in discharge due to climate change respectively.

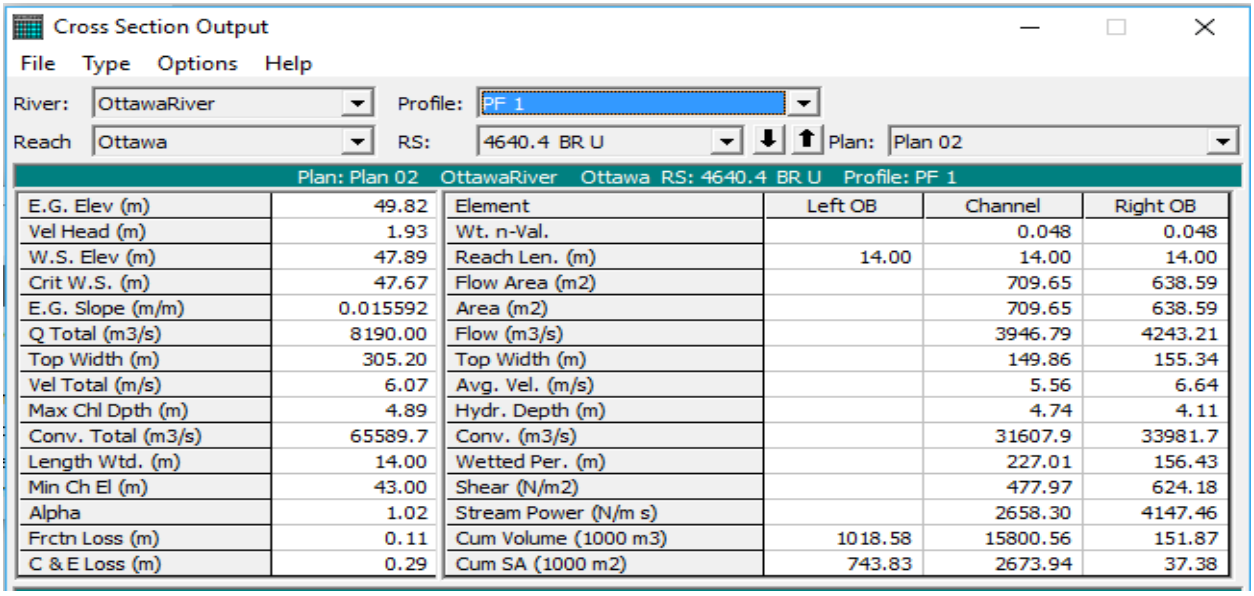

Cross Section Output

File Type Options Help

River: OttawaRiver Profile: PF 1

Reach Ottawa RS: 4640.4 BR U Plan: Plan 02

Plan: Plan 02 OttawaRiver Ottawa RS: 4640.4 BR U Profile: PF 1

		Element	Left OB	Channel	Right OB
E.G. Elev (m)	49.82	Wt. n-Val.		0.048	0.048
Vel Head (m)	1.93	Reach Len. (m)	14.00	14.00	14.00
W.S. Elev (m)	47.89	Flow Area (m2)		709.65	638.59
Crit W.S. (m)	47.67	Area (m2)		709.65	638.59
E.G. Slope (m/m)	0.015592	Flow (m3/s)		3946.79	4243.21
Q Total (m3/s)	8190.00	Top Width (m)		149.86	155.34
Top Width (m)	305.20	Avg. Vel. (m/s)		5.56	6.64
Vel Total (m/s)	6.07	Hydr. Depth (m)		4.74	4.11
Max Chl Dpth (m)	4.89	Conv. (m3/s)		31607.9	33981.7
Conv. Total (m3/s)	65589.7	Wetted Per. (m)		227.01	156.43
Length Wtd. (m)	14.00	Shear (N/m2)		477.97	624.18
Min Ch El (m)	43.00	Stream Power (N/m s)		2658.30	4147.46
Alpha	1.02	Cum Volume (1000 m3)	1018.58	15800.56	151.87
Frctn Loss (m)	0.11	Cum SA (1000 m2)	743.83	2673.94	37.38
C & E Loss (m)	0.29				

Figure 3.3 Hydraulic analysis result table for 100-year return period of portage bridge site

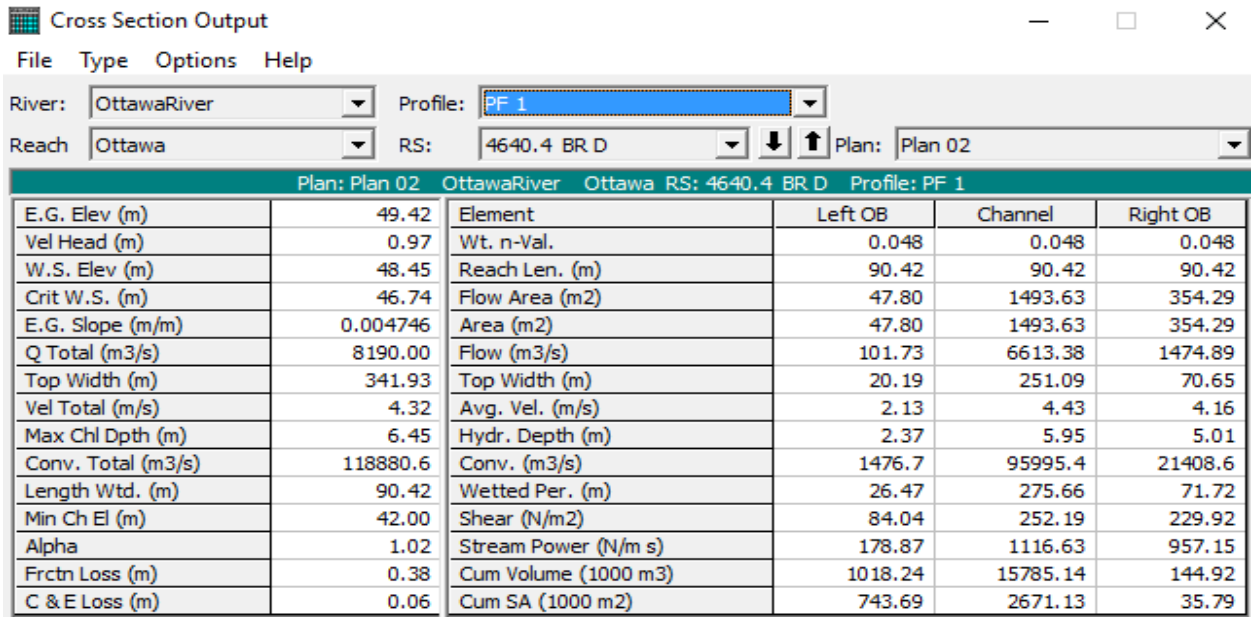

Cross Section Output

File Type Options Help

River: OttawaRiver Profile: PF 1

Reach Ottawa RS: 4640.4 BR D Plan: Plan 02

Plan: Plan 02 OttawaRiver Ottawa RS: 4640.4 BR D Profile: PF 1

		Element	Left OB	Channel	Right OB
E.G. Elev (m)	49.42	Wt. n-Val.	0.048	0.048	0.048
Vel Head (m)	0.97	Reach Len. (m)	90.42	90.42	90.42
W.S. Elev (m)	48.45	Flow Area (m2)	47.80	1493.63	354.29
Crit W.S. (m)	46.74	Area (m2)	47.80	1493.63	354.29
E.G. Slope (m/m)	0.004746	Flow (m3/s)	101.73	6613.38	1474.89
Q Total (m3/s)	8190.00	Top Width (m)	20.19	251.09	70.65
Top Width (m)	341.93	Avg. Vel. (m/s)	2.13	4.43	4.16
Vel Total (m/s)	4.32	Hydr. Depth (m)	2.37	5.95	5.01
Max Chl Dpth (m)	6.45	Conv. (m3/s)	1476.7	95995.4	21408.6
Conv. Total (m3/s)	118880.6	Wetted Per. (m)	26.47	275.66	71.72
Length Wtd. (m)	90.42	Shear (N/m2)	84.04	252.19	229.92
Min Ch El (m)	42.00	Stream Power (N/m s)	178.87	1116.63	957.15
Alpha	1.02	Cum Volume (1000 m3)	1018.24	15785.14	144.92
Frctn Loss (m)	0.38	Cum SA (1000 m2)	743.69	2671.13	35.79
C & E Loss (m)	0.06				

Figure 3.4 Hydraulic analysis result table for 100-year return period downstream at portage bridge site

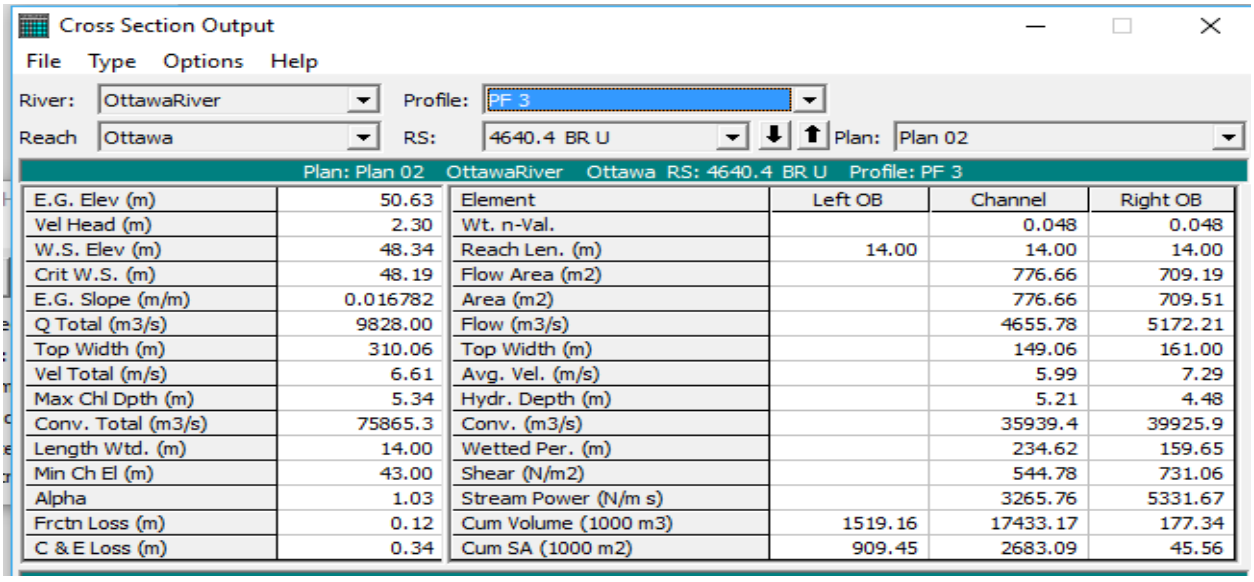

Cross Section Output

File Type Options Help

River: OttawaRiver Profile: PF 3

Reach Ottawa RS: 4640.4 BR U Plan: Plan 02

Plan: Plan 02 OttawaRiver Ottawa RS: 4640.4 BR U Profile: PF 3

		Element	Left OB	Channel	Right OB
E.G. Elev (m)	50.63				
Vel Head (m)	2.30	Wt. n-Val.		0.048	0.048
W.S. Elev (m)	48.34	Reach Len. (m)	14.00	14.00	14.00
Crit W.S. (m)	48.19	Flow Area (m2)		776.66	709.19
E.G. Slope (m/m)	0.016782	Area (m2)		776.66	709.51
Q Total (m3/s)	9828.00	Flow (m3/s)		4655.78	5172.21
Top Width (m)	310.06	Top Width (m)		149.06	161.00
Vel Total (m/s)	6.61	Avg. Vel. (m/s)		5.99	7.29
Max Chl Dpth (m)	5.34	Hydr. Depth (m)		5.21	4.48
Conv. Total (m3/s)	75865.3	Conv. (m3/s)		35939.4	39925.9
Length Wtd. (m)	14.00	Wetted Per. (m)		234.62	159.65
Min Ch El (m)	43.00	Shear (N/m2)		544.78	731.06
Alpha	1.03	Stream Power (N/m s)		3265.76	5331.67
Frctn Loss (m)	0.12	Cum Volume (1000 m3)	1519.16	17433.17	177.34
C & E Loss (m)	0.34	Cum SA (1000 m2)	909.45	2683.09	45.56

Figure 3.5 Hydraulic analysis result table for 100-year return period plus 20% increase in discharge upstream at portage bridge site

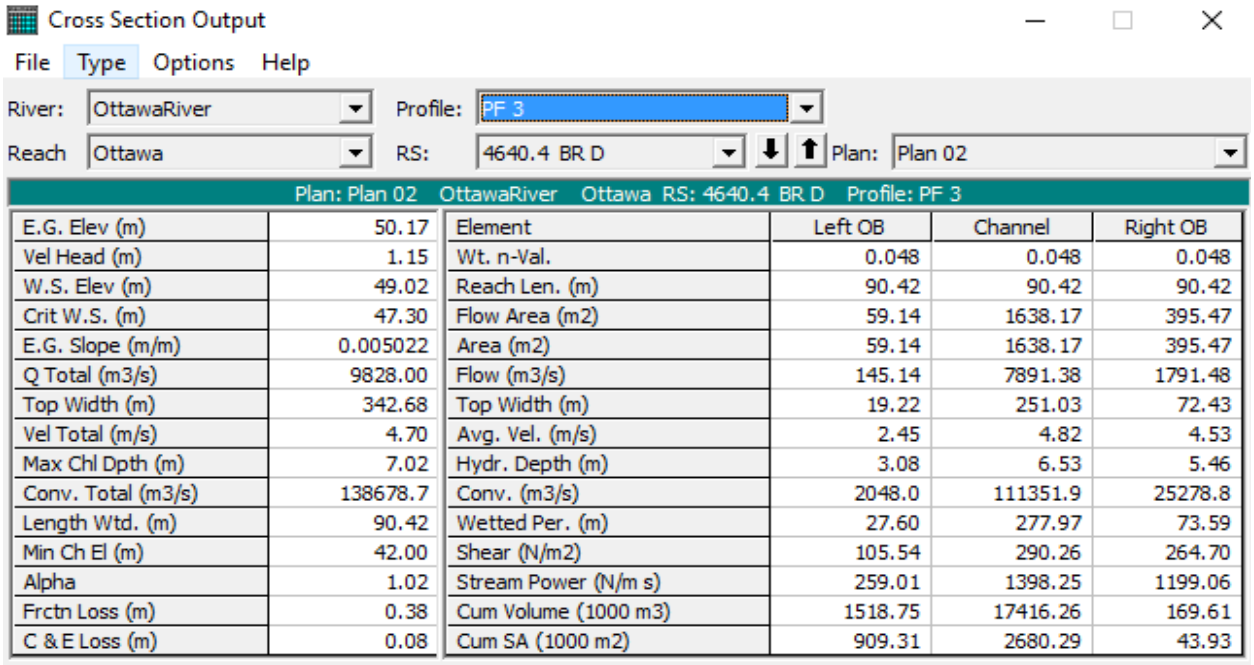

Cross Section Output

File Type Options Help

River: OttawaRiver Profile: PF 3

Reach Ottawa RS: 4640.4 BR D Plan: Plan 02

Plan: Plan 02 OttawaRiver Ottawa RS: 4640.4 BR D Profile: PF 3

		Element	Left OB	Channel	Right OB
E.G. Elev (m)	50.17				
Vel Head (m)	1.15	Wt. n-Val.	0.048	0.048	0.048
W.S. Elev (m)	49.02	Reach Len. (m)	90.42	90.42	90.42
Crit W.S. (m)	47.30	Flow Area (m2)	59.14	1638.17	395.47
E.G. Slope (m/m)	0.005022	Area (m2)	59.14	1638.17	395.47
Q Total (m3/s)	9828.00	Flow (m3/s)	145.14	7891.38	1791.48
Top Width (m)	342.68	Top Width (m)	19.22	251.03	72.43
Vel Total (m/s)	4.70	Avg. Vel. (m/s)	2.45	4.82	4.53
Max Chl Dpth (m)	7.02	Hydr. Depth (m)	3.08	6.53	5.46
Conv. Total (m3/s)	138678.7	Conv. (m3/s)	2048.0	111351.9	25278.8
Length Wtd. (m)	90.42	Wetted Per. (m)	27.60	277.97	73.59
Min Ch El (m)	42.00	Shear (N/m2)	105.54	290.26	264.70
Alpha	1.02	Stream Power (N/m s)	259.01	1398.25	1199.06
Frctn Loss (m)	0.38	Cum Volume (1000 m3)	1518.75	17416.26	169.61
C & E Loss (m)	0.08	Cum SA (1000 m2)	909.31	2680.29	43.93

Figure 3.6 Hydraulic analysis result table for 100-year return period plus 20% increase in discharge downstream at portage bridge site

The stream flow velocity at any point in time at any position is calculated by HEC-RAS using the manning's equation:

$$Q=VA=(1/n)\ AR^{2/3}\sqrt{S} \qquad (3.1)$$

Where:

Q = Flow Rate, (m^3/s)

v = Velocity, (m/s)

A = Flow Area, (m^2)

n = Manning's Roughness Coefficient

R = Hydraulic Radius, (m)

S = Channel Slope, (m/m)

3.4 Scour Depth Prediction

Several research studies have been carried out with the aim of predicting scour, and various equations have been developed. Khwairakpam et al. (2012) provided examples of such studies to include Laursen and Toch (1956), Liu et al. (1961), Shen et al. (1969), Breusers et al. (1977), Jain and Fischer (1984), Melville and Sutherland (1988), Froehlich (1989), Melville (1992), Abed and Gasser (1993), Richardson and Richardson (1994), Lim (1997) and Heza et al. (2007).

Most of these empirical equations were based on results of laboratory and field data, and they differ from one another based on the factors and parameters considered in constructing the scour model, laboratory or field conditions. Out of these equations, the most commonly used pier scour equations in the is the Colorado State University scour equation (Khwairakpam et al. 2012).

The scour depth was calculated using HEC -RAS. HEC RAS scour prediction model is based on the scour equation developed by Colorado State University and recommended by the U.S. Department of Transportation's Hydraulic Engineering Circular No. 18 (HEC-18), Federal Highway Administration (1993), which is expressed as follows:

$$ds = 2.0yK_1K_2K_3K_4b^{0.65}F^{0.43} \qquad (3.2)$$

where ds = scour depth,

y = flow depth at upstream of pier

K_1, K_2, K_3 K_4 = correction factors for pier nose shape, angle of attack, bed conditions and armouring respectively,

b = pier width,

F = Froude number.

It is recommended in the HEC-18 that the limiting value of ds/y is 2.4 for F = 0.8 and 3.0 for F greater than 0.8. The scour equation was developed from laboratory data and was recommended for both live-bed and clear-water conditions (USACE, 1990).

3.5 Finite Element Analysis

A finite element model of a bridge at the site of Portage bridge was developed and calibrated using the finite element analysis software STAAD Pro to simulate the existing bridge circumstances and design. The bridge was analyzed for loads based on the Canadian highway bridge design code. (CHBDC). The model conforms to the initial bridge geometry design to resist a 100-year flood, wind load and other antecedent loads such as dead and live loads.

The model was constructed to study the effect of increased scour depth and increased flood load on the existing bridge. The bridge model was idealized as a beam bridge which consists of a 250 mm reinforced concrete deck supported by 8 reinforced concrete girders spanning continuously over eight 20 m spans. The transverse width of the deck is 17 m and carries 4 lanes of highway each 3.5 m wide. On each extreme side is a shoulder of 1.5m wide each. The center to center spacing between girders is 2.143m with deck overhangs of 1.0m on either side. The girders are supported on beams of 800 mm by 1000 mm depths. Each beam is in turn supported on two 800mm diameter piers, and each has a length of 14.78m from the top of the pile cap. These piers are assumed to be fixed at the base. The girders at the two end spans were supported on roller supports to simulate the support found between the girders and abutment interface at end spans.

Figure 3.7 shows a 3d model of the bridge while

Figure 3.8 and Figure 3.9 shows the transverse and longitudinal sections respectively.

More runs of the models were carried out to study the response when the 100-year flood has increased by 20%. The results were then analyzed to determine their response to the increased flood and wind load. It is desired to check the capacity of these bridges to resist the added loads

and hence determine their safety. The STAAD.pro code input of finite element analysis is included in appendices 4 and 5.

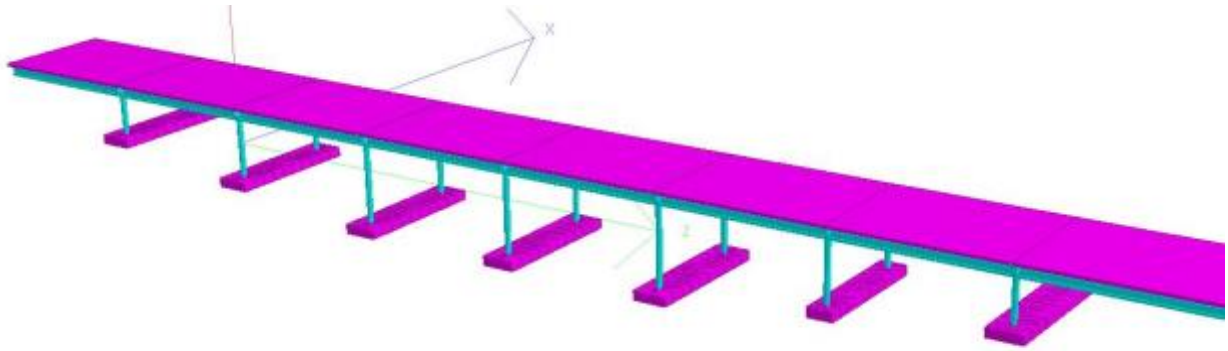

Figure 3.7 3D Model of Bridge Analysis section

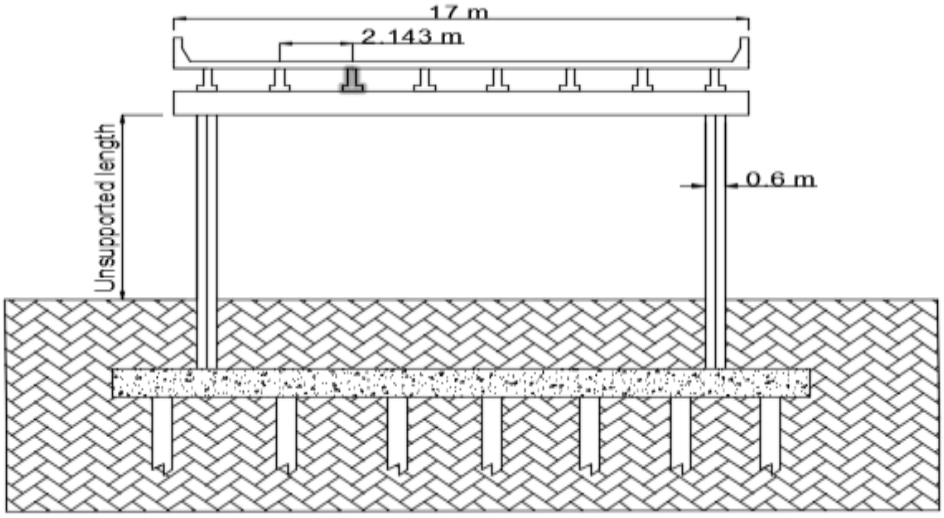

Figure 3.8 Transverse section of Bridge model

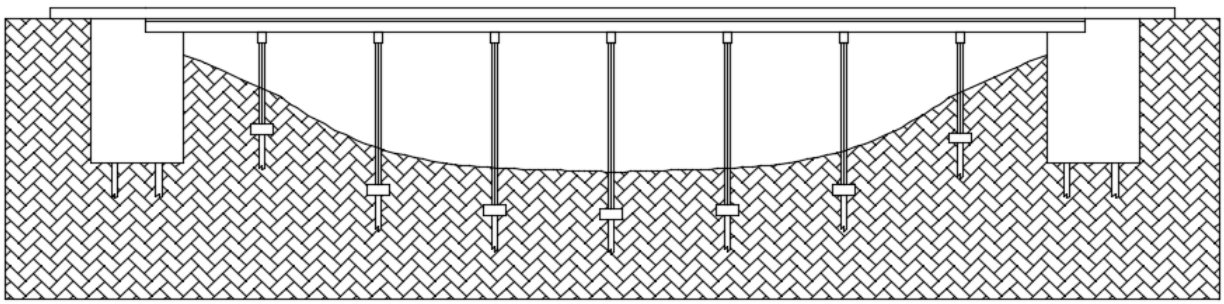

Figure 3.9 Longitudinal view of bridge model.

3.6 Loading

3.6.1 Dead Loads

Dead loads included the weight of all components of the structure and fixtures attached to the bridge, including wearing surface. Unit material weights as specified in Table 3.4 of Canadian Highway Bridge Design Code and reproduced as Table 3.1 in this report was used in calculating dead loads. The weight of water was considered as a dead load in line with the specifications of the CHBDC.

Table 3.1 Unit weights of construction materials (CSA, 2014)

Material	Unit weight, kN/m^3
Bituminous wearing surface	23.5
Reinforced concrete	24
Steel	77
Fresh water	9.8

3.6.2 Hydrostatic Pressure

Static water pressure is assumed to act perpendicular to the surface that is retaining the water (The piers). The pressure of water at a specific point is calculated as the product of the height of water above that point and the density of water.

Hydrostatic pressure = ρgh

where ρ = density;

g = acceleration due to gravity and

h= height of liquid.

3.6.3 Hydrodynamic Pressure

The hydrodynamic pressure, also called the longitudinal effect is the load due to flowing water acting longitudinally on an element and is taken as $C_D\rho Av^2/2$, where the longitudinal drag coefficient, C_D, is as specified in Table 3.11. of CHBDC and reproduced as

Table 3.2 in this report. Other parameters of the hydrodynamic effect are defined as follows:

ρ = density

L = length of a pier along the longitudinal axis

A = Area obstructing flow

V = Velocity of flow.

Table 3.2 Longitudinal drag coefficient (CSA, 2014)

Upstream shape of pier	Longitudinal drag coefficient, C_D
Semicircular nosed	0.7
Square ended	1.4
Wedged nosed < 90	0.8
Pier with debris lodged	1.4

Two profiles were investigated based on stream flow velocity for a 100-year flood and 100-year flood and 20% increase in discharge and a 100-year flood. The scour depth at each event was used to determine the section where the hydrodynamic pressure acts on. Figure 3.10 shows the idealized hydrodynamic pressure on piers. The two profiles are:

Profile 1- 100-year return flood

Flow velocity = 3.8 m/s

Submerged height = 10.5 m

Width of pier = 0.8 m

Pressure = $\frac{1000*11.12*0.8*0.7*3.8^2}{2} = 44.96kN$

Pressure over submerged height = 4.28 kN/m

Profile 2- 100-year return flood plus 20% increase in precipitation

Flow velocity = 3.99 m/s

Submerged height = 12.52 m

Width of pier = 0.8 m

Pressure = $\frac{1000*12.52*0.8*0.7*3.99^2}{2} = 55.8kN$

Pressure over submerged height = 4.46 KN/m

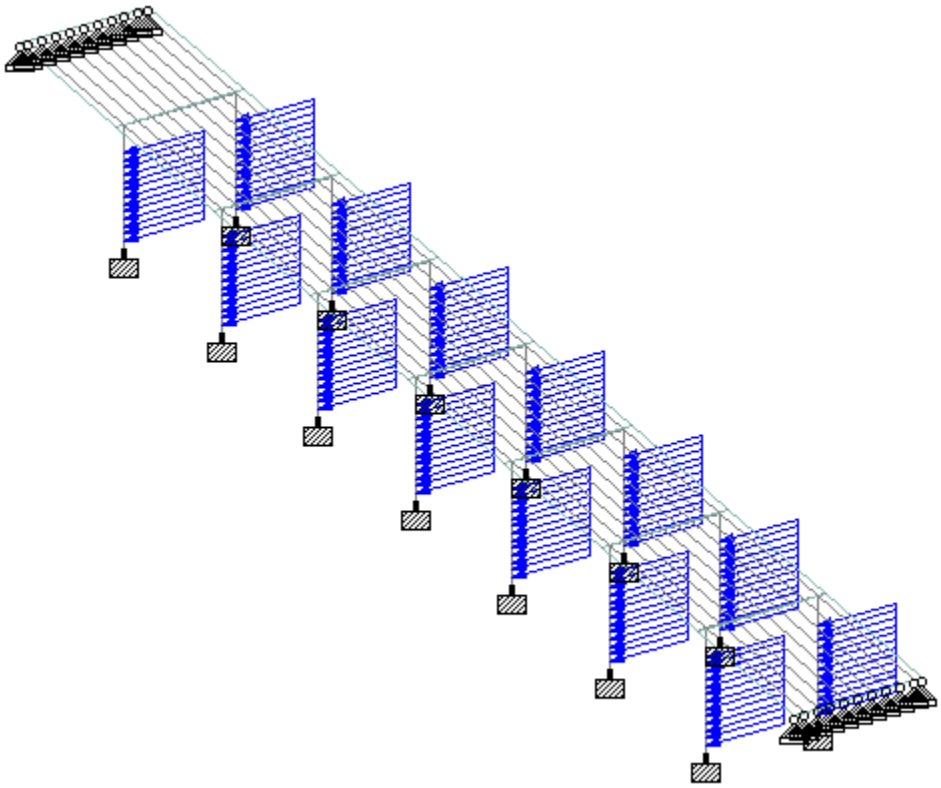

Figure 3.10 Hydrodynamic pressure on bridge piers

3.6.4 Wind Loads

Wind loads were divided into two components as horizontal drag load and vertical load acting simultaneously as specified by CHBDC.

3.6.5 Horizontal drag load

A horizontal wind load of $F_h = qC_eC_gC_h$ was applied to the bridge structure. *Fh* is horizontal wind load, *q* is Reference wind pressure, *Ce* is exposure coefficient and Cg is the gust effect coefficient. *Ce* and *q* are as specified in Tables in the CHBDC, Ce is reproduced here in Table 3.3. Cg = 2.5, *Ch* = 2.0 and the reference wind pressure for study area (Ottawa) is 460 Pa. $F_h = qC_eC_gC_h$

=0.46 x 1.2 x 2.5 x 2.0 = 2.76KN/m^2

Diameter of pier = 0.8m

Fh = 2.76 x 0.8 = 2.208 kN/m

The horizontal wind acts on the exposed portion of the bridge. Portions submerged in water do not experience the wind. Figure 3.11 shows the idealized wind pressure on the bridge piers.

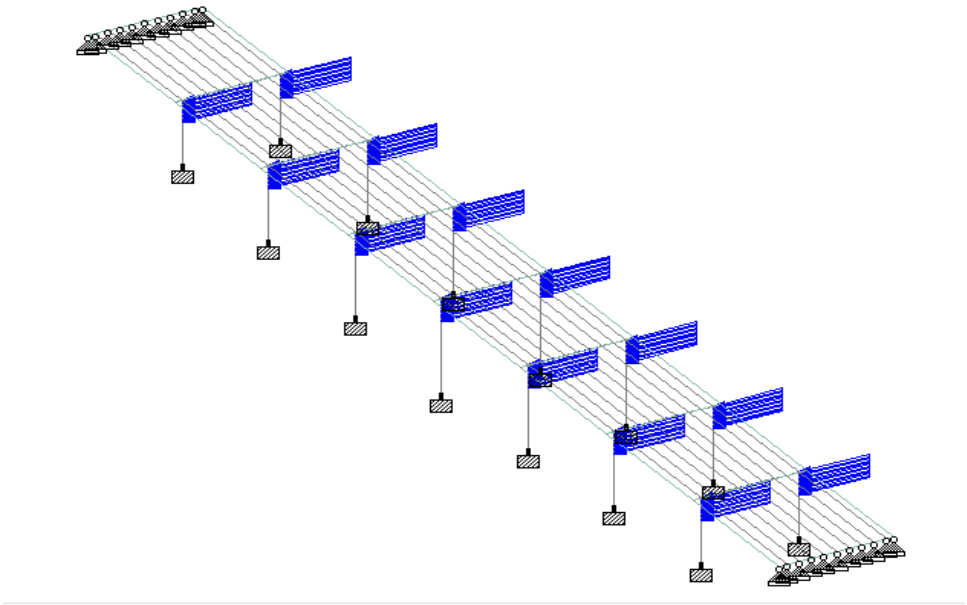

Figure 3.11 Idealized horizontal wind pressure on piers

3.6.6 Vertical Wind Load

A vertical wind is applied as a uniform distributed load over the whole surface of the bridge deck

$F_v = qC_eC_gC_v$, where F_v is vertical wind load, q is Reference wind pressure, C_e is exposure coefficient and C_g is the gust effect coefficient. C_e is as specified in Tables in the CHBDC and reproduced here in

Table 3.3 and C_g = 2.5 and C_v = 1.0.

An additional wind load of same value as Fv is applied as an equivalent line load at the windward quarter point of the transverse width of the deck in accordance with CHBDC

$F_v = qC_eC_gC_v$

q= 0.46 kN/m^2 (Ottawa average wind speed. Source CHBDC)

Fv = 1.2 x 2.5 x 1 x 0.46 =1.38 kN/m

Table 3.3 Wind exposure coefficient (CSA S6-14)

Height above ground of the top of the superstructure, H (m)	Wind exposure coefficient, C_e
0 – 10	1
Over 10 -16	1.1
Over 16 – 25	1.2
Over 25 – 37	1.3
Over 37 – 54	1.4
Over 54 – 76	1.5
Over 76 - 105	1.6

3.6.7 Traffic Loadings

3.6.7.1 Truck Loads

In this study, the bridge deck was loaded with the Canadian CL-W truck. A CL-W truck is the idealized five-axle vehicle as shown in Figure 3.12. Load values, wheel placement, and the lengths have been calibrated for a 625 kN truck, which is the legal limit in Canada. This truck is encompassed in a 3 x 3 m clearance envelope with 1.8 m wheel to wheel spacing as shown in Figure 3.13. The CL-W truck is positioned longitudinally and transversely within a design lane at the location and in the direction, that produces maximum load effect for the design of each bridge element.

3.6.7.2 Lane Loads

The CL-W lane load consists of a CL-W truck load with each axle reduced to 80% of the values given in Figure 6 superimposed with a 9 kN/m lane load applied over an area 3 m wide. As per Code specification. lane loads should not be applied where it reduces the overall load effects, lane loads were not applied in this model. Because girders are continuous over supports, application of the lane load over the entire superstructure would result in lower maximum positive bending moments at mid-spans.

3.6.8 Design Lane

This refers to a longitudinal strip that is a fraction of the deck width and within which a truck or lane load is placed for the purpose of design or evaluation. This model consists of 4 design lanes each 3m in width. The code specifies that when multiple lanes are loaded on a highway bridge, a load reduction factor should be applied to account for the probability of all lanes not being loaded at the same time.

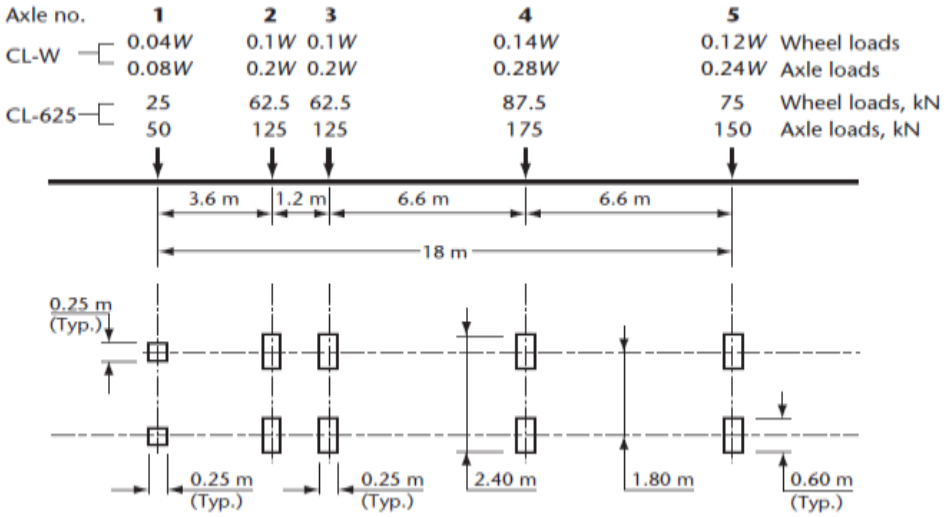

Figure 3.12 CL-W loading (CSA,2014)

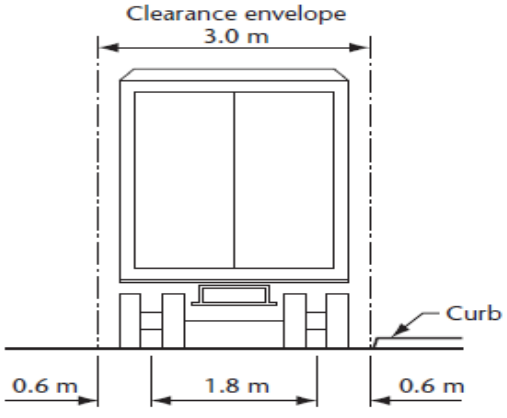

Figure 3.13 Cl-W Load Envelope (CSA, 2014)

3.6.9 Load combinations

Nine ultimate load combinations were investigated as per CHBDC specifications to determine the governing load case for design. Table 3.4 below shows the load combinations.

Table 3.4 Ultimate Load combinations (CSA, 2014)

Ultimate limit states Loads	D	E	P	L	K	W	V	S	EQ	F	A	H
ULS Combination 1	α_D	α_E	α_P	1.7	0	0	0	0	0	0	0	0
ULS Combination 2	α_D	α_E	α_P	1.7	1.15	0	0	0	0	0	0	0
ULS Combination 3	α_D	α_E	α_P	1.7	1	0.45	0.45	0	0	0	0	0
ULS Combination 4	α_D	α_E	α_P	0	1.25	1.4	0	0	0	0	0	0
ULS Combination 5	α_D	α_E	α_P	0	0	0	0	0	1	0	0	0
ULS Combination 6	α_D	α_E	α_P	0	0	0	0	0	0	1.3	0	0
ULS Combination 7	α_D	α_E	α_P	0	0	0.75	0	0	0	0	1.3	0
ULS Combination 8	α_D	α_E	α_P	0	0	0	0	0	0	0	0	1
ULS Combination 9	1.35	α_E	α_P	0	0	0	0	0	0	0	0	0

Table 3.4 legend:

A = ice accretion load;

D = dead load;

E = loads due to earth pressure and hydrostatic pressure, including surcharges but excluding dead load;

EQ = earthquake load;

F = loads due to stream pressure and ice forces or to debris torrents;

H = collision load arising from highway vehicles or vessels;

K = all strains, deformations, and displacements and their effects, including the effects of their restraint and the effects of friction or stiffness in bearings, also, strains and deformations include strains and deformations due to temperature change and temperature differential, concrete shrinkage, differential shrinkage, and creep, but not elastic strains;

L = live load (including the dynamic load allowance, when applicable), including barrier loads; *P* = secondary pre-stress effects;

S = load due to differential settlement and/or movement of the foundation;

V = wind load on traffic; and

W = wind load on structure

Table 3.5 shows the live load factors for the ultimate limit states while

Table 3.6 shows maximum and minimum values of load factors for ultimate limit state.

Table 3.5 Live load factors ultimate limit state (CSA,2014)

	Live load factor				
		Special loads mixed with normal traffic		Special loads travelling alone on bridge under supervision	
Load	Normal traffic	Short spans	Other spans	Short spans	Other spans
ULS combination 1	1.70*	1.70	1.50	1.50	1.35
ULS combination 2	1.60	1.60	1.40	1.40	1.25
ULS combination 3	1.40	1.40	1.25	1.25	1.10

**Also to be applied to the barrier loads.*

Table 3.6 Permanent loads – Maximum and minimum values of load factors for ULS (CSA,2014)

Dead load	**Maximum α_D**	**Minimum α_D**
Factory-produced components, excluding wood	1.10	0.95
Cast-in-place concrete, wood, and all non-structural components	1.20	0.90
Wearing surfaces, based on nominal or specified thickness	1.50	0.65
Earth fill, negative skin friction on piles	1.25	0.80
Water	1.10	0.90
Dead load in combination with earthquakes	**Maximum α_D**	**Minimum α_D**
All dead loads for ULS Combination 5 (see Table 3.1)	1.25	0.80
Earth pressure and hydrostatic pressure	**Maximum α_E**	**Minimum α_E**
Passive earth pressure, considered as a load*	1.25	0.50
At-rest earth pressure	1.25	0.80
Active earth pressure	1.25	0.80
Backfill pressure	1.25	0.80
Hydrostatic pressure	1.10	0.90
Prestress	**Maximum α_P**	**Minimum α_P**
Secondary prestress effects	1.05	0.95

**When passive earth pressure is considered as a resistance, it is factored in accordance with Section 6.*

3.7 Analysis

The bridge model was developed using STAAD Pro finite element analysis and design software and calibrated with all the appropriate loads. A moving load case was defined and used to generate the maximum responses (i.e. the location of the CLW-625 loading or lane loading on this bridge that will generate the maximum responses) on the bridge elements. The maximum response was combined with other live and dead loads described earlier.

4 Results and Discussions

4.1 Hydrological Results and Water Levels for Analyzed 100-Year Storm

The water surface levels for the analyzed 5 kilometers stretch of the Ottawa river ranges between 44.54 m and 51.06 m. The water surface level at the cross section of the bridge location was 47.89 m. Critical flow at bridge section occurs at 47.67 m while the total energy line lies at 49.82 m. This water level is in agreement with the historical water level as measured during an occurrence of the 100-year storm event measured at the Hull station in 1976 and given as 44.74 m.

Figure 4.1 shows the water level and other hydrologic parameters for the river stretch. The water surface level for the 100-year storm event is labeled PF1. while Figure 4.2 shows the water surface levels at the portage bridge site.

The result of water levels for the 100-year storm corresponds with measured water levels when a 100-year storm occurred in 1974. The correspondence of these results of the analysis with measured historical data gives credibility to the calibration of the model.

Chanel flow velocities for the 100-year storm event along the stretch of the river ranges from 1.39 m/s to 4.03 m/s. The velocity just upstream of the bridge is 3.8 m/s while the velocity of flow just downstream of the bridge is 4.03 m/s. The variation in the velocities is due to changes in profile along sections of the river. The discharge at any point along the river reach is related to the velocity of flow and the wetted area by the relationship Q = VA, where A is the wetted area and V is the

velocity of flow. The full output table for the hydraulic analysis is shown in Appendix 1. Figure 4.3 shows the variation in velocities along the river reaches.

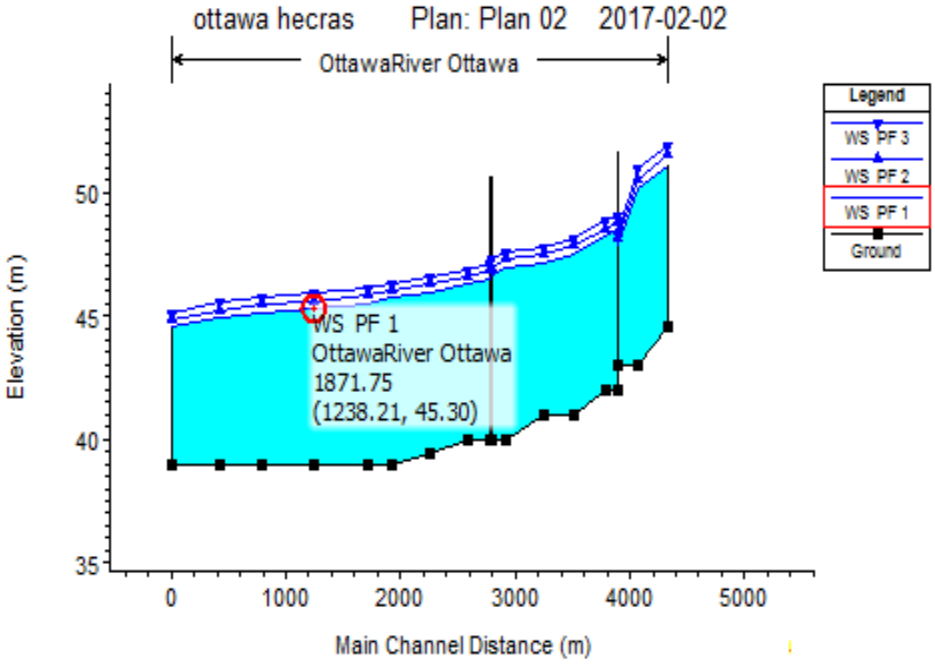

Figure 4.1 Variations in water level for a 100-year storm event along a stretch of Ottawa River

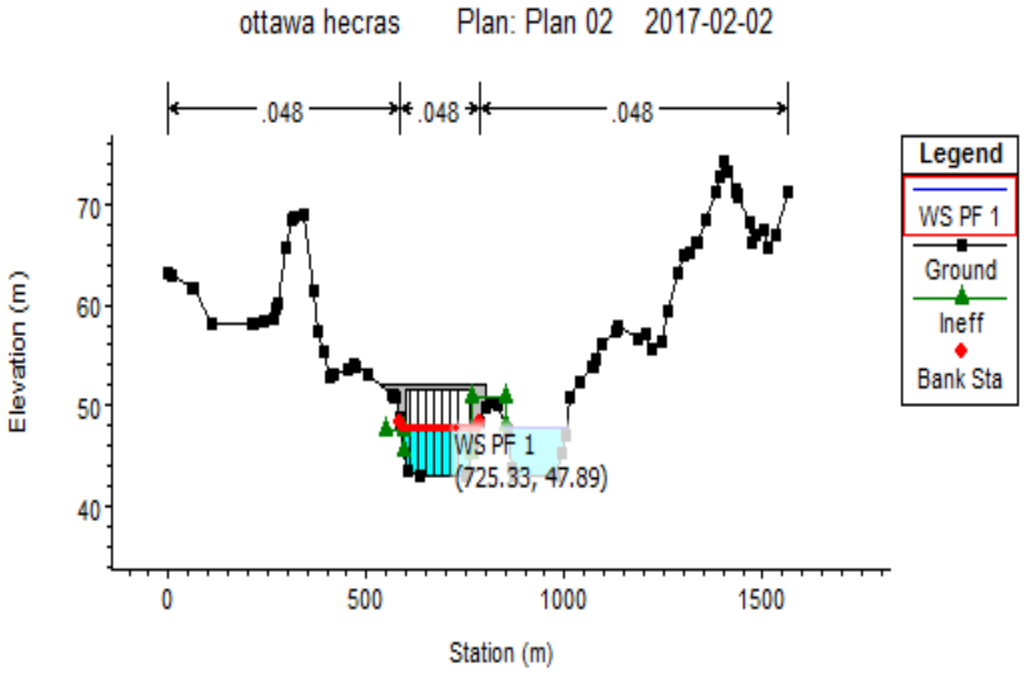

Figure 4.2 Water surface levels at the portage bridge site for 100-year storm event

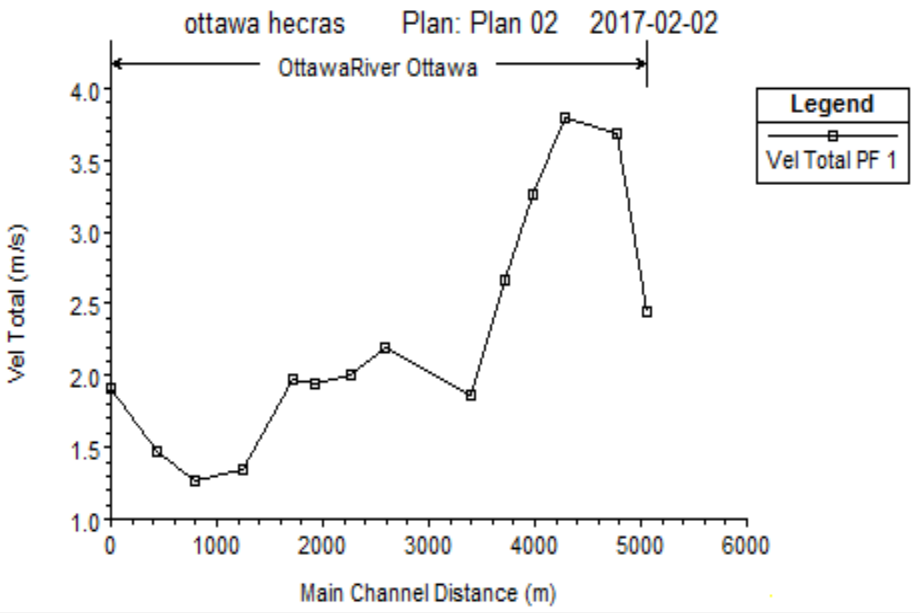

Figure 4.3 Variations in velocities along the river reaches

4.2 Hydrological Results for 100-Year Storm in Projected Changed Climate

For a projected climate with a 20% increase in 100-year storm discharge, the water surface levels for the analyzed 5 kilometer stretch of the Ottawa river ranges between 45.13 m and 51.88 m. This translate to about 1m increase in average water levels. The water surface level at the cross section of the bridge location was 48.34 m. Critical flow at bridge section occurs at 48.19 m while the total energy line lies at 50.63 m. Figure 4.4 shows the water level and other hydrologic parameters for the river stretch. The water surface level for the 100-year storm event in the projected climate is labeled PF3. while

Figure 4.5 shows the water surface levels at the portage bridge site.

Channel flow velocities for the 100-year storm event along the stretch of the river ranges from 1.47 m/s to 4.29 m/s. The velocity just upstream of the bridge is 3.99 m/s while velocity of flow just downstream of bridge is 4.29 m/s. The full output table for the hydraulic analysis is shown in Appendix 1. Figure 4.6 shows the variations in velocities along the river reaches.

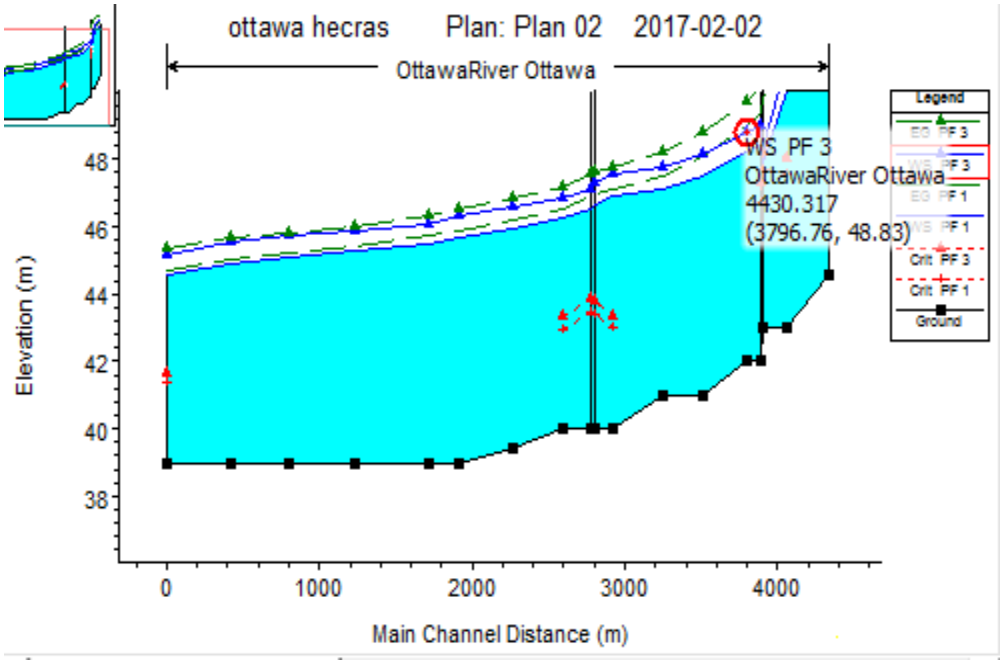

Figure 4.4 Variations in water level for a 100-year storm event along a stretch of Ottawa River for projected climate

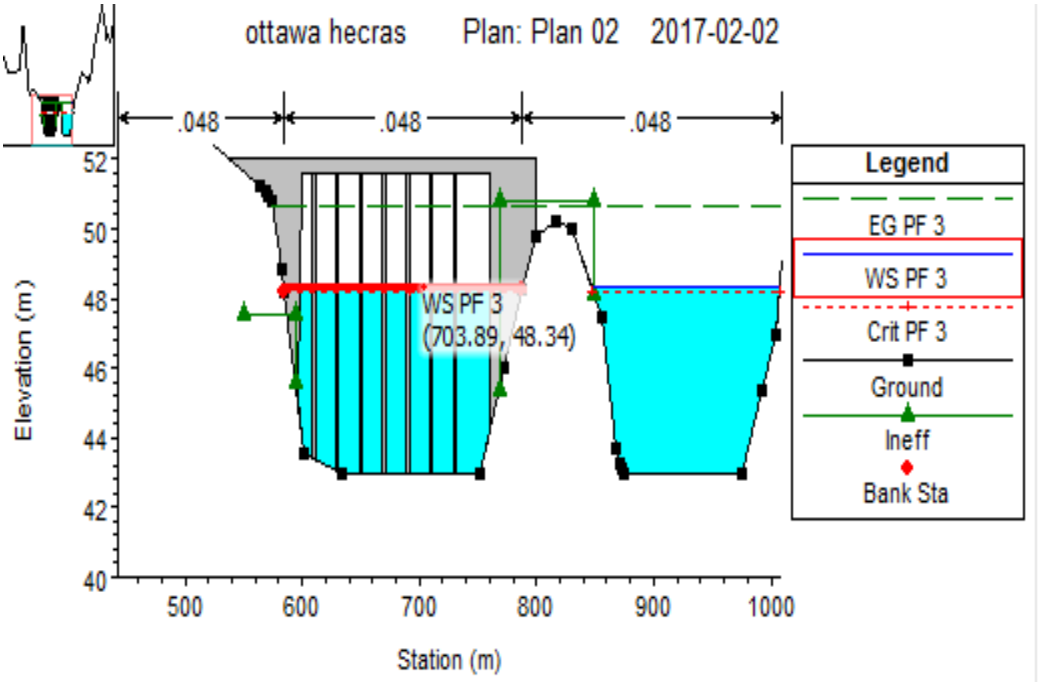

Figure 4.5 Water surface levels at the portage bridge site for 100-year storm event in projected climate

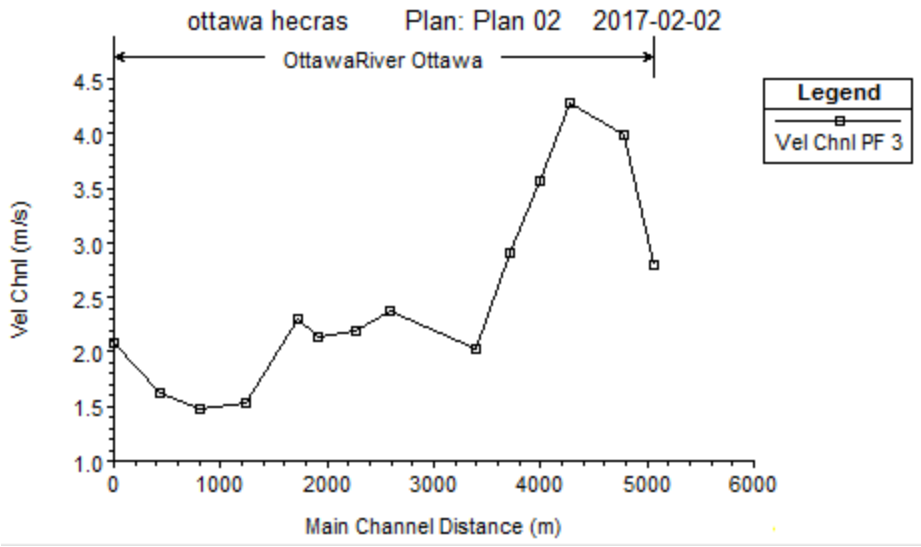

Figure 4.6 Variations in velocities along the river reaches in projected climate

4.3 Design scour for 100-year storm

The scour depths at the base of the bridge piers were computed using the Colorado state university equation (CSU) for live bed scour as recommended in the HEC-18. The piers design scour consisted of a combination of pier scours and contraction scour that is on an elevation of 36.68m as shown in Figure 4.7. The total scour depth computed from the difference between the ground elevation, and the total scour elevation is 6.32 m. A complete description of scour calculations input and output for 100- year storm is included in Appendix 2. The height of the deck was 51.6 m while the water surface stood at 47.18 m. The total depth of water is the difference between the water surface and the sour elevation which was 10.5 m.

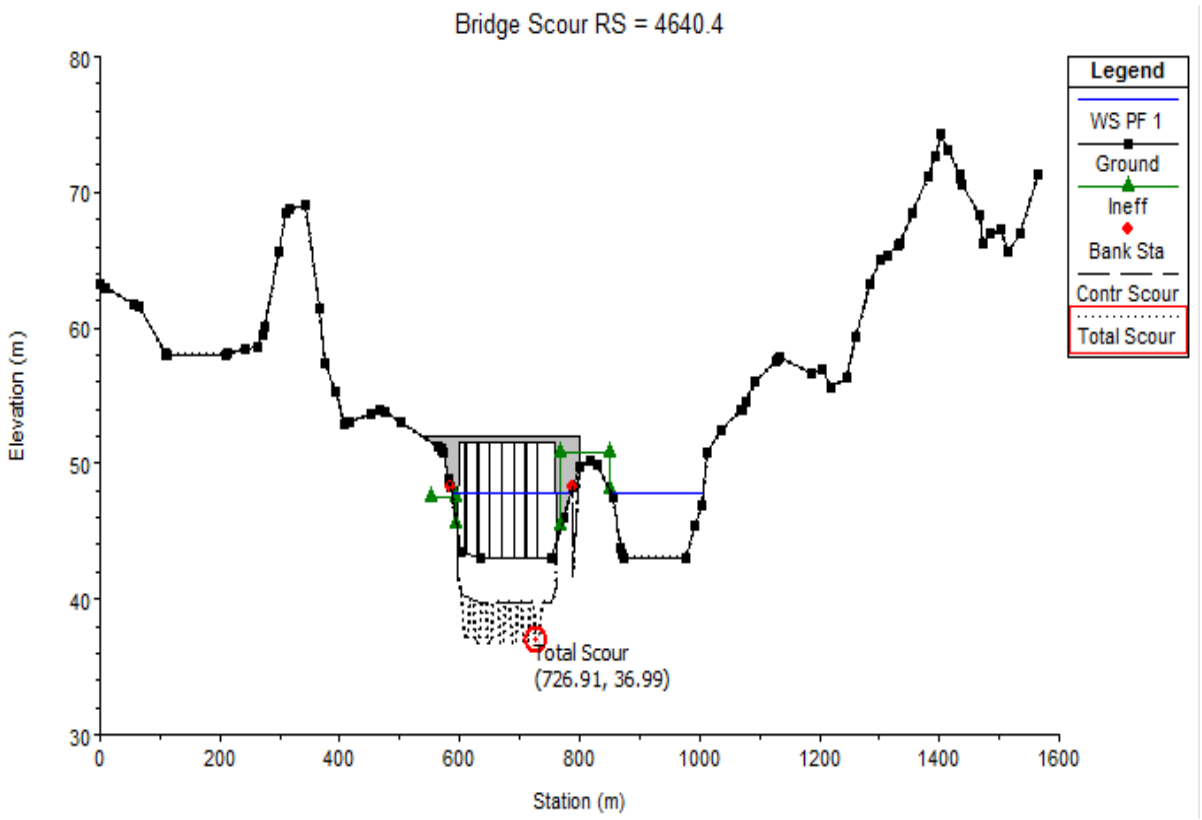

Figure 4.7 Bridge scour in a 100-year storm

4.4 Scour for 100-year storm in projected climate

Again, for the projected climate where the 100-year storm discharge has increased by 20%, the scour depths at the base of the bridge piers was computed using the CSU equation for live bed scour as recommended in the HEC-18. The piers design scour consisted of a combination of pier scours and contraction scour that is on an elevation of 35.82 m in the channel as shown in Figure 4.8. The total scour depth computed from the difference between the ground elevation and the total scour elevation is 7.18 m. A complete description of scour calculations input and output is provided in Appendix 3. Diagram showing scour depths in projected climate is shown in Figure 4.8.

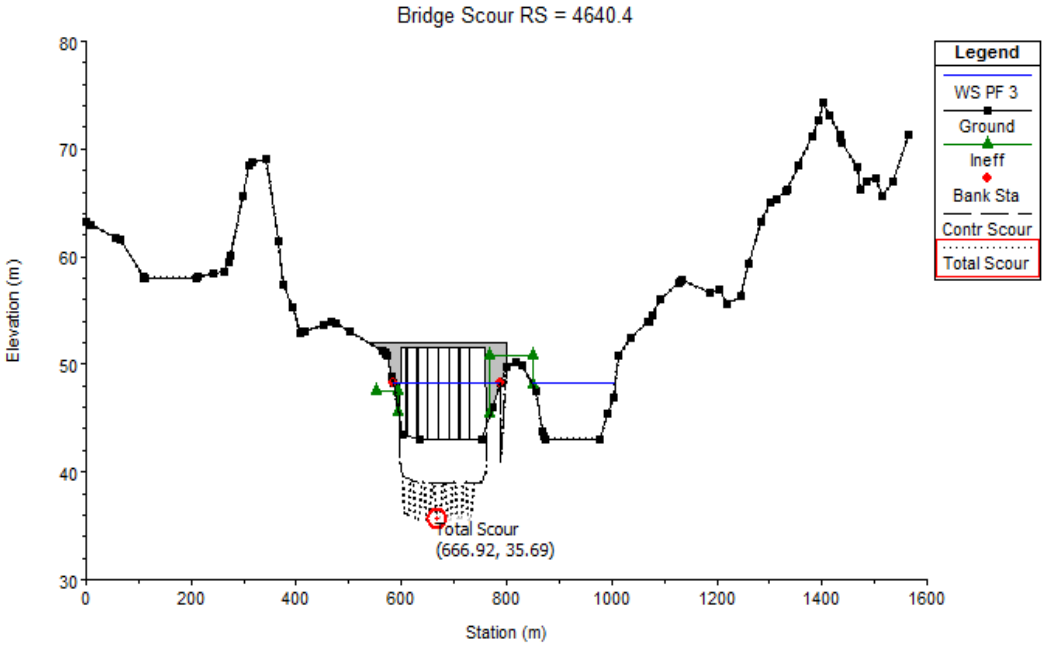

Figure 4.8 Bridge scour for a 100-year storm in projected Climate

4.5 Results of bridge elements under normal design loading

Highway and river bridges are usually analyzed and designed for a lifespan of 100 years. For the present study, the response of the bridge elements, that is, beams, girders and piers to loading was analyzed. The results of two main piers that were found to be critical are discussed here.

4.5.1 Axial and Shear forces

Figure 4.9 shows the arrangement of the piers on the bridge. The piers are numbered 1 to 14, after analysis, piers 7 and 8 were critical as they were exposed to the largest forces. The maximum axial force on pier 7 was controlled by ultimate load combination 3 (Table 3.4).

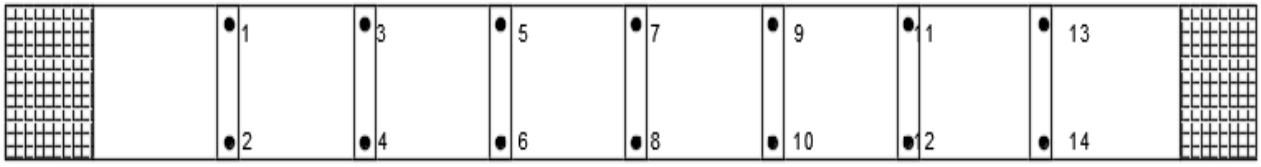

Figure 4.9 Plan of bridge piers arrangement

The maximum axial load on pier 7 is 4483 kN, these load combinations include the dead load, hydrodynamic load and wind load in addition to the vehicle loads. The maximum shear force is 106 kN at the top of the pier. Figure 4.10 and Figure 4.11 shows the axial force and shear force envelopes diagrams for pier 7.

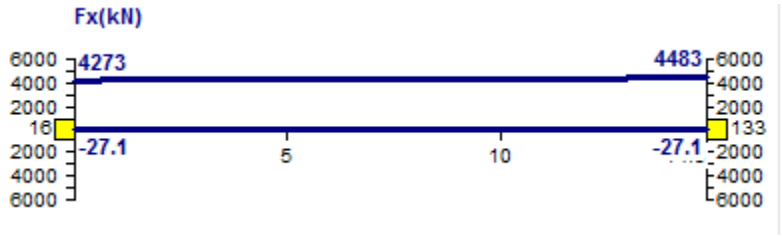

Figure 4.10 Axial load envelope for pier 7

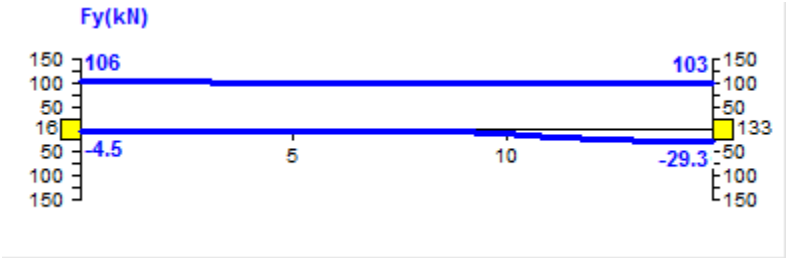

Figure 4.11 Shear force envelope for pier 7

For pier 8, the maximum axial load and shear force was 4482 kN and 104 kN as shown in Figure 4.12 and Figure 4.13, respectively.

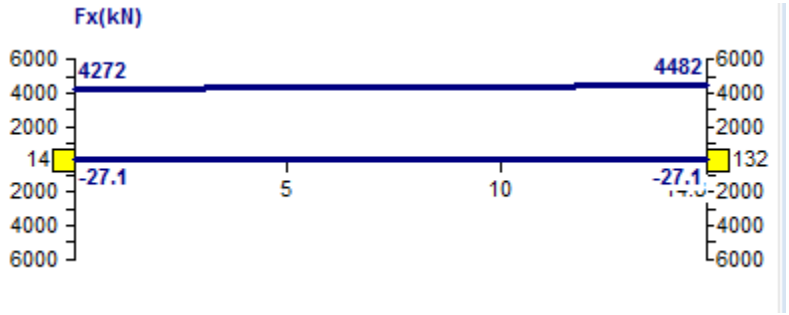

Figure 4.12 Axial load envelope for pier 8

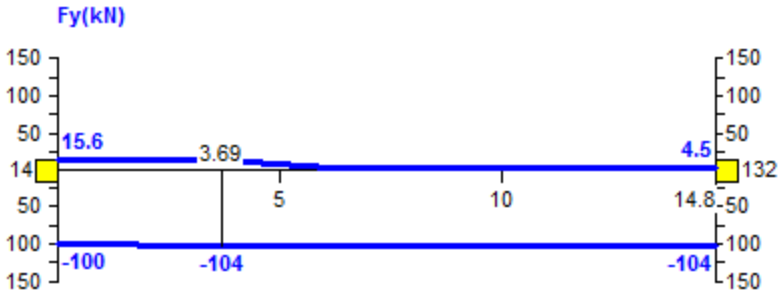

Figure 4.13 Shear force envelope for pier 8

4.5.2 Bending Moments and Design Requirements

Lateral forces and load eccentricity induced bending moments in the pier. The maximum bending moment in pier 7 is 1021 kNm. Figure 4.14 shows the bending moment envelope for pier 7.

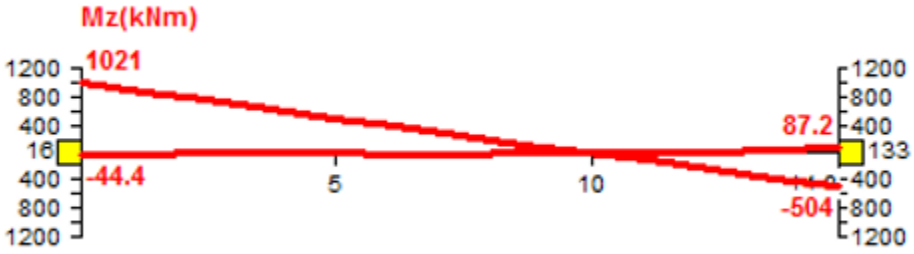

Figure 4.14 Bending moment envelope for pier 7.

For pier 8, the maximum bending moment in the pier is 1018KNm as shown in the bending moment envelope in Figure 4.15.

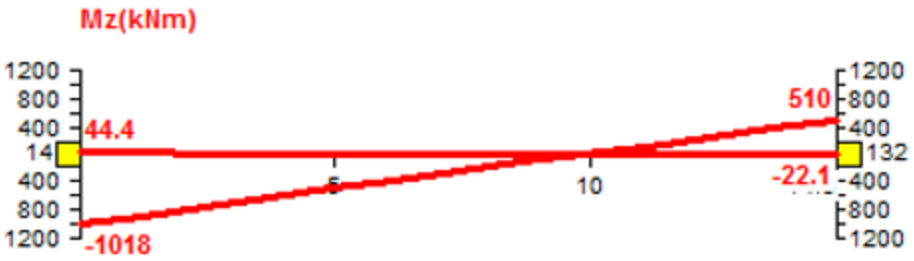

Figure 4.15 Bending moment envelope for pier 8.

The bridge piers were designed according to the Canadian highway bridge design design code. (CSA,2014) .

Material property for piers

Concrete strength f_c' = 30.0 MPa

Concrete Density = 2400 kg/m^3

Aggregate size =20 mm

Cover = 40 mm

Exposure Condition Exterior

Steel yield strength fy = 400 MPa

Modulus = 200000 MPa

Pier 8 - CSA-S6 Design Requirements

Section Diameter = 800 mm

Story height = 14.8 m

Circular Section: Diameter = 800 mm

Pier 7 - CSA-S6 Main Reinforcement

Axial Load = -4482.42 kN

Major axis Moment M, end 1 = 1017.53 kNm

end 2 = -510.47 kNm

Minor axis moment M, end 1 = -22.77 kNm,

end 2 = 11.34 kNm

C_m = 0.40

∂_s = 1.00

C_m = 0.40

∂_s = 1.00

Where:

C_m = factor relating actual moment diagram to an equivalent uniform moment diagram

∂_s = Moment magnification factor accounting for second-order effects of vertical load acting on a structure in a laterally displaced configuration

Area of steel provided = 6900 mm^2

Axial compression capacity = -4482.42 kN

Resultant moment capacity Mz = -1021.19 kNm

Actual distance between bars = 73 mm

Pier 8 - CSA-S6 Shear Reinforcement

Actual spacing of ties = 300 mm

Major Axis:

Design shear force V_f = 104.02 kN

Shear resisted by concrete:

$$V_c = \Phi_c \lambda \beta \sqrt{f_c'} b_w dv \quad (4.1)$$

= 0.65 x 1.00 x 0.297 x √30.00 x 800.00 x 576.00 = 486.75 kN

Shear resisted by steel:

$$V_s = \frac{\phi_s A_v f_{yt} d_v \cot\theta}{s} \quad (4.2)$$

= 0.85 x 0.67 x 400.00 x 576.00 x 1.69 = 220.55 kN

Maximum shear capacity

$$V_{r,max} = 0.25 \Phi_c f_c' b_w dv \quad (4.3)$$

= 0.25 x 0.65 x 30.00 x 800.00 x 576.00 = 2246.40 kN

V_r = 486.75 + 220.55 = 707.30 kN

$V_r > V_f$ = **OK**

Actual area of shear reinforcement (2-10M) = 200 mm2

Maximum spacing of ties = 310 mm

Minor Axis:

Design shear force V_f = 22.12 kN

Shear resisted by concrete:

$$Vc = \Phi_c \lambda \beta \sqrt{f_c'} b_w dv \quad (4.1)$$

$$= 0.65 \times 1.00 \times 0.297 \times \sqrt{30.00} \times 800.00 \times 576.00 = 486.75 \text{ kN}$$

Shear resisted by steel

$$Vs = \frac{\phi_s A_v f_{yt} d_v \cot\theta}{s} \quad (4.2)$$

$$= 0.85 \times 0.67 \times 400.00 \times 576.00 \times 1.69 = 220.55 \text{ kN}$$

Maximum shear capacity

$$V_{r,max} = 0.25 \Phi c \; fc' bw dv \quad (4.3)$$

$$= 0.25 \times 0.65 \times 30.00 \times 800.00 \times 576.00 = 2246.40 \text{ kN}$$

Vr = 486.75 + 220.55 = 707.30 kN

Vr > Vf = **OK**

Actual area of shear reinforcement (2-10M) = 200 mm2

Maximum spacing of ties = 310 mm

Pier 7 - CSA-S6 Design Requirements

Section Diameter: 800 mm

Story height = 14.8 m

Circular Section: Diameter = 800 mm

Pier 8 - CSA-S6 Main Reinforcement

Axial load: = -4482.99 kN

Major axis Moment M, end 1, = -1021.27 kNm

end 2, = 504.39 kNm

Minor axis moment M, end 1, = -22.77 kNm

end 2, = 11.34 kNm

C_m = 0.40

d_s = 1.00

C_m = 0.40

d_s = 1.00

Area of steel provided = 6600 mm2

Axial compression capacity = -4482.99 kN

Resultant moment capacity Mz = 1009.03 kNm

Actual distance between bars = 77 mm

Pier 7 - CSA-S6 Shear Reinforcement

Actual spacing of ties = 300 mm

Major Axis:

Design shear force V_f = 106.26 kN

Shear resisted by concrete

$$V_c = \Phi_c \lambda \beta \sqrt{f_c'} b_w d_v \quad (4.1)$$

= 0.65 x 1.00 x 0.297 x √30.00 x 800.00 x 576.00 = 483.88 kN

Shear resisted by steel

$$V_s = \frac{\phi_s A_v f_{yt} d_v \cot\theta}{s} \quad (4.2)$$

= 0.85 · 0.67 · 400.00 · 576.00 · 1.69 = 220.22 kN

Maximum shear capacity

$$V_{r,max} = 0.25 \Phi_c f_c' b_w d_v \quad (4.3)$$

= 0.25 x 0.65 x 30.00 x 800.00 x 576.00 = 2246.40 kN

V_r = 483.88 + 220.22 = 704.10 kN

$V_r > V_f$ = **OK**

Actual area of shear reinforcement (2-10M) = 200 mm2

Maximum spacing of ties = 310 mm

Minor Axis:

Design shear force V_f = 25.07 kN

Shear resisted by concrete

$$V_c = \Phi c \lambda \beta \sqrt{fc'} bw dv \quad (4.1)$$

= 0.65 · 1.00 · 0.295 · √30.00 · 800.00 · 576.00 = 483.88 kN

Shear resisted by steel

$$V_s = \frac{\phi_s A_v f_{yt} d_v \cot\theta}{s} \quad (4.2)$$

= 0.85 x 0.67 x 400.00 x 576.00 x 1.69 = 220.22 kN

Maximum shear capacity

$$V_{r,max} = 0.25\Phi c\ fc'bwdv \quad (4.3)$$

= 0.25 x 0.65 x 30.00 x 800.00 x 576.00 = 2246.40 kN

Vr = 483.88 + 220.22 = 704.10 kN

Vr > Vf = **OK**

Actual area of shear reinforcement (2-10M) = 200 mm^2

Maximum spacing of ties = 310 mm

4.6 Response of Bridge to Loading and Effects of Scouring In Projected Climate

The same bridge was analyzed for conditions in the projected climate. The vehicle loads, wind loads and self-weight of the structure were kept constant, while the scour depth and hydrodynamic pressure were varied accordingly. The response of the bridge elements was then determined using the new conditions.

4.6.1 Axial and shear forces

The maximum axial forces on pier 7 and 8 remained constant because there was no increment in factors contributing to the axial forces. The maximum shear forces, however, had increased. This is due to the increase in scour depths and the hydrodynamic pressure on the piers. The maximum shear force on pier 7 for the controlling load combination had increased from 106 kN to 149 kN for the projected climate as shown below in Figure 4.16. While for pier 8, the maximum shear force increased to 107 kN as shown in Figure 4.17.

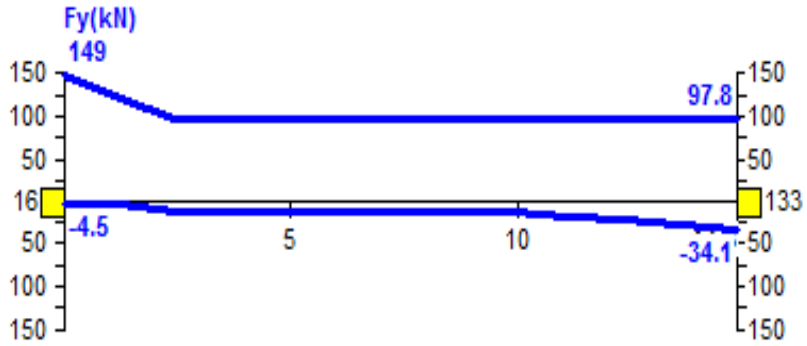

Figure 4.16 Shear force envelope for pier 7 in projected climate

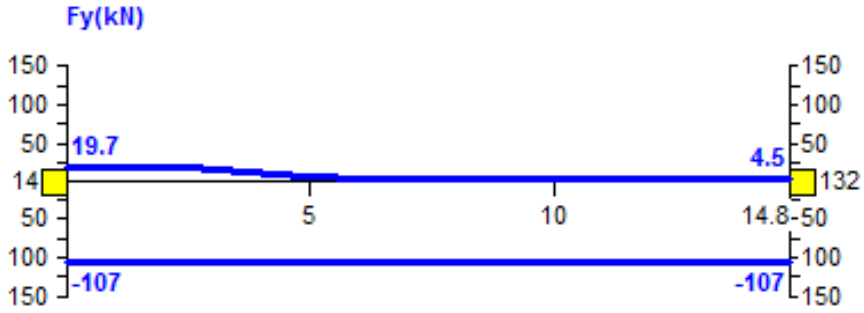

Figure 4.17 Shear force envelope for pier 8 in projected climate

4.6.2 Bending moments and design requirements

The maximum bending moments on the bridge elements for the critical piers has increased. The maximum bending moment in pier 7 increased from 1021 kNm to 1042 kNm while the maximum bending moment for pier 8 increased from 1018 kNm to 1032 kNm. These increments in the maximum bending moment were due to the increase in scour depths, water flow velocity and the depth of flow. Figure 4.18 and Figure 4.19 show the bending moment envelopes for both piers.

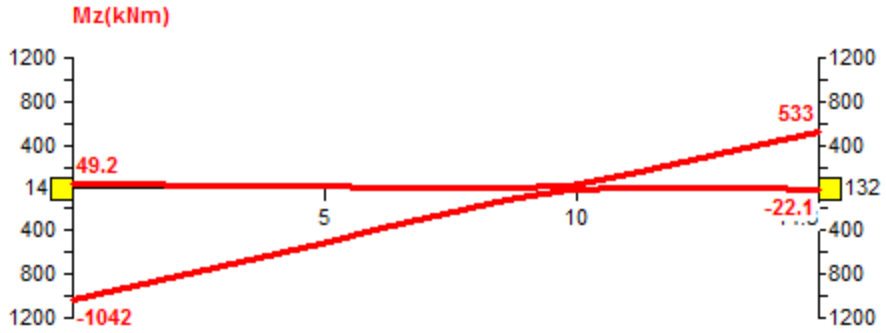

Figure 4.18 Bending moment envelope for pier 7 in projected climate

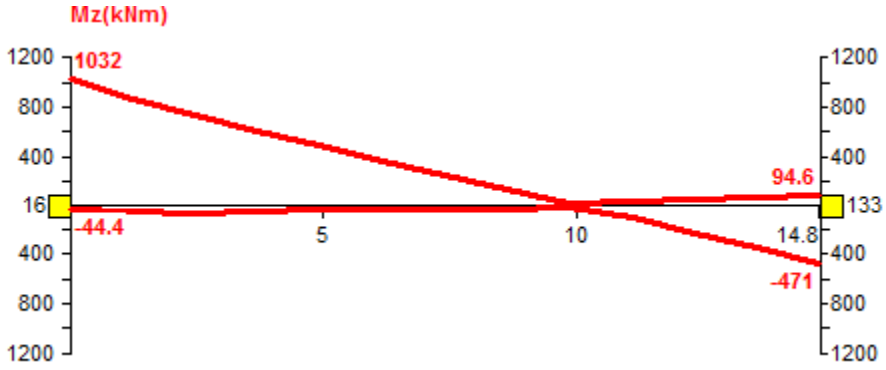

Figure 4.19 Bending moment envelope for pier 8 in projected climate

The piers were designed according to the Canadian standard concrete design code to estimate the reinforcement requirement for the piers in the projected climate scenario.

Pier 7 - CSA-S6 Design Requirements

Section Diameter : 800 mm

Story height = 14.8 m

Circular Section: Diameter = 800 mm

CSA-S6 Main Reinforcement

Axial Load: = -4484.04 kN

Major axis moment M, end 1, = 1042.21 kNm

end 2, = -533.30 kNm

Minor axis moment M, end 1, = -22.77 kNm

end 2, = 11.34 kNm

d_s = 1.00

C_m = 0.40

Area of steel provided = 7500 mm^2

Axial compression capacity = -4484.04 kN

Resultant moment capacity Mz = -1066.84 kNm

Actual distance between bars = 66 mm

Pier 7 - CSA-S6Shear Reinforcement

Actual spacing of ties = 300 mm

Major Axis:

Design shear force V_f = 106.60 kN

Shear resisted by concrete V_c

$$V_c = \Phi_c \lambda \beta \sqrt{f_c'} b_w d_v \quad (4.1)$$

= 0.65 x 1.00 x 0.297 x √30.00 x 800.00 x 576.00 = 487.07 kN

Shear resisted by steel

$$Vs = \frac{\phi_s A_v f_{yt} d_v \cot\theta}{s} \quad (4.2)$$

= 0.85 x 0.67 x 400.00 x 576.00 x 1.69 = 220.58 kN

Maximum shear capacity

$$V_{r,max} = 0.25 \Phi c\ fc' bw dv \quad (4.3)$$

= 0.25 x 0.65 x 30.00 x 800.00 x 576.00 = 2246.40 kN

V_r = 487.07 + 220.58 = 707.66 kN

$V_r > V_f$ = OK

Minimum density of links = 0.67

Shear density of rebar provided = 0.67

Actual area of shear reinforcement (2-10M) = 200 mm2

Maximum spacing of ties = 310 mm

Minor Axis:

Design shear force V_f = 22.12 kN

Shear resisted by concrete

$$V_c = \Phi_c \lambda \beta \sqrt{f_c'} b_w d_v \quad (4.1)$$

= 0.65 x 1.00 x 0.297 x √30.00 x 800.00 x 576.00 = 487.07 kN

Shear resisted by steel

$$Vs = \frac{\phi_s A_v f_{yt} d_v \cot\theta}{s} \quad (4.2)$$

= 0.85 x 0.67 x 400.00 x 576.00 x 1.69 = 220.58 kN

Maximum shear capacity

$V_{r,max} = 0.25\Phi c\ fc'bwdv$ (4.3)

= 0.25 x 0.65 x 30.00 x 800.00 x 576.00 = 2246.40 kN

V_r = 487.07 + 220.58 = 707.66 kN

$V_r > V_f$ = **OK**

Actual area of shear reinforcement (2-10M) = 200 mm2

Maximum spacing of ties = 310 mm

Pier 8 - CSA-S6Design Requirements

Section Property: 800 mm

Story height = 14.8 m

Circular Section: Diameter = 800 mm

Pier 8 - CSA-S6Main Reinforcement

Axial load: = -4482.67 kN

Major axis moment M, end 1, =-1032.43 kNm

end 2, = 471.07 kNm

Minor axis moment M, end 1, = -22.77 kNm

end 2, = 11.34 kNm

C_m = 0.40 Eq. 10-20

d_s = 1.00 Eq. 10-24

Area of steel provided = 6900 mm^2

Axial compression capacity = -4482.67 kN

Resultant moment capacity Mz = 1032.43 kNm

Actual distance between bars = 73 mm

Pier 8 CSA-S6 Shear Reinforcement

Actual spacing of ties = 300 mm

Major Axis:

Design shear force V_f = 100.85 kN

Shear resisted by concrete

$$V_c = \Phi_c \lambda \beta \sqrt{f_c'} b_w d_v \quad (4.1)$$

= 0.65 x 1.00 x 0.297 x √30.00 x 800.00 x 576.00 = 460.91 kN

Shear resisted by steel

$$V_s = \frac{\phi_s A_v f_{yt} d_v \cot\theta}{s} \quad (4.2)$$

= 0.85 x 0.67 x 400.00 x 576.00 x 1.67 = 217.48 kN

Maximum shear capacity

$$V_{r,max} = 0.25 \Phi_c f_c' b_w d_v \quad (4.3)$$

= 0.25 x 0.65 x 30.00 x 800.00 x 576.00 = 2246.40 kN

V_r = 460.91 + 217.48 = 678.39 kN

$V_r > V_f$ = **OK**

Minimum density of links = 0.67

Shear density of rebar provided = 0.67

Actual area of shear reinforcement (2-10M) = 200 mm^2

Maximum spacing of ties = 310 mm

Minor Axis:

Design shear force V_f = 25.07 kN

Shear resisted by concrete

$$V_c = \Phi_c \lambda \beta \sqrt{f_c'} b_w d_v \quad (4.1)$$

= 0.65 x 1.00 x 0.297 x √30.00 x 800.00 x 576.00 = 460.91 kN

Shear resisted by steel

$$V_s = \frac{\phi_s A_v f_{yt} d_v \cot\theta}{s} \quad (4.2)$$

= 0.85 x 0.67 x 400.00 x 576.00 x 1.67 = 217.48 kN

Maximum shear capacity

$$V_{r,max} = 0.25 \Phi_c f_c' b_w d_v \quad (4.3)$$

= 0.25 x 0.65 x 30.00 x 800.00 x 576.00 = 2246.40 kN

V_r = 460.91 + 217.48 = 678.39 kN

$V_r > V_f$ = **OK**

Actual area of shear reinforcement (2-10M) = 200 mm^2

Table 4.1- Summary of Bending Moment, Shear Force and reinforcement requirements

	Present climate		Projected climate	
	Pier 7	Pier 8	Pier 7	Pier 8
Bending Moments (kNm)	1021	1018	1042	1032
Shear forces (kN)	106	104	149	107
Required reinforcement (mm)	6900	6600	7500	6900

4.7 Effects of Age and Exposure Conditions and Climate Change Interactions on Concrete Infrastructures

Bridge infrastructures and other infrastructure built with concrete and steel ages, they deteriorate due to effects of environmental loading that they are exposed to. These deteriorations result in spalling (loss of concrete), which ultimately reduces the sectional dimensions of the member and also the loss of reinforcement. These losses combine to reduce the strength of the members. In a changing climate where the rate of deterioration is exacerbated, the effects of age and exposure conditions on existing infrastructures such as a bridge is somewhat difficult to predict since different exposure conditions will have different effects and are difficult to be simulated accurately.

Experimental analysis by several researchers has in the past tried to predict residual strength based on accelerated corrosion of reinforced, prestressed and fiber reinforced concrete elements. Other methods used to estimate the residual strength of reinforced concrete has been done by testing structural elements from de-commissioned structures or by coring and testing of samples.

Dasar et al. (2017) tested performance reduction of 40-year-old reinforced concrete beams in natural corrosion environments and reported that for every 1% of local cross-sectional loss in the tensile steel bars, a 0.9% reduction in the load-carrying capacity of the reinforced concrete beams occurs. Rodriguez et al. (as cited in Dasar et al. 2017) had reported that a corrosion degree of about 14% caused beam strength to decrease by 23%.

The present study did not investigate the effect of climate change on the age and exposure conditions of the bridge, but it is worthy to note that the effects of climate change will compound the strength loss due to age and exposure conditions.

5 Conclusion and recommendations

A study was carried out to investigate the impact of climate change on bridge infrastructure and to investigate adaptation measures to protect the bridges against these impacts. A bridge on the Ottawa river was used as case study. The model was constructed to study the effect of increased scour depth and increased flood load on the existing bridge. The bridge model was idealized as a beam bridge which consists of a 250 mm reinforced concrete deck on 7 reinforced concrete girders spanning continuously over eight 20 m spans. The transverse width of the deck is 17 m and carries 4 lanes of highway each 3.5 m wide. On each extreme side is a shoulder of 1.5 m wide each. The center to center spacing between girders is 2.143 m with deck overhangs of 1.0 m on either side. The girders are supported on beams of 800 mm by 1000 mm depths. Each beam is in turn supported on two 800mm diameter piers, and each has a length of 14.78 m from the top of the pile cap

The model was analyzed for traffic, wind, hydrostatic and other ancillary loads. Results of analysis for a 100-year storm were compared with results of the analysis for a 100-year storm in a projected climate. Results show that in a projected climate, increased scour depths and hydrodynamic load effects on the bridge piers caused an increase in the shear forces and bending moment and will jeopardize the safety of the bridge. Adaptation measures will have to be carried out to retrofit the bridge to make it safe for use.

5.1 Adapting To Climate Change

River bridge infrastructures can be adapted to the effects of climate change by using the traditional methods of bridge retrofitting or rehabilitation as a result of strength and material deterioration. This is so because even though climate change is a separate phenomenon on its own, its mechanism of effects on infrastructure is by speeding up the rate of deterioration and by increasing physical loads that a structure has to resist.

5.1.1 Jacketing

Jacketing is the process whereby a section of an existing structural member is restored to original dimensions or increased in size by encasement using suitable materials. A steel reinforcement cage

or composite material wrap can be constructed around the damaged section onto which shotcrete or cast-in- place concrete is placed.

For jacketing, the void between the form and the existing member is filled using pumping, or preplaced aggregate concrete. Jacketing is particularly used for the repair of deteriorated columns, piers, and piles and may easily be employed in underwater applications. It is suggested that the bridge piers should be jacketed to increase the shear and moment capacities to meet with the capacity required for the projected climate. Figure 5.1shows a typical cross section of a jacketed pier.

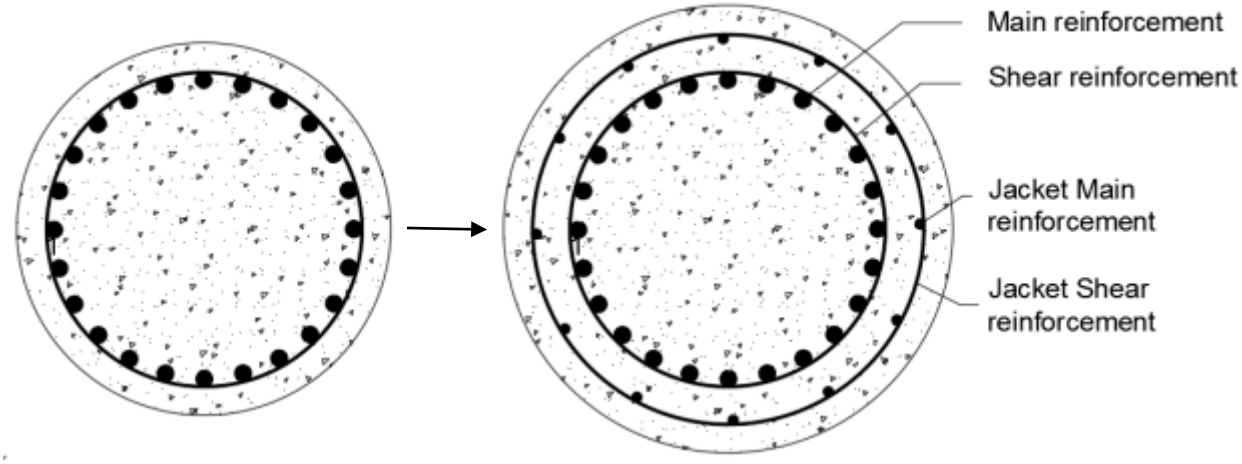

Figure 5.1 Typical cross section of a pier before and after jacketing

5.1.2 Scour Protection

From the present study, it is evident that the single most important effect of climate change on river bridge infrastructure that jeopardizes the safety of bridge and users is scouring as a result of a flood. A way to protect and adapt this bridge is by protection against scour. Many scour protection methods have been studied and deployed in bridges susceptible to scouring. The following scour protection method is suggested to be investigated and if found appropriate be deployed to protect against scour of the bridge

5.1.2.1 Riprap

Riprap is one of the most commonly used bridge pier scour protection measures. it consists of large stones placed around a pier to armor the bed. This armoring prevents the strong vortex flow at the front of the pier from entraining bed sediment and forming a scour hole. The ability of the

riprap layer to provide scour protection is a function of stone size. Stones are sized such that the current of flowing water is not adequate to displace the ripraps. Design and sizing of riprap stones is described in HEC-23 (Lagasse et al. 2006).

Sizing of riprap stones can be determined using the Isbash formula for sizing riprap on a channel bed (Lagasse et al. 2006).

$$d50 = \frac{0.692(kV)^2}{(S_s - 1)2g} \quad (4.4)$$

d50 = Riprap size (m)

V = Design velocity (m/s)

k = Coefficient for pier shape

S_s = Specific gravity of the riprap

g = Acceleration of gravity (9.81 m/s^2)

In ripraps, filters are used in combinations with the stones, and filters should be a combination of geotextile and granular materials.

The selection of geotextile can be based on methods outlined by Koerna (1998), HEC-11 or AASHTO M-288 (Lagasse et al., 2006). Lagasse et al. (2006) advocated the use of Koerna method as it places more emphasis on permeability and less emphasis on particle retension. Geotextile application should exhibit a permeability that is more than 4 times greater than the bed material, that is $K_g/K_s > 4.0$ (Lagasse et al., 2006). K_g and K_s are permeability of geotextile and bed materials respectively.

For the granullar filters, the requirement is the compatibility of the filter with the sand bed material in terms of both particle retention and permeability. By defining upper and lower limits of d_{15} for the filter, the largest size allowable to maintain particle retention and smallest size allowable to ensure the filter has greater permeability than the sand is established. The requirements for the filter to soil relationship are as follows:

$$\frac{d_{15}\ filter}{d_{85}\ soil} < 5 \quad (4.5)$$

$$5 < \frac{d_{15}\ filter}{d_{15}\ soil} < 40 \quad (4.6)$$

The d85 of the filter must be large enough so that the filter does not pass through the riprap. The requirements for filter to riprap relationship are

$$\frac{d_{15}\,riprap}{d_{85}\,filter} < 5 \qquad (4.7)$$

5.2 Future Study

1 This research studied impact of a changing climate on a river bridge infrastructure. On the particular bridge studied as case study, the scour depth was such that the bridge foundations have not been impacted. There would be bridges and scour depths that may be deep enough to affect foundations. Research should in future be carried out for such cases.

2 Material deterioration caused by climate change need to be studied. Infrastructures may be more impacted by chemical reactions as a result of increased environmental loads rather than physical loads.

3 Apart from new built infrastructure and normally existing infrastructure, some infrastructure has experienced extreme event prior in their service life. This type of infrastructure will likely behave differently in a changing climate. Research should be conducted to study climate change interaction with such infrastructures.

4 In some zones of the world, climate change causes a reduction in environmental loads and factors. Some zones will experience reduced temperature, precipitation and even desertification in extremes. A study of how civil infrastructures will be impacted in such zones need be studied.

Appendices

Appendix 1 Output table of hydraulic analysis

Reach	River Sta	Profile	Q Total	Min Ch El	W.S. Elev	Crit W.S.	E.G. Elev	E.G. Slope	Vel Chnl	Flow Area	Top Width	Froude # Chl
			(m3/s)	(m)	(m)	(m)	(m)	(m/m)	(m/s)	(m2)	(m)	
Ottawa	4970	PF 1	8190	44.55	51.06		51.39	0.0016	2.74	3360.4	719.7	0.36
Ottawa	4970	PF 3	9828	44.55	51.88		52.21	0.0014	2.8	3964.7	766.88	0.34
Ottawa	4694.7	PF 1	8190	43	50.09	47.56	50.79	0.0027	3.8	2220.8	424.08	0.47
Ottawa	4694.7	PF 3	9828	43	50.96	47.99	51.66	0.0026	3.99	2698.4	445.31	0.47
Ottawa	4640.4		Bridge									
Ottawa	4430.3	PF 1	8190	42	48.2		48.98	0.0037	4.03	2155.5	456.95	0.54
Ottawa	4430.3	PF 3	9828	42	48.83		49.7	0.0036	4.29	2442.7	459.67	0.54
Ottawa	4139.6	PF 1	8190	41	47.5		48.05	0.0024	3.31	2508.5	464.8	0.44
Ottawa	4139.6	PF 3	9828	41	48.13		48.77	0.0024	3.57	2811	491.33	0.45
Ottawa	3875.3	PF 1	8190	41	47.11		47.48	0.0016	2.71	3076.4	579.81	0.36
Ottawa	3875.3	PF 3	9828	41	47.76		48.19	0.0016	2.91	3485	675.93	0.37
Ottawa	3552.6	PF 1	8190	40	46.92	43.03	47.1	0.0007	1.87	4406.5	719.74	0.24
Ottawa	3552.6	PF 3	9828	40	47.58	43.34	47.79	0.0007	2.03	4911	805.8	0.25

Ottawa	3222.7	PF 1	8190	40	46.26	42.95	46.51	0.0012	2.2	3724.1	693.74	0.3
Ottawa	3222.7	PF 3	9828	40	46.88	43.3	47.17	0.0012	2.38	4158.1	711.04	0.31
Ottawa	2895.2	PF 1	8190	39.45	45.97		46.17	0.0008	2.01	4092.6	683.04	0.26
Ottawa	2895.2	PF 3	9828	39.45	46.58		46.82	0.0009	2.19	4509.8	685.77	0.27
Ottawa	2549.7	PF 1	8190	39	45.71		45.9	0.0007	1.95	4230.9	706.47	0.24
Ottawa	2549.7	PF 3	9828	39	46.3		46.53	0.0008	2.14	4671.3	781.83	0.26
Ottawa	2351.8	PF 1	8190	39	45.5		45.72	0.001	2.17	4137.5	986.25	0.29
Ottawa	2351.8	PF 3	9828	39	46.1		46.35	0.0011	2.31	4750.8	1049.9	0.29
Ottawa	1871.8	PF 1	8190	39	45.3		45.4	0.0004	1.42	6095	1334.6	0.18
Ottawa	1871.8	PF 3	9828	39	45.9		46.01	0.0004	1.53	6915.7	1380.1	0.19
Ottawa	1431.1	PF 1	8190	39	45.12		45.21	0.0004	1.39	6458.6	1475.3	0.18
Ottawa	1431.1	PF 3	9828	39	45.72		45.83	0.0004	1.47	7367.3	1557.8	0.18
Ottawa	1059.9	PF 1	8190	39	44.92		45.04	0.0005	1.52	5578.6	1313	0.2
Ottawa	1059.9	PF 3	9828	39	45.52		45.65	0.0005	1.63	6385.2	1374.9	0.21
Ottawa	633.54	PF 1	8190	39	44.54	41.36	44.73	0.001	1.95	4302	985.74	0.28
Ottawa	633.54	PF 3	9828	39	45.13	41.66	45.34	0.001	2.07	4897	1036	0.28

Appendix 2 Historical discharge data for Ottawa river measured at Carillon (Ottawa river regulation planning board)

MONTHLY AND ANNUAL MEAN DISCHARGES IN CUBIC METRES PER SECOND FROM 1964														ANNUAL EXTREMES	
YEAR	JAN	FEB	MAR	APR	MAY	JUN	JUL	AUG	SEP	OCT	NOV	DEC	ANNUAL MEANS	DAILY MAXIMUM	DAILY MINIMUM
1964	1471	1436	1782	2564	2227	1754	1256	924	851	990	1028	1232	**1459**	3726	560
1965	1257	1286	1426	2078	2851	1511	1017	1247	1785	3163	2605	2243	**1876**	3672	570
1966	2147	1908	2648	3197	2635	2254	1336	1481	1240	1397	1917	3422	**2133**	5410	840
1967	2220	2221	1737	4256	3924	3157	2106	1363	1306	2112	3374	2265	**2500**	5407	974
1968	2016	1913	2339	3480	1799	1596	1659	1280	1184	1150	1223	1361	**1748**	4653	805
1969	1453	1510	1644	3293	3499	2217	1595	1440	1101	1235	2135	1958	**1924**	5134	771
1970	1592	1480	1543	2925	3553	2470	2261	1698	1228	1379	1609	1525	**1941**	4990	842
1971	1396	1354	1484	3512	3536	1579	997	952	880	870	907	1172	**1553**	5704	306
1972	1224	1163	1253	3169	4806	2374	2195	2046	1850	1940	2614	2073	**2228**	6329	863
1973	1975	2071	3615	4137	3841	2765	2065	1563	1362	1665	1703	1904	**2390**	5703	1086
1974	1726	1678	2307	3883	6496	4349	2210	1299	1069	1235	1968	2025	**2524**	8105	611
1975	1922	1748	2005	3206	3057	2060	1109	866	826	975	1162	1612	**1711**	5790	613
1976	1553	1546	2338	5767	3861	1882	1548	1252	1125	1217	1231	1437	**2061**	8190	704
1977	1351	1201	2677	3743	2326	1134	1121	930	973	1323	1571	2012	**1699**	5062	617
1978	1966	1902	1499	3169	2923	1537	1069	958	844	1263	1231	1286	**1634**	4668	701
1979	1454	1428	2537	4113	5023	2231	1466	1273	1296	1934	2483	2850	**2346**	6686	998
1980	2332	1948	2182	3574	2736	1484	1431	1420	1300	2175	2294	1919	**2066**	5329	683
1981	1603	2813	3116	4309	2996	2759	1582	1203	1706	1741	2027	1563	**2276**	6222	907
1982	1394	1374	1558	3176	2283	1426	1100	851	852	1030	1580	2259	**1573**	4585	684
1983	2381	2176	2571	2914	4915	3049	1237	1039	896	1081	1581	1787	**2136**	6907	567
1984	1640	1978	2069	4444	2916	2492	1964	1435	1306	1245	1925	2054	**2119**	5568	873
1985	2094	2015	2699	3646	3793	1539	1340	1623	1134	1109	1350	1593	**1995**	6004	901
1986	1620	1676	1647	3353	2769	2083	1322	1351	1401	1801	1829	1742	**1881**	4647	988
1987	1683	1563	1910	3111	1176	1201	985	816	771	926	1325	1846	**1440**	4767	614
1988	1868	1933	1649	3708	2788	1247	915	1176	1268	2289	3457	2251	**2042**	4665	826
1989	2062	2107	1888	2959	2986	2666	1287	920	854	933	1841	1859	**1859**	3883	566
1990	1919	2061	2499	3222	2628	1552	1444	1018	897	1829	2180	2829	**2006**	4562	775
1991	2262	2235	2412	4796	2542	1312	893	778	842	1177	1502	1881	**1881**	6728	666
1992	1827	1820	1678	3150	2998	1238	1163	1003	1443	1859	2688	2202	**1921**	5337	806
1993	2169	1883	1493	3746	1784	1873	1070	879	942	1896	2416	2216	**1859**	5454	733
1994	1718	1947	1814	2840	2572	2187	2186	1705	1133	1122	1670	1790	**1889**	4600	965
1995	2537	2215	2583	1757	2382	2216	1050	954	699	987	1986	1830	**1764**	3976	588
1996	2054	2291	2043	3034	4212	1944	1582	1387	1036	1237	1705	1915	**2036**	5722	876
1997	2016	2160	2270	4094	4693	1876	1497	990	972	1033	1437	1408	**2035**	6382	798
1998	1589	1554	2290	4687	1396	1107	1177	796	762	819	910	1388	**1536**	7239	535
1999	1737	1959	1921	3295	1279	1420	1355	880	832	1652	2444	2738	**1789**	5401	716
2000	2090	2003	2382	2847	2712	1842	1559	1392	1226	1016	1098	1485	**1804**	4274	617
2001	1449	1657	1518	2872	1756	1439	1016	668	822	1837	2561	2798	**1697**	4081	552

2002	2185	1970	2354	4171	3951	3691	1858	1105	886	826	900	956	**2068**	5894	638
2003	1167	1249	1488	2373	1868	1725	1127	1487	1008	1816	3266	3096	**1807**	4718	788
2004	2470	2040	2289	3217	3865	1936	1875	1091	1255	881	1095	1575	**1966**	4909	636
2005	1942	1736	1373	4141	2499	1570	993	780	698	1068	1614	2258	**1720**	4824	532
2006	2201	2308	2468	4144	2444	1568	1427	1360	1201	2591	3377	3299	**2364**	4587	945
2007	2823	2176	2049	2841	1722	1979	1411	826	720	707	849	1221	**1606**	3635	566
2008	2513	2243	2140	4783	3228	2027	2318	2182	1472	1323	1793	2085	**2341**	6052	1036
2009	2336	2220	2550	4193	3358	2244	1951	1886	1169	1349	1916	1936	**2258**	5617	897
2010	1872	1949	2308	1614	948	789	730	640	981	1896	1867	2711	**1524**	3922	467
2011	2224	2010	2477	3423	3640	2106	1465	899	832	876	1157	1881	**1915**	4931	609
2012	1924	1909	3248	2315	1692	987	620	614	703	1223	2052	1843	**1593**	4810	492
2013	2037	2370	2180	4037	4533	3244	1393	942	992	1440	2745	1980	**2319**	5421	816
2014	2038	1991	1470	3749	4613	2368	1341	1120	1492	2300	2461	2302	**2270**	5213	900
2015	2188	2008	1571	2929	2391	1724	1046	989	1057	874	1432	2408	**1715**	4422	715
2016	2785	2588	3713	4843	3204	1900	1059	932	822	892	978	1582	**2105**	5833	630
2017	1823	2030	3028	5431	6103	---	---	---	---	---	---	---	**---**	8862	1418
Mean	**1913**	**1889**	**2143**	**3523**	**3088**	**1975**	**1411**	**1164**	**1081**	**1410**	**1850**	**1979**	**1942**	**5356**	**744**
YEAR	**JAN**	**FEB**	**MAR**	**APR**	**MAY**	**JUN**	**JUL**	**AUG**	**SEP**	**OCT**	**NOV**	**DEC**	**ANNUAL MEANS**	**DAILY MAXIMUM**	**DAILY MINIMUM**

Appendix 3 Scour calculations input and output for 100- year storm

Contraction Scour

	Left	Channel	Right
Input Data			
Average Depth (m):	5.06	6.09	3.10
Approach Velocity (m/s):	2.42	3.80	1.84
Br Average Depth (m):		4.74	4.11
BR Opening Flow (m3/s):		3946.79	4243.21
BR Top WD (m):		149.86	155.34
Grain Size D50 (mm):	0.05	0.05	0.05
Approach Flow (m3/s):	1249.34	5198.60	1742.06
Approach Top WD (m):	102.23	311.47	305.99
K1 Coefficient:	0.690	0.690	0.690
Results			
Scour Depth Ys (m):		3.23	6.50
Critical Velocity (m/s):		0.31	0.28
Equation:		Live	Live

Pier Scour

All piers have the same scour depth

Input Data	
Pier Shape:	Circular cylinder
Pier Width (m):	0.8
Grain Size D50 (mm):	0.05000
Depth Upstream (m):	6.68
Velocity Upstream (m/s):	3.80
K1 Nose Shape:	1.00
Pier Angle:	0.00
Pier Length (m):	14.00
K2 Angle Coef:	1.00
K3 Bed Cond Coef:	1.10

Grain Size D90 (mm):	1.00000
K4 Armouring Coef:	1.00
Results	
Scour Depth Ys (m):	3.09
Froude #:	0.47
Equation:	CSU equation
Combined Scour Depths	
Pier Scour + Contraction Scour (m):	
Channel: 6.32	

Appendix 4 Scour calculations input and output for 100- year storm in projected climate

Contraction Scour

Left	Channel	Right

Input Data			
Average Depth (m):	5.62	6.90	3.48
Approach Velocity (m/s):	2.44	3.99	1.93
Br Average Depth (m):		5.21	4.48
BR Opening Flow (m3/s):		4655.78	5172.21
BR Top WD (m):		149.06	158.45
Grain Size D50 (mm):	0.05	0.05	0.05
Approach Flow (m3/s):	1467.30	6023.46	2337.24
Approach Top WD (m):	107.20	311.47	348.21
K1 Coefficient:	0.690	0.690	0.690
Results			
Scour Depth Ys (m):	3.99	7.35	
Critical Velocity (m/s):		0.31	0.28
Equation:		Live	Live

Pier Scour

All piers have the same scour depth

Input Data	
Pier Shape:	Circulare cylinder
Pier Width (m):	0.8m
Grain Size D50 (mm):	0.05000
Depth Upstream (m):	7.23
Velocity Upstream (m/s):	3.99
K1 Nose Shape:	1.00
Pier Angle:	0.00
Pier Length (m):	14.00
K2 Angle Coef:	1.00
K3 Bed Cond Coef:	1.10
Grain Size D90 (mm):	1.00000
K4 Armouring Coef:	1.00
Results	
Scour Depth Ys (m):	3.19

Froude #:	0.47
Equation:	CSU equation

Combined Scour Depths

Pier Scour + Contraction Scour (m):

Channel:	7.18

Appendix 5 STAAD Pro input for 100-year design

STAAD SPACE

START JOB INFORMATION

ENGINEER DATE 23-Jan-17

END JOB INFORMATION

INPUT WIDTH 79

UNIT METER KN

JOINT COORDINATES

2 0 5 0; 4 13.2 5 0; 5 14.2 5 0; 6 -1 5 0; 8 0 5 20; 10 13.2 5 20;

11 14.2 5 20; 12 -1 5 20; 14 0 5 40; 16 13.2 5 40; 17 14.2 5 40; 18 -1 5 40;

20 0 5 60; 22 13.2 5 60; 23 14.2 5 60; 24 -1 5 60; 26 0 5 80; 28 13.2 5 80;

29 14.2 5 80; 30 -1 5 80; 32 0 5 100; 34 13.2 5 100; 35 14.2 5 100;

36 -1 5 100; 37 1.65 5 0; 38 1.65 5 20; 39 1.65 5 40; 40 1.65 5 60;

41 1.65 5 80; 42 1.65 5 100; 43 3.3 5 0; 44 3.3 5 20; 45 3.3 5 40; 46 3.3 5 60;

47 3.3 5 80; 48 3.3 5 100; 49 4.95 5 0; 50 4.95 5 20; 51 4.95 5 40;

52 4.95 5 60; 53 4.95 5 80; 54 4.95 5 100; 55 6.6 5 0; 56 6.6 5 20;

57 6.6 5 40; 58 6.6 5 60; 59 6.6 5 80; 60 6.6 5 100; 61 8.25 5 0; 62 8.25 5 20;

63 8.25 5 40; 64 8.25 5 60; 65 8.25 5 80; 66 8.25 5 100; 67 9.9 5 0;

68 9.9 5 20; 69 9.9 5 40; 70 9.9 5 60; 71 9.9 5 80; 72 9.9 5 100; 73 11.55 5 0;

74 11.55 5 20; 75 11.55 5 40; 76 11.55 5 60; 77 11.55 5 80; 78 11.55 5 100;

79 0 5 120; 80 13.2 5 120; 81 14.2 5 120; 82 -1 5 120; 83 1.65 5 120;

84 3.3 5 120; 85 4.95 5 120; 86 6.6 5 120; 87 8.25 5 120; 88 9.9 5 120;

89 11.55 5 120; 90 0 5 -20; 91 13.2 5 -20; 92 14.2 5 -20; 93 -1 5 -20;

94 1.65 5 -20; 95 3.3 5 -20; 96 4.95 5 -20; 97 6.6 5 -20; 98 8.25 5 -20;

99 9.9 5 -20; 100 11.55 5 -20; 109 0 5 -40; 110 13.2 5 -40; 111 14.2 5 -40;

112 -1 5 -40; 113 1.65 5 -40; 114 3.3 5 -40; 115 4.95 5 -40; 116 6.6 5 -40;

117 8.25 5 -40; 118 9.9 5 -40; 119 11.55 5 -40; 120 0 -9.78 100;

121 13.2 -9.78 100; 122 0 -9.78 -20; 123 13.2 -9.78 -20; 124 0 -9.78 0;

125 13.2 -9.78 0; 126 0 -9.78 80; 127 13.2 -9.78 80; 128 0 -9.78 20;

129 13.2 -9.78 20; 130 0 -9.78 60; 131 13.2 -9.78 60; 132 0 -9.78 40;

133 13.2 -9.78 40;

MEMBER INCIDENCES

1 93 90; 2 6 2; 3 12 8; 4 18 14; 5 24 20; 6 30 26; 7 36 32; 8 90 122; 9 2 124;
10 8 128; 11 14 132; 12 20 130; 13 26 126; 14 32 120; 15 90 109; 16 2 90;
17 8 2; 18 14 8; 19 20 14; 20 26 20; 21 32 26; 22 79 32; 23 90 94; 24 2 37;
25 8 38; 26 14 39; 27 20 40; 28 26 41; 29 32 42; 30 94 113; 31 37 94; 32 38 37;
33 39 38; 34 40 39; 35 41 40; 36 42 41; 37 83 42; 38 94 95; 39 37 43; 40 38 44;
41 39 45; 42 40 46; 43 41 47; 44 42 48; 45 95 114; 46 43 95; 47 44 43;
48 45 44; 49 46 45; 50 47 46; 51 48 47; 52 84 48; 53 95 96; 54 43 49; 55 44 50;
56 45 51; 57 46 52; 58 47 53; 59 48 54; 60 96 115; 61 49 96; 62 50 49;
63 51 50; 64 52 51; 65 53 52; 66 54 53; 67 85 54; 68 96 97; 69 49 55; 70 50 56;
71 51 57; 72 52 58; 73 53 59; 74 54 60; 82 97 116; 83 55 97; 84 56 55;
85 57 56; 86 58 57; 87 59 58; 88 60 59; 89 86 60; 90 97 98; 91 55 61; 92 56 62;
93 57 63; 94 58 64; 95 59 65; 96 60 66; 97 98 117; 98 61 98; 99 62 61;
100 63 62; 101 64 63; 102 65 64; 103 66 65; 104 87 66; 105 98 99; 106 61 67;
107 62 68; 108 63 69; 109 64 70; 110 65 71; 111 66 72; 112 99 118; 113 67 99;
114 68 67; 115 69 68; 116 70 69; 117 71 70; 118 72 71; 119 88 72; 120 99 100;
121 67 73; 122 68 74; 123 69 75; 124 70 76; 125 71 77; 126 72 78; 127 100 119;
128 73 100; 129 74 73; 130 75 74; 131 76 75; 132 77 76; 133 78 77; 134 89 78;
135 100 91; 136 73 4; 137 74 10; 138 75 16; 139 76 22; 140 77 28; 141 78 34;
142 91 123; 143 4 125; 144 10 129; 145 16 133; 146 22 131; 147 28 127;
148 34 121; 149 91 110; 171 4 91; 172 10 4; 173 16 10; 174 22 16; 175 28 22;
176 34 28; 177 80 34; 178 91 92; 179 4 5; 180 10 11; 181 16 17; 182 22 23;
183 28 29; 184 34 35;

ELEMENT INCIDENCES SHELL

150 82 81 35 36; 151 36 35 29 30; 152 30 29 23 24; 153 24 23 17 18;
154 18 17 11 12; 155 12 11 5 6; 156 6 5 92 93; 187 93 92 111 112;

DEFINE PMEMBER

1 23 38 53 68 90 105 120 135 178 PMEMBER 1
4 26 41 56 71 93 108 123 138 181 PMEMBER 2
3 25 40 55 70 92 107 122 137 180 PMEMBER 3

ELEMENT PROPERTY

150 TO 156 187 THICKNESS 0.35
DEFINE MATERIAL START
ISOTROPIC CONCRETE
E 2.17185e+007
POISSON 0.17
DENSITY 23.5616
ALPHA 1e-005
DAMP 0.05
END DEFINE MATERIAL
MEMBER PROPERTY AMERICAN
15 TO 22 30 TO 37 45 TO 52 60 TO 67 82 TO 89 97 TO 104 112 TO 119 127 TO 134 -
149 171 TO 177 PRIS YD 1 ZD 0.6 YB 0.75 ZB 0.25
1 TO 7 23 TO 29 38 TO 44 53 TO 59 68 TO 74 90 TO 96 105 TO 111 120 TO 126 -
135 TO 141 178 TO 184 PRIS YD 1 ZD 0.8
8 TO 14 142 TO 148 PRIS YD 0.8
CONSTANTS
BETA 180 MEMB 15 TO 22 30 TO 37 45 TO 52 60 TO 67 82 TO 89 97 TO 104 -
112 TO 119 127 TO 134 149 171 TO 177
MATERIAL CONCRETE ALL
SUPPORTS
79 TO 89 109 TO 119 PINNED
120 TO 133 FIXED
DEFINE MOVING LOAD
TYPE 1 LOAD 25 62.5 62.5 87.5 75
DIST 3.6 1.2 6.6 6.6 WID 1.8
TYPE 2 LOAD 25 62.5 62.5 87.5 75
DIST 3.6 1.2 6.6 6.6 WID 1.8
TYPE 3 LOAD 25 62.5 62.5 87.5 75
DIST 3.6 1.2 6.6 6.6 WID 1.8
TYPE 4 LOAD 25 62.5 62.5 87.5 75
DIST 3.6 1.2 6.6 6.6 WID 1.8

LOAD 1 LOADTYPE Dead TITLE SELF WEIGHT

SELFWEIGHT Y -1

LOAD 2 LOADTYPE Dead TITLE VERTICAL WIND

ELEMENT LOAD

150 TO 156 187 PR GY -1.38

LOAD 3 LOADTYPE Dead TITLE HORIZONTAL WIND

MEMBER LOAD

8 TO 14 142 TO 148 UNI GX -2.208 0 3.46

LOAD 5 LOADTYPE Dead TITLE HYDRODYNAMIC LOAD

MEMBER LOAD

8 TO 14 142 TO 148 UNI GX -4.28 3.42 13.92

LOAD GENERATION 20

TYPE 1 1.2 5 -40 ZINC 8

LOAD GENERATION 20

TYPE 2 4.2 5 -40 ZINC 8

LOAD GENERATION 20

TYPE 3 7.2 5 -40 ZINC 8

LOAD GENERATION 20

TYPE 4 10.2 5 -40 ZINC 8

LOAD 87 LOADTYPE Dead TITLE WEARING SURFACE

ELEMENT LOAD

150 TO 156 187 PR GY -0.01

LOAD COMB 86 COMBINATION LOAD CASE PIER 1 ULTIMATE COMBO 1

1 1.2 87 1.5 6 1.7 27 1.7 49 1.7 69 1.7

LOAD COMB 88 COMBINATION LOAD CASE PIER 1 ULTIMATE COMBO 3

1 1.2 87 1.5 2 0.45 3 0.45 6 1.5 27 1.5 49 1.5 69 1.5

LOAD COMB 89 COMBINATION LOAD CASE PIER 1 COMBO 4

1 1.2 87 1.5 2 1.4 3 1.4

LOAD COMB 90 COMBINATION LOAD CASE PIER 10 ULTIMATE COMBO 1

1 1.2 87 1.5 16 1.7 35 1.7 56 1.7 76 1.7

LOAD COMB 91 COMBINATION LOAD CASE PIER 10 ULTIMATE COMBO 3

1 1.2 87 1.5 2 0.45 3 0.45 15 1.7 35 1.7 55 1.7 75 1.7

LOAD COMB 92 COMBINATION LOAD CASE PIER 10 ULTIMATE COMBO 4

1 1.2 87 1.5 2 1.4 3 1.4

PERFORM ANALYSIS PRINT ALL

DEFINE ENVELOPE

86 88 89 ENVELOPE 1 TYPE STRENGTH

90 TO 92 ENVELOPE 2 TYPE STRENGTH

END DEFINE ENVELOPE

LOAD LIST ENV 2

START CONCRETE DESIGN

CODE CANADIAN

CLB 0.04 MEMB 8

DESIGN COLUMN 8

MINSEC 10 MEMB 11

DESIGN COLUMN 11

END CONCRETE DESIGN

FINISH

Appendix 6 STAAD Pro input for projected climate

STAAD SPACE

START JOB INFORMATION

ENGINEER DATE 23-Jan-17

END JOB INFORMATION

INPUT WIDTH 79

UNIT METER KN

JOINT COORDINATES

2 0 5 0; 4 13.2 5 0; 5 14.2 5 0; 6 -1 5 0; 8 0 5 20; 10 13.2 5 20;

11 14.2 5 20; 12 -1 5 20; 14 0 5 40; 16 13.2 5 40; 17 14.2 5 40; 18 -1 5 40;

20 0 5 60; 22 13.2 5 60; 23 14.2 5 60; 24 -1 5 60; 26 0 5 80; 28 13.2 5 80;

29 14.2 5 80; 30 -1 5 80; 32 0 5 100; 34 13.2 5 100; 35 14.2 5 100;

36 -1 5 100; 37 1.65 5 0; 38 1.65 5 20; 39 1.65 5 40; 40 1.65 5 60;

41 1.65 5 80; 42 1.65 5 100; 43 3.3 5 0; 44 3.3 5 20; 45 3.3 5 40; 46 3.3 5 60;

47 3.3 5 80; 48 3.3 5 100; 49 4.95 5 0; 50 4.95 5 20; 51 4.95 5 40;

52 4.95 5 60; 53 4.95 5 80; 54 4.95 5 100; 55 6.6 5 0; 56 6.6 5 20;

57 6.6 5 40; 58 6.6 5 60; 59 6.6 5 80; 60 6.6 5 100; 61 8.25 5 0; 62 8.25 5 20;

63 8.25 5 40; 64 8.25 5 60; 65 8.25 5 80; 66 8.25 5 100; 67 9.9 5 0;

68 9.9 5 20; 69 9.9 5 40; 70 9.9 5 60; 71 9.9 5 80; 72 9.9 5 100; 73 11.55 5 0;

74 11.55 5 20; 75 11.55 5 40; 76 11.55 5 60; 77 11.55 5 80; 78 11.55 5 100;

79 0 5 120; 80 13.2 5 120; 81 14.2 5 120; 82 -1 5 120; 83 1.65 5 120;

84 3.3 5 120; 85 4.95 5 120; 86 6.6 5 120; 87 8.25 5 120; 88 9.9 5 120;

89 11.55 5 120; 90 0 5 -20; 91 13.2 5 -20; 92 14.2 5 -20; 93 -1 5 -20;

94 1.65 5 -20; 95 3.3 5 -20; 96 4.95 5 -20; 97 6.6 5 -20; 98 8.25 5 -20;

99 9.9 5 -20; 100 11.55 5 -20; 109 0 5 -40; 110 13.2 5 -40; 111 14.2 5 -40;

112 -1 5 -40; 113 1.65 5 -40; 114 3.3 5 -40; 115 4.95 5 -40; 116 6.6 5 -40;

117 8.25 5 -40; 118 9.9 5 -40; 119 11.55 5 -40; 120 0 -9.78 100;

121 13.2 -9.78 100; 122 0 -9.78 -20; 123 13.2 -9.78 -20; 124 0 -9.78 0;

125 13.2 -9.78 0; 126 0 -9.78 80; 127 13.2 -9.78 80; 128 0 -9.78 20;

129 13.2 -9.78 20; 130 0 -9.78 60; 131 13.2 -9.78 60; 132 0 -9.78 40;

133 13.2 -9.78 40;

MEMBER INCIDENCES

1 93 90; 2 6 2; 3 12 8; 4 18 14; 5 24 20; 6 30 26; 7 36 32; 8 90 122; 9 2 124;
10 8 128; 11 14 132; 12 20 130; 13 26 126; 14 32 120; 15 90 109; 16 2 90;
17 8 2; 18 14 8; 19 20 14; 20 26 20; 21 32 26; 22 79 32; 23 90 94; 24 2 37;
25 8 38; 26 14 39; 27 20 40; 28 26 41; 29 32 42; 30 94 113; 31 37 94; 32 38 37;
33 39 38; 34 40 39; 35 41 40; 36 42 41; 37 83 42; 38 94 95; 39 37 43; 40 38 44;
41 39 45; 42 40 46; 43 41 47; 44 42 48; 45 95 114; 46 43 95; 47 44 43;
48 45 44; 49 46 45; 50 47 46; 51 48 47; 52 84 48; 53 95 96; 54 43 49; 55 44 50;
56 45 51; 57 46 52; 58 47 53; 59 48 54; 60 96 115; 61 49 96; 62 50 49;
63 51 50; 64 52 51; 65 53 52; 66 54 53; 67 85 54; 68 96 97; 69 49 55; 70 50 56;
71 51 57; 72 52 58; 73 53 59; 74 54 60; 82 97 116; 83 55 97; 84 56 55;
85 57 56; 86 58 57; 87 59 58; 88 60 59; 89 86 60; 90 97 98; 91 55 61; 92 56 62;
93 57 63; 94 58 64; 95 59 65; 96 60 66; 97 98 117; 98 61 98; 99 62 61;
100 63 62; 101 64 63; 102 65 64; 103 66 65; 104 87 66; 105 98 99; 106 61 67;
107 62 68; 108 63 69; 109 64 70; 110 65 71; 111 66 72; 112 99 118; 113 67 99;
114 68 67; 115 69 68; 116 70 69; 117 71 70; 118 72 71; 119 88 72; 120 99 100;
121 67 73; 122 68 74; 123 69 75; 124 70 76; 125 71 77; 126 72 78; 127 100 119;
128 73 100; 129 74 73; 130 75 74; 131 76 75; 132 77 76; 133 78 77; 134 89 78;
135 100 91; 136 73 4; 137 74 10; 138 75 16; 139 76 22; 140 77 28; 141 78 34;
142 91 123; 143 4 125; 144 10 129; 145 16 133; 146 22 131; 147 28 127;
148 34 121; 149 91 110; 171 4 91; 172 10 4; 173 16 10; 174 22 16; 175 28 22;
176 34 28; 177 80 34; 178 91 92; 179 4 5; 180 10 11; 181 16 17; 182 22 23;
183 28 29; 184 34 35;

ELEMENT INCIDENCES SHELL

150 82 81 35 36; 151 36 35 29 30; 152 30 29 23 24; 153 24 23 17 18;
154 18 17 11 12; 155 12 11 5 6; 156 6 5 92 93; 187 93 92 111 112;

DEFINE PMEMBER

1 23 38 53 68 90 105 120 135 178 PMEMBER 1
4 26 41 56 71 93 108 123 138 181 PMEMBER 2
3 25 40 55 70 92 107 122 137 180 PMEMBER 3

ELEMENT PROPERTY

150 TO 156 187 THICKNESS 0.35
DEFINE MATERIAL START
ISOTROPIC CONCRETE
E 2.17185e+007
POISSON 0.17
DENSITY 23.5616
ALPHA 1e-005
DAMP 0.05
END DEFINE MATERIAL
MEMBER PROPERTY AMERICAN
15 TO 22 30 TO 37 45 TO 52 60 TO 67 82 TO 89 97 TO 104 112 TO 119 127 TO 134 -
149 171 TO 177 PRIS YD 1 ZD 0.6 YB 0.75 ZB 0.25
1 TO 7 23 TO 29 38 TO 44 53 TO 59 68 TO 74 90 TO 96 105 TO 111 120 TO 126 -
135 TO 141 178 TO 184 PRIS YD 1 ZD 0.8
8 TO 14 142 TO 148 PRIS YD 0.8
CONSTANTS
BETA 180 MEMB 15 TO 22 30 TO 37 45 TO 52 60 TO 67 82 TO 89 97 TO 104 -
112 TO 119 127 TO 134 149 171 TO 177
MATERIAL CONCRETE ALL
SUPPORTS
79 TO 89 109 TO 119 PINNED
120 TO 133 FIXED
DEFINE MOVING LOAD
TYPE 1 LOAD 25 62.5 62.5 87.5 75
DIST 3.6 1.2 6.6 6.6 WID 1.8
TYPE 2 LOAD 25 62.5 62.5 87.5 75
DIST 3.6 1.2 6.6 6.6 WID 1.8
TYPE 3 LOAD 25 62.5 62.5 87.5 75
DIST 3.6 1.2 6.6 6.6 WID 1.8
TYPE 4 LOAD 25 62.5 62.5 87.5 75
DIST 3.6 1.2 6.6 6.6 WID 1.8

LOAD 1 LOADTYPE Dead TITLE SELF WEIGHT

SELFWEIGHT Y -1

LOAD 2 LOADTYPE Dead TITLE VERTICAL WIND

ELEMENT LOAD

150 TO 156 187 PR GY -1.38

LOAD 3 LOADTYPE Dead TITLE HORIZONTAL WIND

MEMBER LOAD

8 TO 10 12 TO 14 142 TO 148 UNI GX -50 0 2.26

LOAD 5 LOADTYPE Dead TITLE HYDRODYNAMIC LOAD

MEMBER LOAD

8 TO 14 142 TO 148 UNI GX -4.3 2.26 14.78

LOAD GENERATION 20

TYPE 1 1.2 5 -40 ZINC 8

LOAD GENERATION 20

TYPE 2 4.2 5 -40 ZINC 8

LOAD GENERATION 20

TYPE 3 7.2 5 -40 ZINC 8

LOAD GENERATION 20

TYPE 4 10.2 5 -40 ZINC 8

LOAD 87 LOADTYPE Dead TITLE WEARING SURFACE

ELEMENT LOAD

150 TO 156 187 PR GY -0.01

LOAD COMB 4 COMBINATION LOAD CASE 4

1 1.2 5 1.3

LOAD COMB 86 COMBINATION LOAD CASE PIER 1 ULTIMATE COMBO 1

1 1.2 87 1.5 6 1.7 27 1.7 49 1.7 69 1.7

LOAD COMB 88 COMBINATION LOAD CASE PIER 1 ULTIMATE COMBO 3

1 1.2 87 1.5 2 0.45 3 0.45 6 1.5 27 1.5 49 1.5 69 1.5

LOAD COMB 89 COMBINATION LOAD CASE PIER 1 COMBO 4

1 1.2 87 1.5 2 1.4 3 1.4

LOAD COMB 90 COMBINATION LOAD CASE PIER 10 ULTIMATE COMBO 1

1 1.2 87 1.5 16 1.7 35 1.7 56 1.7 76 1.7

LOAD COMB 91 COMBINATION LOAD CASE PIER 10 ULTIMATE COMBO 3

1 1.2 87 1.5 2 0.45 3 0.45 15 1.7 35 1.7 55 1.7 75 1.7

LOAD COMB 92 COMBINATION LOAD CASE PIER 10 ULTIMATE COMBO 4

1 1.2 87 1.5 2 1.4 3 1.4

PERFORM ANALYSIS PRINT ALL

DEFINE ENVELOPE

86 88 89 ENVELOPE 1 TYPE STRENGTH

90 TO 92 ENVELOPE 2 TYPE STRENGTH

END DEFINE ENVELOPE

LOAD LIST ENV 2

START CONCRETE DESIGN

CODE CANADIAN

CLB 0.04 MEMB 8

DESIGN COLUMN 8

MINSEC 10 MEMB 11

DESIGN COLUMN 11

END CONCRETE DESIGN

FINISH

References

Alexander, L. V., Zhang, X., Peterson, T. C., Caesar, J., Gleason, B., Tank, A. M. Burn. (2006). Global observed changes in daily climate extremes of temperature and precipitation. *Journal of Geophysical Reseach*.

ASCE Committee on Adaptation to a Changing Climate. (2015). Adapting Infrastructure and Civil Engineering Practice to a Changing Climate. (J. R. Olsen, Ed.)

Bentley Systems Incorporated. (2012). *STAAD.Pro V8i (SELECT series 4) Technical Reference Manual.* Pennsylvania: Bentley Systems Incorporated.

Buurman, J., & Babovic, V. (2016). Adaptation Pathways and Real Options Analysis: An approach to deep uncertainty in climate change adaptation policies. *Policy and society*. Retrieved from http://dx.doi.org/10.1016/j.polsoc.2016.05.002

Canadian Standards Association. (2004). *CSA Standard A23.3-04 Design of Concrete Structures.* Toronto: Canadian Standards Association.

Canadian Standards Association. (2014). *CSA S6-14. Canadian Highway Bridge Design Code.* Mississauga: Canadian Standards Association.

Chase, K. J., & Holnbeck, S. R. (2004). *Evaluation of Pier-Scour Equations for Coarse-Bed Streams.* Reston, Virginia: U.S. Geological Survey.

Cheng, L. (2012). *Evaluation Of Lateral Behavior Of Pile-Supported Bridges Under Scour Conditions.* University of Kansas, Civil, Environmental, and Architectural Engineering and the Graduate Faculty. unpublished Thesis.

Chiotti, Q., & Lavender, B. (2008). *Ontario; From impacts to adaptation: Canada in a changing climate.* Ottawa: Government of Canada.

Colombo, S., McKenney, D., Lawrence, K., & Gray, P. (2007). *Climate Change Projections for Ontario :Practical Information for policy makers and planners.* Toronto: Ontario Ministry of Natural Resources.

Crowley, T. J. (2000). Causes of Climate Change Over the Past 1000 Years. *Science Magarzine, 289*. Retrieved from www.sciencemag.org

Das, S., Das, R., & Mazumdar, A. (2013). Circulation characteristics of horseshoe vortex in scour region around circular piers. *Water Science and Engineering*, 59-77.

Dasar, A., Hamada, H., Sagawa, Y., & Yamamoto, D. (2017). Deterioration progress and performance reduction of 40-year-old reinforced concrete beams in natural corrosion environments. *Elsevier*.

Demuzere, M., Orru, K., Heidrich, O., Olazabal, E., Geneletti, D., Orru, H., Faehnle, M. (2014). Mitigating and adapting to climate change: Multi-functional and multi-scale assessment of green urban infrastructure. *Journal of Environmental Management*, 107-115.

DuraCrete. (1998). probabilistic performance based durability design of concrete structures. *Modelling of degradation*, p. 174.

Environment and Climate Change Canada. (2017, June 8). Retrieved from The Canadian Centre for Climate Modelling and Analysis (CCCma): http://www.ec.gc.ca/ccmac-cccma/default.asp?lang=En&n=4A642EDE-1

Environment and natural resources Canada. (2015). *Causes of climate change.* Retrieved April 2017, from https://www.canada.ca/en/environment-climate-change/services/climate-change/causes.html

Ferdous, A., Daley, M., Perry, G., Evelyn, L., & Andrea, L. (2014). *Ottawa River Flood Risk Mapping from Shirley's Bay to Cumberland.* Rideau Valley Conservation Authority.

Fischer, E., & Subhash C. Jain. (1984). Live- Bed Scour at Bridge Piers. *Journal of Hydraulic Engineering*.

Forster, P., Ramaswamy, V., Artaxo, P., Berntsen, T., Fahey, R. B., Haywood, J., Dorland, R. V. (2007). Changes in atmospheric constituents and in radiative forcing. Contribution of Working Group I to the Fourth Assessment Report of the Intergovernmental Panel on Climate Change. In D. Q. Solomon S. (Ed.), *Climate Change 2007: The Physical Science Basis* (pp. 131-217). Cambridge, United Kingdom / New York, NY, USA.: Cambridge University Press.

Groisman, P. Y., & Knight, R. W. (2008). Prolonged Dry Episodes over the Conterminous United States: New Tendencies Emerging during the Last 40 Years. *merican Meteorological Society*.

Intergovernmental Panel on Climate Change (IPCC)(2007a). (2007). Climate Change 2007: Impacts, Adaptation and Vulnerability, Contribution of Working Group II to the Fourth Assessment. (O. C. M.L Parry, Ed.) *Report of the Intergovernmental Panel on Climate Change.*

IPCC. (2014). Climate Change 2014: Synthesis Report. Contribution of Working Groups I, II and III to the Fifth Assessment Report of the Intergovernmental Panel on Climate Change. 117-130.

IPCC. (2017, June 5). *What is a GCM*. Retrieved from IPCC SITE: http://www.ipcc-data.org/guidelines/pages/gcm_guide.html

Jacob, D., Barring, L., Christensen, O. B., Christensen, J. H., Castro, M. d., Deque, M., Sanchez, E. (2007). An inter-comparison of regional climate models for Europe: model performance in present-day climate.

Kallias, A. N., & Imam, B. M. (2013). *Effect of Climate Change on the Deterioration of Steel Bridges*. International Association for Bridge and Structural Engineering.

Khwairakpam, P., Ray, S. S., Das, S., Das, R., & Mazumdar, A. (2012, June). Scour Hole Characteristics Around a Vertical Pier Under Clearwater Scour Conditions. *ARPN Journal of Engineering and Applied Sciences, 7*(6).

Kunkel, K. E., Andsager, K., & Easterling, D. R. (1999). Long-Term Trends in Extreme Precipitation Events over the Conterminous United States and Canada. *Jounal of Climate, ii*.

Lagasse, P., Clopper, P., Zevenbergen, L., & Girard, L. (2006). *Countermeasures to Protect Bridge Piers From Scour*. National Cooperative Highway Research Program Transportation Research Board National Research Council.

Marie, C., Palhol, F., & Andre, L. (2016). Adaptation of transport infrastructures and networks to climate change. *Transportation Research Procedia*, 86-95.

Meehl, G. A., Zwiers, F., Evans, J., Knutson, T., Mearns, L., & Whetton, P. (2000). Trends in Extreme Weather and Climate Events: Issues Related to Modeling Extremes in Projections of Future Climate Change. *Bulletin of the American Meteorological Society*.

Melville, B. W., & Sutherland, A. J. (1988). Design Method for Local Scour at Bridge Piers. *Journal of Hydraulic Engineering, 114*(10).

Ortega, N. F., & Robles, S. I. (2014). Assessment of Residual Life of concrete structures affected by reinforcement corrosion. *Housing and Building National Research Center*.

Paasche, Y., & Storen, E. W. (2014). How Does Climate Impact Floods? Closing the Knowledge Gap. *Earth and Space Science*.

Rood, R. (2007). *Definition of Climate: Average versus Accumulation.* University of Michigan. Retrieved from https://www.wunderground.com/blog/RickyRood/definition-of-climate-average-versus-accumulation.

Saeki, T. (2002). Effect Of Carbonation On Chloride penetration in concrete. *Third RILEM workshop on Testing and Modelling the Chloride Ingress into Concrete.* Madrid, Spain.

Stewart, M. G., Wang, X., & Nguyen, M. N. (2011). Climate change impact and risks of concrete infrastructure deterioration. *Engineering Structures, 33*, 1326–1337. Retrieved 02 25, 2017, from www.elsevier.com/locate/engstruct.

Xiaoming, W., Nguyen, M., Stewartt, M. G., Syme, M., & Leitch, A. (2010). Analysis of Climate Change Impacts on the Deterioration of Concrete Infrastructure – Part 1: Mechanisms, Practices, Modelling and Simulations – A review. CSIRO, Canberra.

Yin-hui, W., Yi-song, Z., Lue-qin, X., & Zheng, L. (2015). *Analysis of Water Flow Pressure on Bridge Piers.* Hindawi Publishing Corporation Mathematical Problems in Engineering Volume 2015, Article ID 687535, 8 pages http://dx.doi.org/10.1155/2015/687535.

Zhang, X., Brown, R., Vincent, L., Skinner, W., Feng, Y., & Mekis, E. (2010). *Canadian climate trends, 1950 - 2007.* Canadian Councils of Resource Ministers.